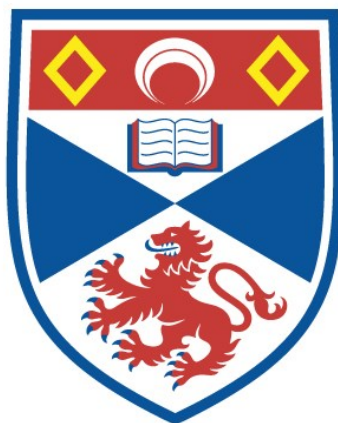


THE DEVELOPMENT OF AN IMPROVED KINETIC
FLOW TECHNIQUE AND ITS APPLICATION TO THE
PYROLYSIS OF METHYL BROMIDE

Gordon Robert Woolley

A Thesis Submitted for the Degree of PhD
at the
University of St Andrews



1965

Full metadata for this item is available in
St Andrews Research Repository
at:

<http://research-repository.st-andrews.ac.uk/>

Please use this identifier to cite or link to this item:

<http://hdl.handle.net/10023/14802>

This item is protected by original copyright

THE DEVELOPMENT OF
AN IMPROVED KINETIC FLOW TECHNIQUE
AND ITS APPLICATION TO
THE PYROLYSIS OF METHYL BROMIDE

being a Thesis
presented by

GORDON ROBERT WOOLLEY, B.Sc.,

to the
UNIVERSITY OF ST. ANDREWS

in application for the
DEGREE OF DOCTOR OF PHILOSOPHY.

November 1965.



ProQuest Number: 10171136

All rights reserved

INFORMATION TO ALL USERS

The quality of this reproduction is dependent upon the quality of the copy submitted.

In the unlikely event that the author did not send a complete manuscript and there are missing pages, these will be noted. Also, if material had to be removed, a note will indicate the deletion.



ProQuest 10171136

Published by ProQuest LLC (2017). Copyright of the Dissertation is held by the Author.

All rights reserved.

This work is protected against unauthorized copying under Title 17, United States Code
Microform Edition © ProQuest LLC.

ProQuest LLC.
789 East Eisenhower Parkway
P.O. Box 1346
Ann Arbor, MI 48106 – 1346

Tu 5363

(ii)

DECLARATION

I hereby declare that the following Thesis is a record of results of experiments carried out by me, that it is my own composition, and that it has not previously been presented in application for a Higher Degree.

The experiments were carried out in the Chemistry Research Laboratories of St. Salvator's College, St. Andrews, under the supervision of Dr. C. Horrex.

CERTIFICATE

I hereby certify that Gordon Robert Woolley has been engaged upon research work for twelve terms under my supervision, that he has fulfilled the conditions of Ordinance No. 16 (St. Andrews), and that he is qualified to submit the accompanying Thesis in application for the degree of Doctor of Philosophy.

UNIVERSITY CAREER

I entered the University of St. Andrews in October, 1955 and graduated in 1959 with First Class Honours in Chemistry. Since October, 1962 I have been an Assistant Lecturer in the Department of Chemistry, St. Salvator's College, St. Andrews.

The work described in this Thesis was carried out under the direction of Dr. C. Horrex during the period October, 1959, to May, 1965.

ACKNOWLEDGEMENT

I should like to record my gratitude to my supervisor, Dr. C. Horrex, for the help, interest and encouragement he has given throughout the practical and theoretical aspects of this work.

I am indebted to the Trustees of the Carnegie Trust for the Scottish Universities for a Research Scholarship for the period 1959 to 1962. I wish to record my indebtedness to the late Professor John Read, F.R.S., and to Professor J. I. G. Cadogan for research facilities during the period of the research.

I should also like to thank Dr. David Calvert for his willing advice and for many helpful discussions, Mr. T. Norris, Mr. A. McGhee and Mr. M. Zechewski for help with the constructional work, Mr. W. D. Woolley, Dr. R. K. Boyd and my several research colleagues for many fruitful discussions, and also Mrs. M. Smith and Miss J. Brown who typed the manuscript.

CONTENTS

Declaration	(ii)
Certificate	(iii)
University Career	(iv)
Acknowledgements	(v)
Contents	(vi)
List of Illustrations	(ix)
List of Tables	(xi)
INTRODUCTION	1
1. Bond Dissociation Energies	4
2. Toluene as a radical acceptor	9
3. Radical reactions	14
4. Halide pyrolyses with particular reference to bromides	21
5. Previous determinations of $D(\text{CH}_3\text{--Br})$	31
APPARATUS AND EXPERIMENTAL PROCEDURE	
1. Description of the apparatus	38
2. Injection of reactants	39
3. Purification of reactants	40
4. Reactant injection calibration	42
5. Calibration of flow capillaries	44
6. Circulation pump flow rate	45
7. Pressure gradient in the flow system	46
8. The Mass Spectrometer	47
9. Early experiments	53
10. Apparatus modifications	57

APPARATUS AND EXPERIMENTAL PRECEDURE (Cont'd.)

11. Further calibrations	60
12. Typical run procedure	62
13. Tests for surface reaction	65

DESCRIPTION OF EXPERIMENTS PERFORMED AND
EXPERIMENTAL RESULTS

1. Introductory	68
2. Seasoning of furnace	69
3. Effect of variation of methyl bromide partial pressure	72
4. Effect of variation of contact time	73
5. Effect of variation of toluene partial pressure	76
6. Effect of variation of carrier gas pressure	78
7. Effect of temperature variation (unpacked furnace)	80
8. Effect of temperature variation (packed furnace)	81

DISCUSSION

A. The empirical rate equation, evaluation of the rate constants and their temperature dependence	83
1 The rate equation	83
2. Toluene dependence of rate law	86
3. Effect of variation of contact time and carrier gas pressure	88
4. Evaluation of k_T , k_C and k_A and their temperature dependence	89
B. Reaction sequences and mechanistic considerations	94
C. Analysis of the rate equation	100
D. General assessment of the method	109

SUMMARY

112

APPENDICES

I	Calculation of contact times	115
II	Gas distribution data	117
III	Seasoning rate data	119
IV	Variation of partial pressure with contact time	121
V	Temperature coefficient data (unpacked furnace)	123
VI	Temperature coefficient data (packed furnace)	125
VII	Rate of molecular diffusion to furnace wall	126
VIII	An assessment of errors and error limits	128
IX	Effect of contact time variation and removal of toluene dependence	130
X	Furnace seasoning	135
XI	Flow conditions and design characteristics	136

REFERENCES

141

LIST OF ILLUSTRATIONS AND GRAPHS

	Facing page
1. Flow system	38
2. Furnace temperature profile	39
3. Reactant injection	40
4. Diaphragm valve	40
5. Flow system gas calibration	40
6. Toluene injection calibration	42
7. Methyl bromide injection calibration	43
8. Flow capillary calibration	44
9. Flow capillary calibration	45
10. Circulation pump flow rate	45
11. Circulation pump efficiency	45
12a. Pressure gradient in flow system	46
12b. Pressure gradient in flow system	46
13. Mass spectrometer electrical requirements	47
14. Outline of trap current stabilised filament supply	50
15. E.H.T. variation controls	51
16. Potentials on the ion gun plates	52
17. Variation of peak height with repeller-box voltage	52
18. Mass spectrometer resolution	52
19. Peak shape	52
20. Typical early run data	54
21. Variation of leak ratio with argon pressure	58
22. Sampling system	58
23. Stainless steel valve	59
24. Collection trap	61
25. Gas distribution (temperature variation)	62
26. Gas distribution (pressure variation)	62

27. Mass spectrometer response to methyl bromide	62
28. Typical experimental data	65
29. Gas distribution (temperature variation)	67
30. Gas distribution (pressure variation)	67
31. Seasoning rates of furnaces	70
32. Examination of furnace coating	71
33. Variation of methyl bromide pressure	72
34. Variation of contact time	73
35. Variation of toluene/methyl bromide ratio	76
36. Variation of toluene pressure	77
37. Variation of carrier gas pressure	78
38. Temperature variation (unpacked furnace)	80
39. Temperature variation (packed furnace)	82
40. Variation of argon and toluene pressures	83
41. Correlation between graphs in figure 40	86
42. Toluene and methyl bromide pressure data	86
43. Combined data of first order constants	87
44. Extrapolation for α and α_0	90
45. Data for 0.4 and 0.8 mm. toluene	92
46. Arrhenius plot of k_T	92
47. Arrhenius plot of k_0	92
48. Toluene variation for lined furnace	101
49. Comparison with other work	104
50. Removal of toluene dependence from contact time	133
51. Theoretical and experimental decomposition rates	134

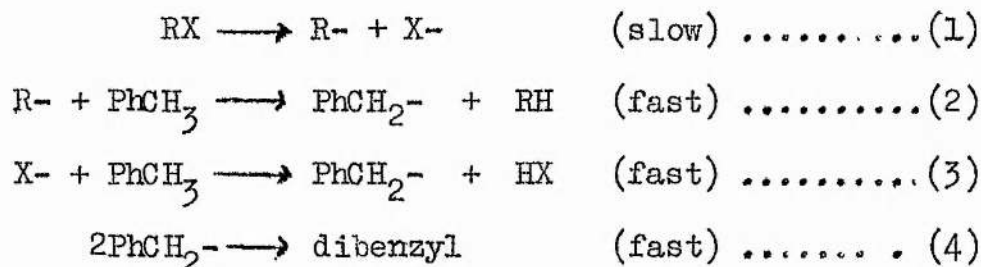
LIST OF TABLES

I	Variation of methyl bromide partial pressure	72
II	Contact time variation	74
III	Variation of toluene partial pressure	77
IV	Variation of carrier gas pressure	79
V	Temperature variation (unpacked furnace)	123
VI	Temperature variation (packed furnace)	125
VII	Data for α_0	91
VIII	Data for k_T and k_0	93
IX	Removal of toluene dependence from contact time variation	133

INTRODUCTION

Investigations of the rates of decomposition of organic halides have played an important part in the creation of recent lists of bond strengths in organic compounds, and of heats of formation of radicals. Such data are very useful for our understanding of the principles of molecular reactivity and it is important that these lists of values shall be as accurate as possible. The work described in this thesis was undertaken with the aim of improving one particular technique of investigation and testing the method on an example of importance.

The particular method chosen for study was the toluene radical acceptor technique where the following reactions are said to occur:-



In order to reduce the possibility of side reactions as much as possible, the usual recommended procedure is to choose operating conditions which give only small percentages of decomposition of RX. By using a flow technique, adequate quantities of one compound are usually collected for analysis. When bromo compounds have been pyrolysed, the hydrogen bromide formed has been determined and the stoichiometry assumed.

Using values of $d[\text{HBr}]/dt$ to measure the rate of reaction (1) resulted in the derivation of first order velocity constants, but the proof of first order character has not been convincing in many cases. For some compounds the temperature coefficient of such first order constants has been studied and energies of activation deduced. In other cases it has been assumed that the Arrhenius temperature independent factor should be 10^{13} sec^{-1} and the values of velocity constants at a single temperature have yielded energies of activation through use of the equation

$$\log_{10} k(\text{sec}^{-1}) = 13 - (E/4.57T).$$

The deduced energies of activation have been equated to the enthalpies of reaction (1), leading to the relationship

$$\begin{aligned} E &= \Delta H \text{ for reaction (1)} \\ &= \Delta H_f (\text{R}\cdot) + \Delta H_f (\text{X}\cdot) - \Delta H_f (\text{RX}) \end{aligned}$$

It is clear that the data on series of compounds such as $\text{PhCH}_2\text{-X}$ and $\text{CH}_3\text{-X}$ should yield consistent values of ΔH_f for the $\text{PhCH}_2\cdot$ and $\text{CH}_3\cdot$ radicals. This has not always been found. In some cases the methods of analysis of the data may have been at fault. Mearns(19) in this Department, has shown, in a study of the decomposition of $\text{Ph}\cdot\text{CH}_2\text{Br}$, that Szwarc's value of E is too low and his use of a constant A factor is not justified.

The purpose of the research work described in this thesis has been to produce a more searching method of investigation into this field by applying mass spectrometry as an analytical tool. The advantages foreseen included:-

(a) the possibility of analysing simultaneously for reactants and products emerging from a flow type reactor, obtaining data which can be followed with time in order to assess the seasoning (if any) of the reactor surface;

(b) the opportunity to base rate constants on reactant concentration, rather than on product concentrations and an assumed stoichiometry;

(c) the possibility of amassing a substantial quantity of analytical data in a reasonable time while retaining the power of a flow technique to study the initial stages of a reaction.

In order to prove the technique which was developed, the work was concentrated on the decomposition of methyl bromide. The only pyrolytic work on this compound has been done by Szwarc who considers the reaction complex under his conditions and prefers not to attach any weight to the activation energy found experimentally, although it agrees with the value deduced from reliable thermochemical data.

In addition, it is often convenient to relate data to the first member of a series, and it is important that the bond dissociation energies of such 'reference' compounds should be firmly supported by experimental evidence.

1. Bond Dissociation Energies

It is necessary to distinguish between the two terms used in the representation of the energies of chemical bonds: The first, and more useful, is the bond dissociation energy (B.D.E.) or simply dissociation energy. This is defined as the energy difference between the parent molecule (in its equilibrium configuration) and the two fragments (in their equilibrium ground state configurations) after breaking the bond. Thus the bond dissociation energy of a bond AB - C is the change in energy ΔE_0° for the reaction



occurring in the ideal gas state at absolute zero. The strict definition is therefore D_0° where the superscript refers to products in their ground states and the subscript to the zeroth vibrational level (23). Occasionally $\Delta H_{25^\circ C}^\circ$ of the reaction is used instead (80), but frequently literature values are not clearly stated.

For a dissociation reaction, ΔC_p° is generally positive but small and so $\Delta H_{25}^\circ > D_0^\circ$. The difference rarely exceeds 1 k.cal/mole (for example D_0° (H - H) = 103.24 k.cal/mole and $\Delta H_{298^\circ K}^\circ$ for $H_2 \rightarrow H\cdot + H\cdot$ is 104.18 k.cal/mole) and frequently the accuracy of the $\Delta H_{25^\circ C}^\circ$ value does not justify the correction to absolute zero.

It is of interest to relate the B.D.E. to other molecular properties.

Thus the BDE is equal to the difference between the heats of formation of the fragments and the parent molecule.

$$D(AB-C) = \Delta H_f(AB\cdot) + \Delta H_f(C\cdot) - \Delta H_f(ABC).$$

The heat of reaction is the sum of the B.D.E's of bonds formed minus the sum of B.D.E's of bonds broken. Thus for the reaction $AB + C \rightarrow A + BC$, $\Delta H = D(B-C) - D(A-B)$.

The heat of atomization (Q_a) is equal to the sum of all the dissociation energies involved as the molecule is degraded stepwise into separate atoms.

In a unimolecular decomposition in which two radicals or atoms are formed the activation energy for the process will be very close if not equal to the B.D.E. This assumes that the reverse reaction, the recombination of the two atoms or radicals, has zero or very small activation energy. In the determination of this activation energy it is necessary to inhibit any potential chain reactions involving the products otherwise the value obtained cannot be related to the B.D.E. For most exothermic radical-molecule reactions, the activation energy is also very small.

Finally it should be pointed out that the dissociation energy of a bond depends upon the groups attached to the atoms carrying the broken bond. The C-C single bond dissociation energy in ethane is 84 k.cal/mole but in hexaphanylene it is only 10 k.cal/mole.

The second term is that of the 'bond energy' or 'average bond energy' (E). This is a quantity assigned to each of the bonds in a molecule such that the sum is equal to the heat of atomization of the molecule. For this term to be of value it is necessary to assume the constancy of bond energies from one molecule to another. Thus the bond energy, $C\rightarrow Cl$, in methyl chloride may be estimated from the heat of atomization of CH_3Cl and a knowledge of $E(C-H)$; this latter value would be taken as one quarter of the heat of atomization of methane.

Many discrepancies in such methods have come about as a result of the uncertainty of the latent heat of sublimation of carbon. This is now fairly well established at 170 k.cal/mole(20,21). Such an elementary treatment has obvious failings; nevertheless, with careful use, heats of formation of molecules can be calculated to within a few kilocalories of the observed value from a set of average bond energies (see for example, Pitzer(22)). Some of the difficulties of such schemes have been discussed by Cottrell(23).

More recent refined treatments of bond energy schemes have involved nearest neighbour corrections and the state of hybridization of atoms(24), the use of bond distance/bond energy relations(25), steric corrections(26) and the use of the valency states of the atoms involved -- the aim being to obtain an additivity scheme. Bernstein(25) for instance has developed a scheme allowing the calculation of heats of atomization at 298^oK of almost all hydrocarbons to ± 1 k.cal./mole.

Perhaps one should mention here a third type of bond energy referred to as the coordinate bond energy. This is for the heterolytic breaking of a bond i.e. for the reaction $\text{RY} \longrightarrow \text{R}^+ + \text{Y}^-$.

This is relevant to ionic reactions and may become important in the gas phase as a result of Maccoll's work (see the section on halide decomposition). In solution, where such a term might be of value, solvent interaction interferes with the treatment.

To return to bond dissociation energies, several schemes have been proposed for the calculation of such quantities but these are often either very complex or inaccurate. Recently the publications of Errede(27, 28) give a simple equation determined empirically from published data. The bond dissociation energy for a series of $\text{C}-\text{C}$ or $\text{C}-\text{X}$ bonds is given by $D = 71\epsilon_i\epsilon_j$ for a bond R_i-R_j ; the ϵ value of a group $\text{R} = (\text{A}_1\text{A}_2\text{A}_3)\text{C}-$ is related to the substituents on the carbon atom attached to the bond in question by

$$\epsilon = 0.43 + 0.162(\epsilon_1 + \epsilon_2 + \epsilon_3)$$

This formula holds provided the A_i does not have a centre of unsaturation α to one of the central carbon atoms. The ϵ values of more complex radicals cannot be calculated by the equation but must be found experimentally. Errede points out that the ϵ values listed may be related to Pauling's electronegativity, E , since ϵ is given by \sqrt{E}/r where r is the bond length. The ϵ_i for a group is very nearly equal to $[E_c + \sum \epsilon_i] / 6$ where E_c is Pauling's electronegativity for carbon (=2.5).

The values calculated by Errede's method agree with other literature values to within $\pm 1 - 2$ k.cal./mole in most cases.

The experimental methods of investigation of bond dissociation energies viz. thermal equilibrium, kinetics, electron impact and spectroscopic methods are summarized and discussed in the literature by Cottrell(23), Sehon and Szwarc(29), Szwarc(30), Reed(31), Mortimer(32), Steacie(33), Kondratev(34) and Trotman-Dickenson(35). Electron impact data are available from Field and Franklin(11).

Spectroscopic data of diatomic molecules are discussed in detail by Herzberg(36) and by Gaydon(37). The application of spectroscopy to polyatomic molecules is somewhat limited. The difficulties lie in a knowledge of the precise nature and degree of excitation of the fragments. However data on the simpler polyatomics has been of use in supplementing results from the other methods.

Any factors which influence the heat of formation of the radicals or the parent molecule will be reflected in the relevant bond dissociation energy. Changes in radical resonance energy and the effect of changing ionic character of the relevant bonds were suggested as main contributing factors by Baughan et al.(38). Szwarc(39) has discussed his results on halogenated methyl bromides in terms of the steric repulsions increasing as the atomic size increases. The C—Br bond lengths in the series $\text{CH}_3\text{—Br} \longrightarrow \text{CX}_3\text{—Br}$ are about constant and so the decrease in dissociation energy along the series may be, in part at any rate, attributed to this repulsion.

The resonance stabilization of the radicals formed will increase with increasing number of halogen atoms, with decreasing separation of the p orbitals and with decreasing electronegativity of the halogen atoms.

It has been suggested that the stabilization of a radical R- be measured by the difference $D(\text{CH}_3\text{---H}) - D(\text{R---H})$. Then such radicals as CCl_3^- , for example, would have about 12 K.cal/mole of total stabilization.

Skinner(40) has discussed the calculation of $Q_{\text{F}}(\text{R-})$ and then compares calculated and experimental values of $D(\text{R---X})$.

Ideally, it is desirable that different determinations of dissociation energies should all yield ~~and~~ consistent heats of formation of radicals.

2. Toluene as a radical acceptor.

Toluene, along with many other radical acceptors such as propylene, nitric oxide and cyclohexene, has found numerous applications as a radical scavenger in kinetic studies. It reacts very efficiently with radicals, preventing the development of chains, to produce the relatively stable benzyl radical (PhCH_2^-) and it has been used in the determination of numerous bond strengths, many of these by the toluene carrier technique (30, 35, 41).

Its application is limited to the study of those molecules containing a bond weaker than the $\text{Ph}\cdot\text{CH}_2\text{---H}$ bond in toluene. The

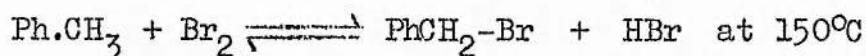
energy of activation for the decomposition of the radical formed must also be greater than that for any reaction involving toluene. At temperatures where toluene decomposes it is desirable that the products of the main decomposition differ from those of toluene decomposition. (This was not the case in the work described in this thesis and was one of the early difficulties which had to be overcome by a change in technique.)

The method has proved useful in halide studies especially bromides where HBr is formed as an end product. Szwarc and Ghosh(42) have demonstrated how to distinguish between radical decomposition and HBr elimination to yield unsaturated compounds. In radical reactions for every RBr decomposing, one each of HBr, RH and dibenzyl are formed whilst dibenzyl does not appear in the elimination reaction.

The bond dissociation energy of toluene, $D(\text{Ph.CH}_2\text{---H})$ has been the subject of much investigation. Several pyrolytic studies of toluene yield varying values. Szwarc's value (43) of 77.5 kcal/mol had tended to become accepted but was criticised by Steacie et al (44) who found dimethyldiphenyls in the products and that variations in contact time, pressure and surface/volume ratio affected the rate constant. More recently Takahasi (45) found similar variations and Price(46) in a thorough analysis obtained a first order rate constant for the decomposition:

$$\log_{10} k(\text{sec}^{-1}) = 14.8 - 85000/2.3 RT \text{ in the range } 640 \text{ to } 870^\circ\text{C}$$

Anderson et al(47) using a thermal and photochemical bromination of toluene obtained 89.5k.cal/mole at room temperature as an upper limit. Benson and Buss(48), who review the various attempts to determine $D(\text{PhCH}_2\text{---H})$, tried to measure K_{eq} for



and obtained a value $D(\text{PhCH}_2\text{---H}) = 84 \text{ k.cal/mole}$.

Schissler and Stevenson(49) using an electron impact method showed that the appearance potentials of C_7H_7^+ from toluene and from dibenzyl led to a value of 77.0 for $D(\text{PhCH}_2\text{---H})$. Trotman-Dickenson et al.(50) warned of the uncertainty of electron impact data because the benzyl positive ion isomerises(51,52) and they obtained values of 83.3 and 84.6 k.cal/mole from pyrolyses of ethyl benzene and n-propylbenzene respectively and preferred the latter value. They also pointed out that Anderson et al.(47) used a value of zero for the activation energy of a benzyl radical attacking a bromine molecule whereas in fact it is more likely to be about 5 k.cal/mole, which would give a value of $D(\text{PhCH}_2\text{---H}) = 85 \text{ k.cal/mole}$. A value of 86.5 can be deduced (50) from the work of Busfield and Ivin(53) although this may carry a large error.

Lossing et al.(54) also criticised the value of Schissler and Stevenson(49) and suggest it is not complementary to Szwarc's value. Takahasi (45) pointed out that a value of 77.5 k.cal/mole is too low because the difference $D(\text{CH}_3\text{---H}) - D(\text{Ph}\cdot\text{CH}_2\text{---H}) = 103 - 77.5 = 25.5$ is too large compared with the extra resonance energy of the benzyl radical calculated at about 14 k.cal/mole (55). On the other hand

Brickstock and Pople(81) calculated the resonance energy of benzyl at 21.9 k.cals/mole and compared it with experimental values of 23.5 k.cals/mole based on the hydrocarbons and 17.0 based on the bromides. Franklin and Lumpkin(82) quoted a value of 18.0 k.cal based on the data of Roberts and Skinner.

Smith (8) in an extensive examination of the decomposition obtained a rate constant given by $\log_{10} k(\text{sec}^{-1}) = 15.1 - 84700/2.3RT$ over the temperature range 750 to 880°C but does not feel justified in assigning this activation energy to the bond dissociation process. Rhind(56) in an examination of the pyrolysis of ethylbenzene using toluene as a radical acceptor was able to assign a value of 84 k.cals/mole to the rate determining step for the breakdown of toluene.

A resumé of several determinations is shown in the table and it will be seen that a value of about 84 k.cals/mole for $D(\text{PhCH}_2\text{---H})$ would appear to be well established.

$D(\text{PhCH}_2\text{---H})$ k.cal./mole.	Temp. range °C	Method used	Reference
77.0	-	Appearance potential	49
77.5	680 - 850	Toluene carrier	43
84.0	150	Equilibrium	48
84.0	476 - 785	Flow & static	56
84.6	603 - 727	$\Delta H_f(B_2^{\bullet})$ from Ph.Et	50
84.7	750 - 880	Flow system	8
85.0	640 - 870	Flow system	46
89.5	{ 82 - 132	Photochemical bromination	47
	{ 166	Thermal bromination	47

In gas phase photoytic studies of toluene and deuterotoluenes at 60°C, Cher(57) concludes that the rate of abstraction by methyl radicals of hydrogen atoms from the ring is 0.17 times the rate of abstraction from the side chain. He suggested that side chain and ring attacks proceeded through geometrically different transition states. Abstraction from the ring resulted in a tolyl radical which reacted with toluene to form a benzyl radical, which in turn reacted with a methyl radical to produce the main product ethylbenzene, while the abstraction from the side chain proceeded via a 3-centre transition complex of the type suggested by Johnston and Parr(58).

Burkley and Rebbert(59), in experiments aimed at determining the rate of H abstraction by methyl from primary, secondary and tertiary positions alpha to the aromatic ring, deduced the E_a values for such reactions. Their experiments involved the gas phase photolysis of acetone-toluene mixtures and they claimed that methyl radical abstraction from the ring was of minor importance.

Berezin et al.(60) have also studied this abstraction reaction at 60→96°C. using tritiated toluene. They showed that, at 85°C, the rate of abstraction of tritium from the side chain is 156 times the rate of abstraction of the para-hydrogen in the ring. They suggested that methyl reacts with π bonds of the ring to form a free radical of the cyclo-hexadiene type which subsequently dissociated to yield a product carrying a tritium atom bound to an allylic position on a tertiary carbon atom. Reaction of the methyl with the

carbon-tritium bond in the methyl group was rapid and accounted for 99% of the total methane.

In the pyrolysis of toluene at 750°C using hydrogen as a carrier gas, Meyer and Burr(61) claimed much simplified kinetics with only methane and benzene as products in approximately equal amounts. To explain their results that ring abstraction is the major effect they had to assume that one primary process was a split of toluene into Ph and CH₃⁻ followed by abstraction from carrier hydrogen or toluene. They concluded that both Ph⁻ and Me⁻ abstracted from the ring and not the sidechain under their conditions. Benson and Buss(48) had pointed out that entropy considerations favour PhCH₃ → Ph⁻+CH₃⁻ over PhCH₃ → PhCH₂⁻ + H⁻ despite the larger activation energy of the former.

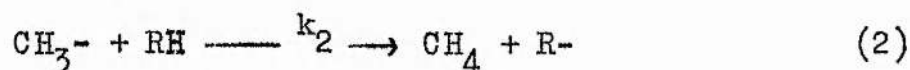
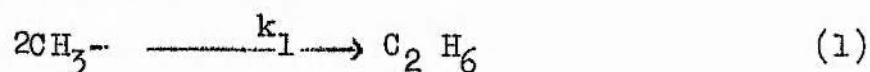
3. Radical reactions.

Reactions of radicals abstracting a hydrogen atom from toluene proceed with activation energies of about 5 to 10 k.cals/mole. The particular reactions relevant to the present work are for methyl radicals and for bromine atoms attacking toluene.

A considerable amount of data is available on methyl radical reactions since they are particularly convenient to study. The products methane and ethane are easily separated and analysed, the radical does not break down or decompose at normal temperatures and is easily prepared with an isotopic label. The best thermal source is ditertiarybutyl-peroxide but its activation energy of 38 k.cals/mole

makes it only of value in the temperature range $100 \rightarrow 200^\circ\text{C}$. Azomethane and acetyl peroxide have also been used as thermal sources. The other main source of methyl radicals is photolysis of compounds which contain a methyl group, for example, acetone, dimethyl mercury, azomethane and similar compounds.

Data are generally based on the rates of the competitive reactions:

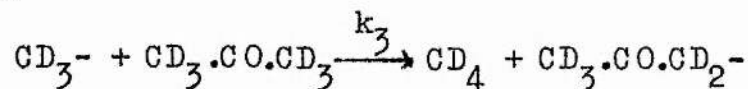


One can deduce $k_2/k_1^{1/2}$ and hence determine $E_2 - \frac{1}{2}E_1$.

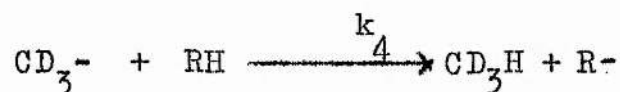
The value of k_1 appears to be well established as a result of work by Gomer and Kistiakowsky(62) using the combination rate of methyl radicals from a rotating sector method of intermittent illumination on acetone and dimethyl mercury. A value for k_1 of $10^{13.6} \exp(-0.700/RT) \text{ mol}^{-1} \text{ cc. sec.}^{-1}$ was deduced which was in agreement with the A factor expected from collision theory, with a probability factor of unity and zero energy barrier. The rate constant was however pressure dependent, falling off with decreasing pressure. This is expected since under conditions of equilibrium the forward and reverse rates of reaction (1) above must both vary to the same extent with pressure and k_{-1} is a unimolecular decomposition which would exhibit such behaviour. Miller and Steacie(83) suggest that a value of 1-2 k.cal/mole for E is possible for the methyl radical recombination process. Some second order processes for methyl attacking various substrates

are quoted by Frost and Pearson(63). A value of P of 10^{-3} to 10^{-4} is required for collision theory interpretation. The activation energies deduced are about 10 k.cals/mole.

Another method of finding k_1 involves the use of acetone- d_6 . The CD_3 radicals form methane by:



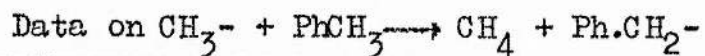
and



It follows that

$$\frac{R_{CD_4}}{R_{CD_3H}} = \frac{k_3 [CD_3\cdot CO\cdot CD_3]}{k_4 [RH]}$$

Experimental conditions are such as to keep $[CD_3\cdot CO\cdot CD_3/RH]$ effectively constant and the rate ratio is determined mass spectrometrically to give the k_3/k_4 ratio. Then values of k_3 and k_4/k_2 may be found by separate experiments whence k_2 is available. Below is a table of some reported data for methyl attacking toluene. The A-factors for the process are of about the expected order of magnitude for a bimolecular reaction.



<u>k. (cc mol⁻¹ sec⁻¹)</u>	<u>E. (k.cal/mole)</u>	<u>Reference</u>
-	12 ± 2	64
-	13.03 ± 0.27 ^a	65
(3.8 ± 0.8) × 10 ⁵ ^b	-	57
(2.3 ± 0.4) × 10 ⁴ ^c	-	57
-	8.3	66
-	5.6	67
-	7.3	68
-	7.4 ± 0.3	59

a Average of toluene attack by several CH₃⁻ sources.

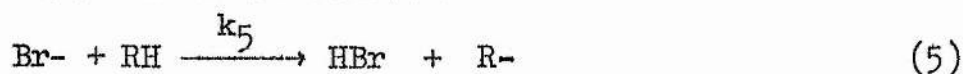
b Side chain abstraction of H-

c Ring abstraction of H-

Some of the features of methyl radical attack on toluene have been discussed in the preceding section. The rate of abstraction of H- from the side chain appears to predominate over ring abstraction in the gas phase (59). Some evidence (69, 70) has been proposed for ring abstraction based on experiments with toluene α-d₃ but these are in solution and probably the ring abstraction occurs after ring addition since methyl radicals are known to add to the ring in the liquid phase (70).

A knowledge of the activation energies of hydrogen abstraction reactions by bromine atoms is of value in the calculation of more accurate bond dissociation energies.

Consideration of the reaction:



suggests that a value of $D(\text{R}-\text{H})$ may be deduced from the relation

$$\begin{aligned} D(\text{R}-\text{H}) &= \Delta H_5 + D(\text{H}-\text{Br}) \\ &= (E_5 - E_{-5}) + D(\text{H} - \text{Br}). \end{aligned}$$

Since the heats of formation of H , $\text{Br}\cdot$ and HBr are well established, we have an accurate knowledge of $D(\text{H} - \text{Br})$, thus allowing the determination of $D(\text{R}-\text{H})$, once E_5 and E_{-5} are known. Trotman-Dickenson et al.(71) list activation energies for the forward reaction in (5) for several hydrocarbons. These values were as expected. The value for E_{-5} however is less well known; Trotman-Dickenson has estimated a value of this quantity, basing his calculations on the Polanyi relation $E_a = \alpha\Delta H + C$, but he points out that the estimated value may be dubious and he emphasized the need for more experimental evidence on alkyl radical reactions with hydrogen bromide. Since the method of study was one of competitive rates, the results of Trotman-Dickenson were related to the rate of bromination of methyl bromide. Their results on the bromination of methane were not sufficiently accurate to allow the methane reaction to be used as a standard of reference.

A brief discussion of the kinetics of bromine atoms attacking hydrocarbons was given by Van Artsdalen et al.(72) who described in detail the bromination of isobutane. The particular case of bromine attacking toluene was quoted by Van Artsdalen et al.(47)

for the photochemical and thermal bromination of toluene. Infra red analyses showed that the reaction yielded mainly benzyl bromide and hydrogen bromide. The photochemical reaction was studied in the range $82 \rightarrow 130^{\circ}\text{C}$ and the thermal reaction at 166°C . An activation energy of 7.2 k.cal/mole was assigned to



The E_a for the reverse of this reaction was estimated at 5 k.cals/mole based on the temperature dependence of HBr inhibition in the photochemical reaction.

Data on the relative efficiencies of Br_2 , argon and CO_2 as third bodies in the bromine atom recombination reaction was given by Givens and Willard(73). The table below gives some relevant data on bromine atom reactions.

Reaction	E (k.cals/mole)	Temp range ($^{\circ}\text{C}$)	Reference
$\text{Br}\cdot + \text{PhCH}_3 \rightarrow \text{HBr} + \text{Ph}\cdot\text{CH}_2\cdot$	7.2 ± 0.6	$80 \rightarrow 130$	47
$\text{HBr} + \text{Ph}\cdot\text{CH}_2\cdot \rightarrow \text{PhCH}_3 + \text{Br}\cdot$	$\gg 5.0 \pm 1.2$	$80 \rightarrow 130$	47
$\text{Br}\cdot + \text{CH}_4 \rightarrow \text{CH}_3\cdot + \text{HBr}$	17.8 ± 0.4	$150 \rightarrow 230$	72, 75
$\text{Br}\cdot + \text{CH}_4 \rightarrow \text{CH}_3\cdot + \text{HBr}$	18.3	100	71
$\text{CH}_3\cdot + \text{HBr} \rightarrow \text{CH}_4 + \text{Br}\cdot$	about 2	$150 \rightarrow 230$	72, 75
$\text{Br}\cdot + \text{CH}_3\text{Br} \rightarrow \text{CH}_2\text{Br}\cdot + \text{HBr}$	15.6 ± 1.0	$150 \rightarrow 230$	75

It should be pointed out that the assignment of 5 k.cals/mole activation energy to the reaction:



by Anderson et al. (47) leads to a high value of 89.5 for the C - H bond dissociation energy in toluene. A value higher than 5 k.cal/mole would bring the bond strength more in line with literature values.

The results of Van Artsdalen and collaborators on bromination rates of hydrocarbons have been suspect because they quote rather high A factors; for example, Benson and Buss (76) suggested that their assumptions of a rapid attainment of steady state concentrations of bromine atoms were invalid for the more reactive of the compounds used. They also suggested that the reactions were partly heterogenous but there was not evidence for this.

Several relations have been proposed to correlate activation energies of processes of the above types. Probably the best known is Hirschfelder's rule (77) for a bimolecular process involving atoms or radicals, which states that, when written in the exothermic direction, the activation energy for the reaction is about 5.5% of the energy of the bond being broken. For the endothermic direction the E_a becomes 5.5% plus the ΔE of the reaction. The value 5.5 was found by semiempirical calculation.

Semenov deduced theoretically an approximate equation for an exothermic abstraction or addition reaction of small radicals or atoms that $E_a = 11.5 - 0.25 q$, where q is the heat evolved in the reaction. The equation is of limited use and appears not to hold for halogen atoms.

Trotman-Dickenson(78) showed that good agreement can be expected between the observed activation energies for hydrogen abstraction by methyl from the lower members of the paraffin series and the E_a deduced from Polanyi's relation, $E_a = 0.49[D(C-H) - 74.3]$

Eyring's relation, $E = \alpha\Delta H + C$, where α and C are constants for a series of reactions, was shown by Butler and Polanyi to hold for sodium atoms reacting with alkyl halides. Szabo(79) quoted a relation $E = \sum_i D_i(\text{broken}) - \alpha \sum_j D_j(\text{formed})$ for homogeneous gas reactions which took into account the strengths of bonds broken and formed where α is again constant for a given type of reaction.

4. Halide pyrolyses with particular reference to bromides

On pyrolysis, monochloro and monobromoalkanes yield halogen acid and an olefin. In the case of the chlorides a radical chain process is absent and the mechanism involves the unimolecular elimination of hydrogen chloride. The bromides can display three reaction mechanisms: (1) a radical chain process, (2) a radical nonchain process and (3) unimolecular elimination of hydrogen bromide. Pyrolysis of the iodides produces iodine, an olefin and the corresponding paraffin -- the mechanisms in these cases are less well established, although it has been shown that unimolecular elimination of hydrogen iodide and iodine catalysed decomposition are both feasible.

Maccoll et al. have been responsible for much of the pyrolytic work on bromides and Szwarc and co-workers have also examined these

compounds using the toluene carrier technique. Benson also has reported on halide pyrolyses; his work appears to be particularly applied to iodides (115). Szabo(41) gives a brief survey of such work (see also (85)). Some relevant data on bromides is tabulated below. Additional references are quoted in those cited.

In most cases vessel conditioning was necessary to obtain reproducible data and to avoid chain decomposition at the walls.

To obtain information on the radical chain present in the pyrolysis of ethyl bromide, photolysis experiments were performed in the temperature range 150-300° and a rate equation $-d[\text{EtBr}]/dt = \text{Const. } I_0^{1/2} [\text{EtBr}]$ was deduced (104). The quantum yield was high and the first order rate constant gave an activation energy of 10.5 k.cals/mole. At low pressures a second order reaction became important. Blades et al.(105), in an isotope effect investigation, demonstrated that the inhibited decomposition of ethyl bromide was primarily a molecular process and that the rate controlling step involved a C-H bond fission.

Kale and Maccoll(106) provided further evidence for a unimolecular decomposition of isopropyl bromide. The pyrolysis was carried out at low pressures (0.5 to 48 mm Hg.) to verify the Lindemann theory. They found their rate constants gave a better fit to the Rice-Ramsperger theory than to the Lindemann-Hinshelwood theory.

The major factor determining the rate of dehydrobromination is the environment of the C-Br bond. Relative rates for this process

<u>Compound</u>	<u>Mechanism</u>	<u>Temp(°C)</u>
C ₂ H ₅ Br	Chain mechanism and uni-molecular decomposition	310 → 476 523 → 633
	Homogeneous 1st order if inhibited	380 → 430
	Unimolecular elimination	467 → 667
n-C ₃ H ₇ Br	1.5 order, homogeneous	300 → 380
	1.5 order	350 → 500
i-C ₃ H ₇ Br	1st order	310 → 350
	Homogeneous	
	Unimolecular elimination	310 → 350
n-C ₄ H ₉ Br	1st order up to 50% dec. if max. inhibition	370 → 420
sec.-C ₄ H ₉ Br	Homogeneous, 1st order	300 → 350
	Unimolec. + 15% chain	
tert-C ₄ H ₉ Br	Homogeneous, 1st order	230 → 280
	Unimolecular elimination	430 → 630
iso-C ₄ H ₉ Br	Homogeneous, 1st order if max. inhibition	360 → 420
tert-C ₅ H ₁₁ Br	Homogeneous, 1st order Unimolecular elimination	220 → 270

+ Units of R are k.cals/mole.

* Units are l^{1/2} mol.^{-1/2} sec.⁻¹

<u>Overall rate constant</u> ⁺	<u>Remarks</u>	<u>Reference</u>
$6 \times 10^{11} \exp(-46.4/RT) \text{sec}^{-1}$	Surface reaction present	86, 87
$8.5 \times 10^{12} \exp(-52.2/RT) \text{sec}^{-1}$	Isotope effect investigation	88
$2.8 \times 10^{13} \exp(-53.9/RT) \text{sec}^{-1}$		89
$8.0 \times 10^{13} \exp(-53.7/RT) \text{sec}^{-1}$	Shock tube method	103
$2.29 \times 10^9 \exp(-33.8/RT) *$	Retarded by propylene	90
$3.8 \times 10^9 \exp(-42.0/RT) \text{sec}^{-1} \text{mm}^{-1/2}$		91
$1.0 \times 10^{13} \exp(-50.7/RT) \text{sec}^{-1}$	Early determination in presence of toluene	92
$4.17 \times 10^{13} \exp(-47.8/RT) \text{sec}^{-1}$	Vessel conditioning necessary	94, 93
$4.0 \times 10^{13} \exp(-47.7/RT) \text{sec}^{-1}$	Toluene carrier	92
$4.2 \times 10^{13} \exp(-47.8/RT) \text{sec}^{-1}$	Shock tube	103
$1.5 \times 10^{13} \exp(-50.9/RT) \text{sec}^{-1}$	Inhibition by olefinic substance	95
$4.27 \times 10^{12} \exp(-43.8/RT) \text{sec}^{-1}$	No inhibition by chain-breakers	96
$1.1 \times 10^{13} \exp(-45.5/RT) \text{sec}^{-1}$		97
$1.51 \times 10^{13} \exp(-46.5/RT) \text{sec}^{-1}$	No chain with cyclohexene	98
$1.0 \times 10^{14} \exp(-42.0/RT) \text{sec}^{-1}$	No inhibition by chainbreakers; 4 centre transition state	99
$3.2 \times 10^{13} \exp(-41.5/RT) \text{sec}^{-1}$	Shock tube method	100
$1.12 \times 10^{13} \exp(-50.4/RT) \text{sec}^{-1}$		101
$3.98 \times 10^{13} \exp(-40.5/RT) \text{sec}^{-1}$	No inhibition or acceleration by cyclohexene etc. Secondary H eliminated	102

and corresponding activation energies (Maccoll and Thomas(107) for a series of compounds are given in the tables below.

C-H	C-Br		
	Primary	Secondary	Tertiary
Primary	1	170	32,000
Secondary	3.5	380	46,000
Tertiary	6.3	-	130,000

Rates are relative to EtBr taken as unity at 380°C

C-H	C-Br		
	Primary	Secondary	Tertiary
Primary	53.9	47.8	42.2
Secondary	50.7	43.8	40.5
Tertiary	50.4	-	39.0

Activation energies for HBr elimination

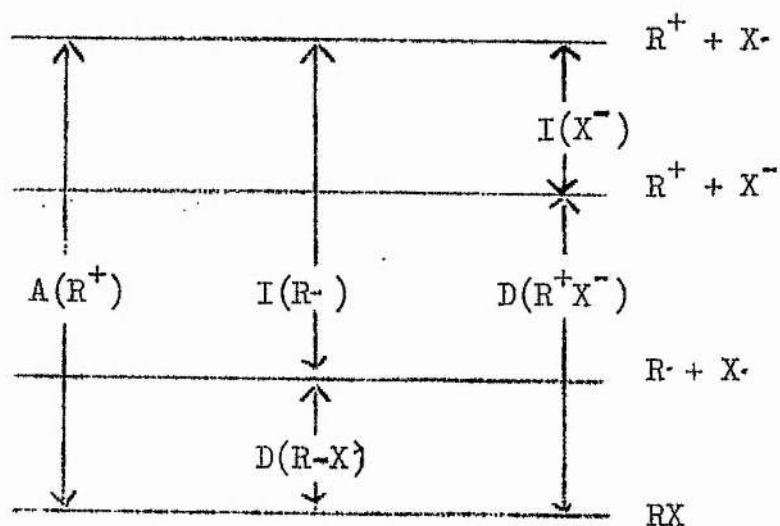
There did not appear to be a simple relation between the activation energy for the elimination reaction and the bond dissociation energy $D(R-Br)$ (See table below).

	<u>EtBr</u>	<u>Sec-C₃H₇Br</u>	<u>Tert BuBr</u>
E_{HBr}	53.9	47.8	42.2
$D(\text{R-Br})$	67.2	67.6	63.8
$D(\text{R}^+\text{Br}^-)$	183.7	156.3	140.3
Rate ratio	1	170	32,000

However, Maccoll and Thomas claimed a clear correlation between the activation energy for HBr elimination and the heterolytic dissociation energy, $D(\text{R}^+\text{Br}^-)$, for the process $\text{RBr} \rightarrow \text{R}^+ + \text{Br}^-$, all species being in the gas phase. The heterolytic bond dissociation energies were calculated from appearance potential, ionization potential and homolytic bond dissociation energy data. Two useful relations which follow from the gas phase ionization energetics diagram below are:

$$(a) \quad D(\text{R}^+\text{X}^-) = A(\text{R}^+) - I(\text{X}^-)$$

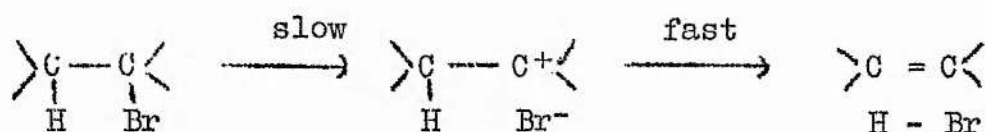
$$(b) \quad D(\text{R}^+\text{X}^-) = I(\text{R}\cdot) + D(\text{R-X}) - I(\text{X}^-)$$



Energetics of gas phase ionization.

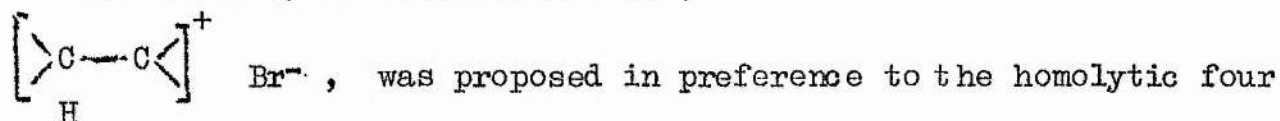
Such calculations led to heats of heterolytic dissociation of around 200 k.cals/mole, greatly in excess of any observed activation energy. Maccoll(85) suggested that a value of about 150 k.cals/mole may be subtracted as the coulombic energy of the ion-pair transition state, thus giving a value similar to the observed activation energies.

The ion-pair transition state was first proposed by Ingold(108), who suggested the sequence



for a unimolecular gas reaction. This is the same as the E1 mechanism in polar solvents except that the ions stay as a pair.

The heterolytic transition state,



centre transition state (109), $\begin{array}{c} >C-C< \\ \vdots \quad \vdots \\ H \quad Br \end{array}$, which would involve the halogen atom, a β -hydrogen atom and the two carbon atoms to which these are bonded.

The β -hydrogen atom was suggested to have a role similar to the polar solvent in the S_N1 and E1 mechanisms in solution reactions — the role of the solvent being to stabilize the polar transition state.

Thus activation consisted of an elongation and polarization of the C-Br bond with some assistance from the polarized C-H bond.

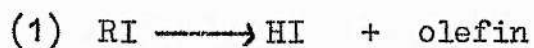
In agreement with Maccoll's correlation between $D(R^+X^-)$ and the hydrogen halide elimination activation energy, Lossing et al.(110) have shown that, for a series of conjugated molecules, a linear relation exists between $D(R^+X^-)$ and the charge, calculated by molecular orbital theory, on the carbon atom formally carrying the positive charge. Maccoll has compared the gas phase elimination rates with S_N1 and $E1$ rates in solution. He demonstrated that these gas phase and solution correlations could be extended to include not only the very simple members but also α -methyl, α -chloro and β -methyl substituted alkyl halides and suggested that the ideas could be extended to other gas phase eliminations. For example, olefin forming elimination from esters bears a resemblance to $E2$ reaction in solution, and hydrogen halide catalysis of the dehydration of alcohols may be the gas phase analogue of acid catalysis in solution.

A condition for a reaction to be 'quasi-heterolytic' is the presence of a polar group. Since such groups differ in their degree of polarity the possibility exists of a gradation in gas phase mechanisms from completely heterolytic to completely homolytic.

Herndon et al.(111), as a result of pyrolytic work on secondary chlorides which differed greatly in their solvolytic reactivity, suggested that the 'quasi-heterolytic' mechanism was not correct in detail but they then pointed out that the discovered parallel reactivities to solvolytic reactions became difficult to explain.

The iodides differ from the bromides in that in the former there

is not a system in which the C-I bond scission is rate determining and very few in which it is important. Organic iodide pyrolyses have been discussed by Benson (112, 113, 114); for alkyl iodides two rate limiting mechanisms are operative:



These are followed by rapid reaction between the alkyl iodide and hydrogen iodide which maintains the latter at a low stationary state. Mechanism (1) describes the pyrolyses of *i*-PrI, EtI, *t*-BuI, CH_3COI , while (2) is the mechanism for *n*-PrI, *i*-BuI, *n*-BuI. *Sec*-BuI and 1:2 diiodoethane involve both (1) and (2).

In *i*-PrI and *n*-PrI, although both pyrolyse to yield C_3H_6 , C_3H_8 and I_2 , they serve to illustrate the two general rate laws:-

$$- d [\text{i-PrI}] / dt = k_1 [\text{i-PrI}] \quad (a)$$

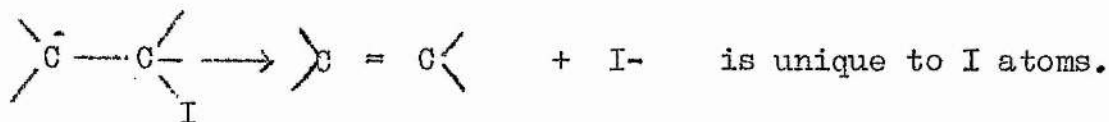
$$- d [\text{n-PrI}] / dt = k_n [\text{nPrI}] [\text{I}_2]^{1/2} \quad (b)$$

It was found that alkyl iodides containing a primary iodine atom followed rate law (b) while those with secondary or tertiary iodine atoms followed rate law (a).

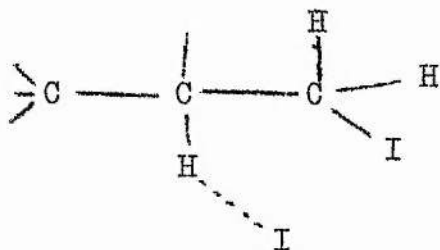
The spontaneous elimination of HI by the iodides is an example of a genuine 4-centre molecular reaction (compare Maccoll's theory.) This elimination is most rapid when the I atom is attached to a secondary or tertiary carbon atom. For primary atom attachment, however, a fast competing step is an I atom catalysed elimination

with an activation energy equal to the endothermicity of the reaction.

Benson (115) suggested that the concerted elimination reaction



That the 4-centre elimination reaction is faster for secondary and tertiary iodides, while the I atom assisted elimination is faster for primary iodides lies in the supposition of a transition state of the type:



With primary iodides, I attacks the relatively weakly bound secondary or tertiary H atom, while for the secondary and tertiary iodides the I attack would be on the more strongly bound primary hydrogen atom. For sec-BuI, attack can occur on a secondary or primary H atom and thus both processes compete.

Holmes and Maccoll (116) have examined the pyrolyses of isopropyl and s-butyl iodides. These authors, like Benson, found the isopropyl iodide decomposition to be a first order process, with an I₂ catalysed decomposition of importance at the lower temperatures. The first order rates for sec-BuI were complicated by the fact that HI was found in amount up to 50% of the I₂ produced. At the lower temperatures an autocatalytic reaction was again important.

The thermal decompositions of monochloro-alkanes occur by the unimolecular elimination of hydrogen chloride. For example, 1-chloropropane shows a homogeneous first order decomposition to propylene and HCl(109). This 'rule', however, should not be extended to multichloroalkanes; 1,1,2-trichloroethane, for example, decomposes at about 400° to yield vinylidene chloride, cis and trans dichloroethylene and HCl; decomposition in the presence of toluene has shown (117) that a radical chain and a unimolecular mechanism operate simultaneously.

Iane et al.(118) have pointed out that in the series CH_3X , $\text{C}_2\text{H}_5\text{X}$, $(\text{CH}_3)_2\text{CHX}$, $(\text{CH}_3)_3\text{CX}$ the dissociation energy decreases regularly if $\text{X} = \text{H}$, but it is approximately constant for the first three members, if $\text{X} = \text{Cl}$ or Br , although lower for the tertiary butyl halides. They have interpreted this constant dissociation energy as a balance between increasing stability of the halides along the series and increasing stabilization of the radicals produced along the series. The low values for $(\text{CH}_3)_3\text{X}$ are readily understood since steric effects will lower the stability of these halides.

The C-F bond in CH_3F is estimated to be about as strong as the C-H bonds in methane. Several bond dissociation energies of fluorocarbons are quoted by Errede(28) and the C-H bond strengths in trifluoromethane, pentafluoroethane and heptafluoropropane have been determined by Pritchard and Thommarson(119). The value of $D(\text{CF}_3\text{-H})$ is quoted as 102 ± 2 k.cal/mole. The C-F bond dissociation energy in methyl fluoride has been measured by electron impact methods by Lossing et al.(124) and by Tsuda, Melton and Hamill(74). The values are quoted on p 35.

5. Previous determinations of $D(\text{CH}_3\text{-Br})$

There have been several determinations both direct and indirect of the bond dissociation energy in methyl bromide and related halides. The value generally accepted for $D(\text{CH}_3\text{-Br})$ is 67.5 k.cal/mole determined by Sehon and Szwarc (39). In a toluene carrier pyrolytic study on halogenated bromomethanes they found their rate constant dependent upon toluene pressure and so analysed their data for these compounds using the Arrhenius expression $k = A \exp.(-E/RT)$, with a fixed value of $2 \times 10^{13} \text{ sec}^{-1}$ for A. This value of A was determined from work on the pyrolysis of methyl bromide taking $D(\text{CH}_3\text{-Br})$ as 67.5 k.cals/mole, this latter value being computed from well established thermochemical data. The value of k used was that corresponding to the lowest temperatures with toluene pressures of about 10mm Hg.

The decomposition of methyl bromide at three different toluene pressures (5, 11 and 20 mm Hg.) gave three parallel straight lines with frequency factors near to 10^{13} sec^{-1} and an activation energy of 67 ± 2 k.cal/mole. They considered the agreement between this and the value calculated from the thermochemical data to be fortuitous. They studied both chloro- and bromo-substituted methyl bromides and they considered that the decompositions started with the unimolecular step $\text{RBr} \longrightarrow \text{R}\cdot + \text{Br}\cdot$. Since both radicals were then removed by fast reactions with excess of toluene, the rate of the unimolecular

process was measured by the rate of formation of HBr. The pyrolyses were reported to be essentially first order homogeneous processes and the rate constants were found to be independent of the contact times. In only CCl_3Br and CBr_4 were the rate constants unaffected by variation of toluene pressure. Since this was the case the temperature independent factor for CCl_3Br decomposition was determined experimentally and was found to be $3 \times 10^{13} \text{ sec}^{-1}$, in good agreement with the methyl bromide case. This close agreement was Szwarc and Schon's justification for a constant frequency factor throughout the series.

The gradation in the series of C-Br bond dissociation energies determined pyrolytically showed good agreement with the values deduced from sodium flame reactions. Evans and Polanyi(129) related the variation of the activation energy for the reaction $\text{R-Br} + \text{Na} \longrightarrow \text{R}^- + \text{Na}^+\text{Br}^-$ in a series of kindred compounds to the variation in bond dissociation energies by the formula $\Delta E = \alpha \Delta D$. The proportionality constant, α , was taken to be 0.27, and by assuming $D(\text{CH}_3\text{-Br})$ to be 67.5 k.cal/mole, and by using Polanyi's sodium atom reaction activation energy results, Schon and Szwarc(39) computed values of $D(\text{C-Br})$ as shown in the table below. (data in k.cals/mole.)

Compound	D(C-Br) computed from Na flame	D(C-Br) from pyrolysis	Other worker*
CH ₃ Br	(67.5)	(67.5)	See later
CH ₂ ClBr	61.2	61.0	
CHCl ₂ Br	54.5	53.5	
CCl ₃ Br	50.8	49.0	51.0. ≤ 52.0 55.5
CH ₂ Br ₂	58.6	62.5	
CHBr ₃	50.1	55.5	
CBr ₄		49.0	≤ 50.0

* Data of various workers quoted by Sehon and Szwarc (39).

The low values, deduced from Na flame data, for the polybromo-methanes were explained by the fact that the Evans-Polanyi treatment did not allow for the additional resonance stabilization of the transition state R---Br---Na for molecules containing more than one identical reactive site, and this effect becomes more important as the number of 'active' halogens increases.

The particular experimental details of the methyl bromide pyrolysis used by Sehon and Szwarc will be given in the discussion. However, it may be noted here that in addition to large differences between the halides in their behaviour to variation of toluene pressure, considerable differences in the degree of heterogeneity were observed. For example, the methyl bromide decomposition was estimated to be 4% heterogeneous in an unpacked furnace at the lower temperature used, but no surface effects at the high temperatures were

observed. CCl_3Br , on the other hand, in an unpacked vessel was 11% and 2.5% heterogeneous at the lower and upper ends of the temperature range, respectively, and carbon tetrabromide showed 32% heterogeneity at 695°K .

Other experimental determinations of $D(\text{CH}_3\text{-Br})$ have involved electron impact methods and calculations from appearance potentials of the appropriate ions. On the whole these show moderately good agreement with the pyrolysis work.

From data on the appearance potentials of the positive ions from methane and the monohalogenated methanes and using a value of 10.1eV for the ionization potential of CH_3^+ (122), Branson and Smith (121) calculated $D(\text{CH}_3\text{-Br}) \leq 3.1\text{eV}$ (=71.4 k.cal./mole). They considered this value to be an upper limit, pointing out that the difference in energy between the C-X bond in the halide and the C-H bond in methane should be reflected in the total dissociation energy. Accordingly the energy of the $\text{CH}_3\text{-Br}$ bond should be 0.9eV less than the bond in methane and it followed that the bond energies in CH_3Br and CH_3I should be 2.9eV (=66.8 k.cals/mole) and 2.3eV (=53.1 k.cals/mole) respectively.

Lossing et al. (124) deduced a value for the appearance potential of the CH_3^+ radical ion of $12.83 \pm 0.06\text{eV}$. compared with the value of $13.2 \pm 0.3\text{eV}$. of Branson and Smith (121). Basing their calculations on an ionization potential of the methyl radical of $9.95 \pm 0.03\text{eV}$., Lossing et al. deduced bond dissociation energies of the methanes as shown in the table below. The more recent data of Tsuda, Melton and

Hamill(74) is shown for comparison.

Bond	Energy in k.cals/mole	
	Lossing et al.	Tsuda et al.
D(CH ₃ -Br)	66.4 ± 2	70.1
D(CH ₃ -I)	50.7 ± 1.5	52.8
D(CH ₃ -Cl)	80.5 ± 3	83.9
D(CH ₃ -F)	107.0 ± 12	104.9
D(CH ₃ -H)	102.8 ± 1.5	103.8

McDowell and Cox(125) give a value of 55.6 for the methyl iodide bond dissociation energy, again based on electron impact data, and a recent kinetic investigation by Goy and Pritchard(130) produced a value of 35.0 k.cal/mole for the activation energy of the reaction $I_2 + CH_3 \rightarrow CH_3I + I$. This, along with an activation energy for the reverse reaction of 19.2 k.cal/mole (131), and a value for D(I-I) of 35.5 k.cal/mole leads to D(CH₃ - I) = 51.3 k.cal/mole. Lossing et al. were unable to suggest a reason for their apparently low value of A(CH₃⁺). They argued for the exclusion of several plausible explanations.

Reed and Sneddon(21) have estimated the dissociation energies of several CH₃-X compounds. They claimed good agreement with previous workers but their value for D(CH₃-Br) of 2.33eV. (= 54 k.cal/mol.) is low. Their methyl iodide value (2.30eV.) is more in agreement with published data, but their methane bond dissociation energy

$D(\text{CH}_3\text{-H}) = 4.12\text{eV}$. is lower than that presently accepted. Other values are given in the table below, which may be compared with data discussed above.

<u>Bond</u>	<u>Dissociation Energy</u>	
	<u>eV</u>	<u>k.cals/mol.</u>
$D(\text{CH}_3\text{-H})$	4.12	95.0
$D(\text{CH}_3\text{-Cl})$	3.4	78.4
$D(\text{CH}_3\text{-Br})$	2.33	53.7
$D(\text{CH}_3\text{-I})$	2.3	53.1
$D(\text{Cl}_2\text{CH-H})$	3.46	79.7
$D(\text{ClCH}_2\text{-Cl})$	3.19	73.5
$D(\text{Cl}_2\text{CH-Cl})$	2.89	66.6
$D(\text{BrCH}_2\text{-Br})$	2.59	59.8
$D(\text{Br}_2\text{CH-Br})$	2.67	61.6

A thermochemical determination (126) of the heats of formation of mercury dialkyls in a bomb calorimeter and use of thermochemical data (127, 128) allowed the calculation of the heats of formation of the alkyl halides. These are tabulated below along with the calculated bond dissociation energies (a C-H bond dissociation energy in the hydrocarbon was assumed). An uncertainty of ± 2 k.cals/mole is quoted.

Halide	ΔH_f° (in k.cal/mole)	C-X bond diss. En.
$\text{CH}_3\text{Br}(g)$	- 8.6	67.8 k.cals/mole
$\text{C}_2\text{H}_5\text{Br}(l)$	-22.1	66.5 " "
$\text{CH}_3\text{I}(l)$	- 2.3	53.4 " "
$\text{C}_2\text{H}_5\text{I}(l)$	-10.13	52.6 " "

A table giving the various values for the bond dissociation energy in methyl bromide is given below.

$D(\text{CH}_3\text{-Br})$ k.cals/mole	Method	Reference
≤ 71.5	Electron impact	121
70.1	Electron impact	74
67.8	Thermochemical	126
67.4	Thermochemical	40
(67.0)	Pyrolysis	39
66.4	Electron impact	124
53.7	Electron impact	21

A value of about 67.0 k.cals/mole would seem the most appropriate.

Flow System.

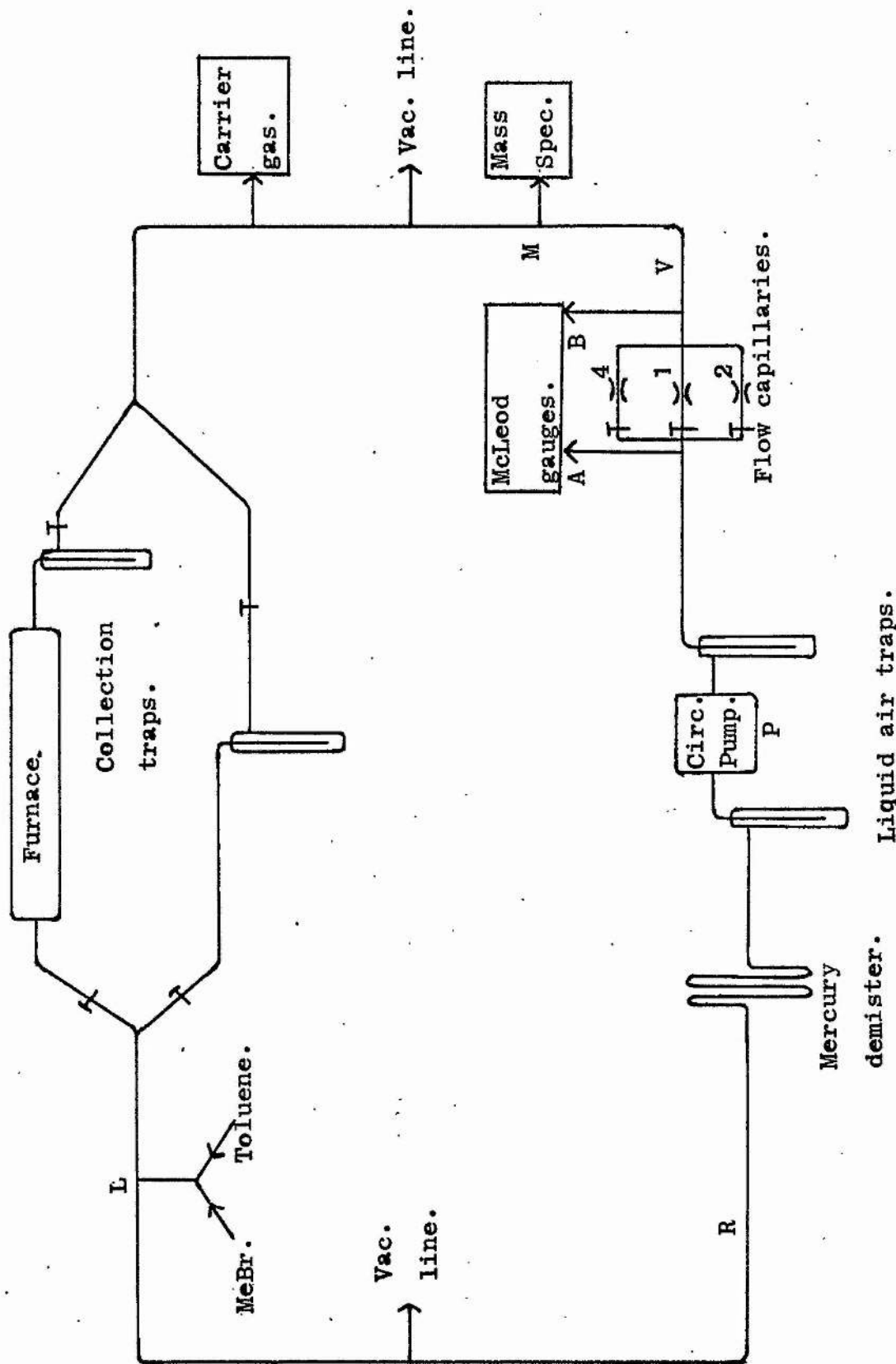


FIG. 1.

APPARATUS AND EXPERIMENTAL PROCEDURE.1. Description of the apparatus.

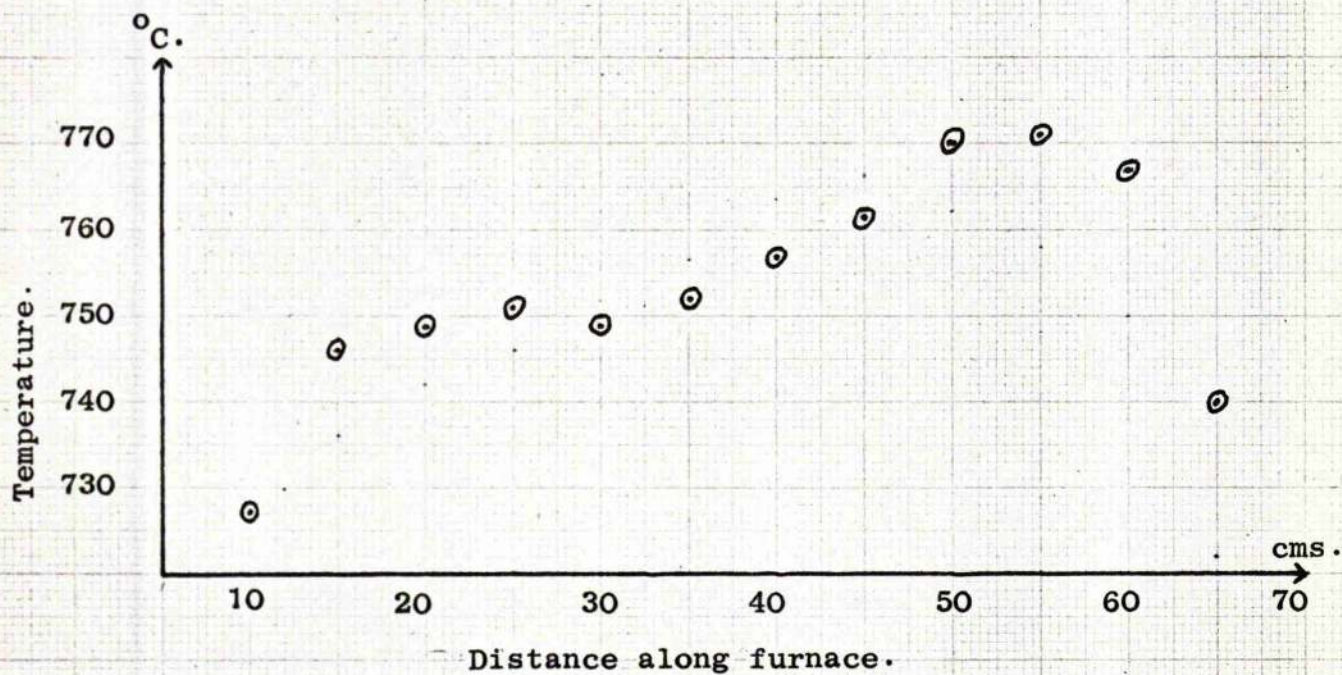
This was a conventional type of flow system in which the flow of gas could be adjusted to give contact times in the reaction zone of from about 0.5 sec. up to about 5 secs. It is shown diagrammatically in fig. 1 and was capable of evacuation to 10^{-5} mm Hg. pressure. The reactants were injected continually, at point L, into about 1 mm of argon carrier gas. Circulation was by a mercury diffusion pump, P, which had a liquid air trap on the low pressure side and, on the high pressure side a liquid air trap followed by a mercury demister to prevent the diffusion of any mercury to other parts of the system.

Variation in contact time was obtained by circulation of the gases via a restriction to flow constituted by one, or a combination of three, flow capillaries. After suitable calibration, which is described later, observations of the McLeod gauge readings on either side of these flow capillaries enabled the flow rates in moles/second to be calculated and hence the contact times deduced (see appendix 1).

Large bulbs were placed at V (fig. 1) making the flow system volume over 20 litres. This was to prevent an observable drop in pressure in the system due to bleeding through the metrosil sampling leak of the mass spectrometer.

FURNACE TEMPERATURE PROFILE.

(a) Early smoothing at about 760°C.



(b) After smoothing at 709°C.

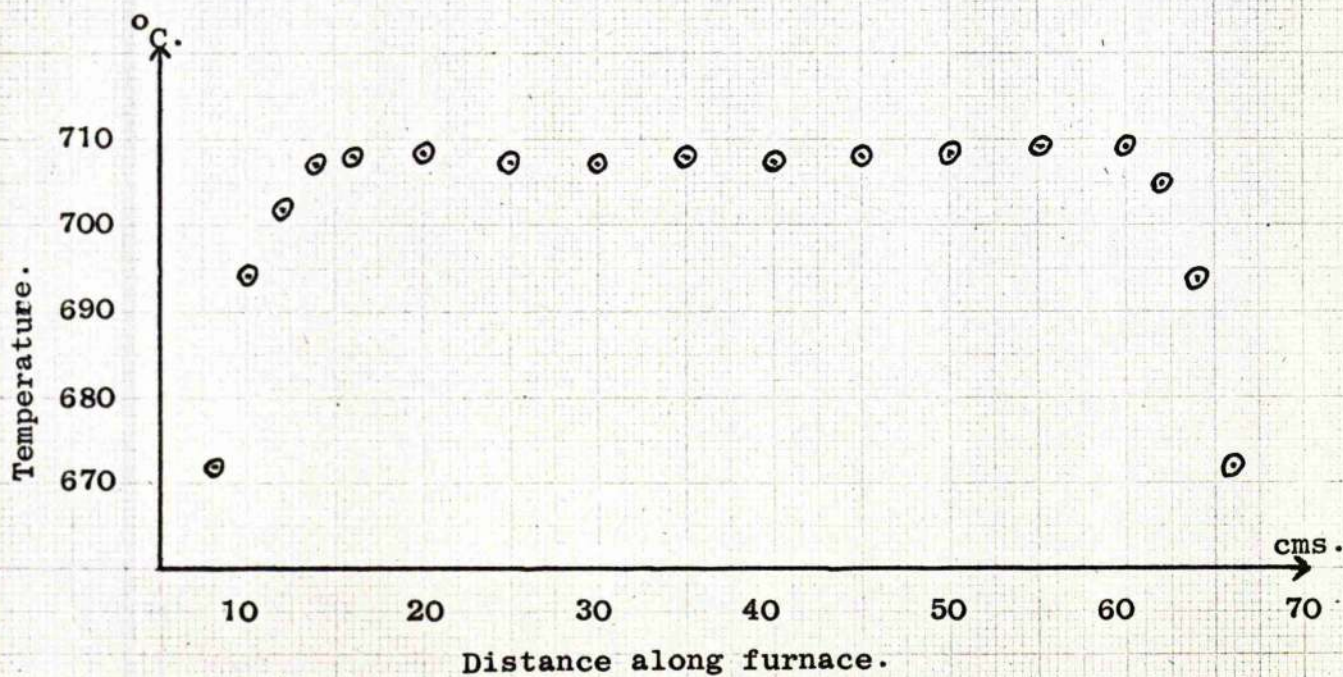


FIG. 2.

An analysis of products of decomposition was available, after suitable calibration, by this sampling of the gases at point M.

The furnace was of 1.25 in. diameter silica tube of heated volume 280 ml. and could be heated to above 800°C. Its detailed construction is described by Barraclough (1).

Temperature profiles along the furnace were drawn and the parallel resistors adjusted to smooth this profile to ± 2 C° at 720°C (see fig. 2).

The furnace volume was measured by removing the furnace and measuring the volume of water required to fill it between the limits of the flat portion of the temperature profile.

Temperature control was obtained by use of a Sunvic type RT2 temperature controller which gave temperature variations of not more than ± 0.5 C° at 800°C. The furnace temperature was measured by a chromel-alumel thermocouple. This had been previously calibrated by Barraclough (1) against the melting points of pure tin, lead and zinc.

2. Injection of reactants.

The reactants were injected together at point L (fig. 1) into the flow system. The injection, from a reservoir, was via a suitable fine capillary and a neoprene diaphragm valve (see fig. 4). The toluene injection rate was controlled by a water bath surrounding the reservoir. The methyl bromide injection valve was similar,

REACTANT INJECTION.

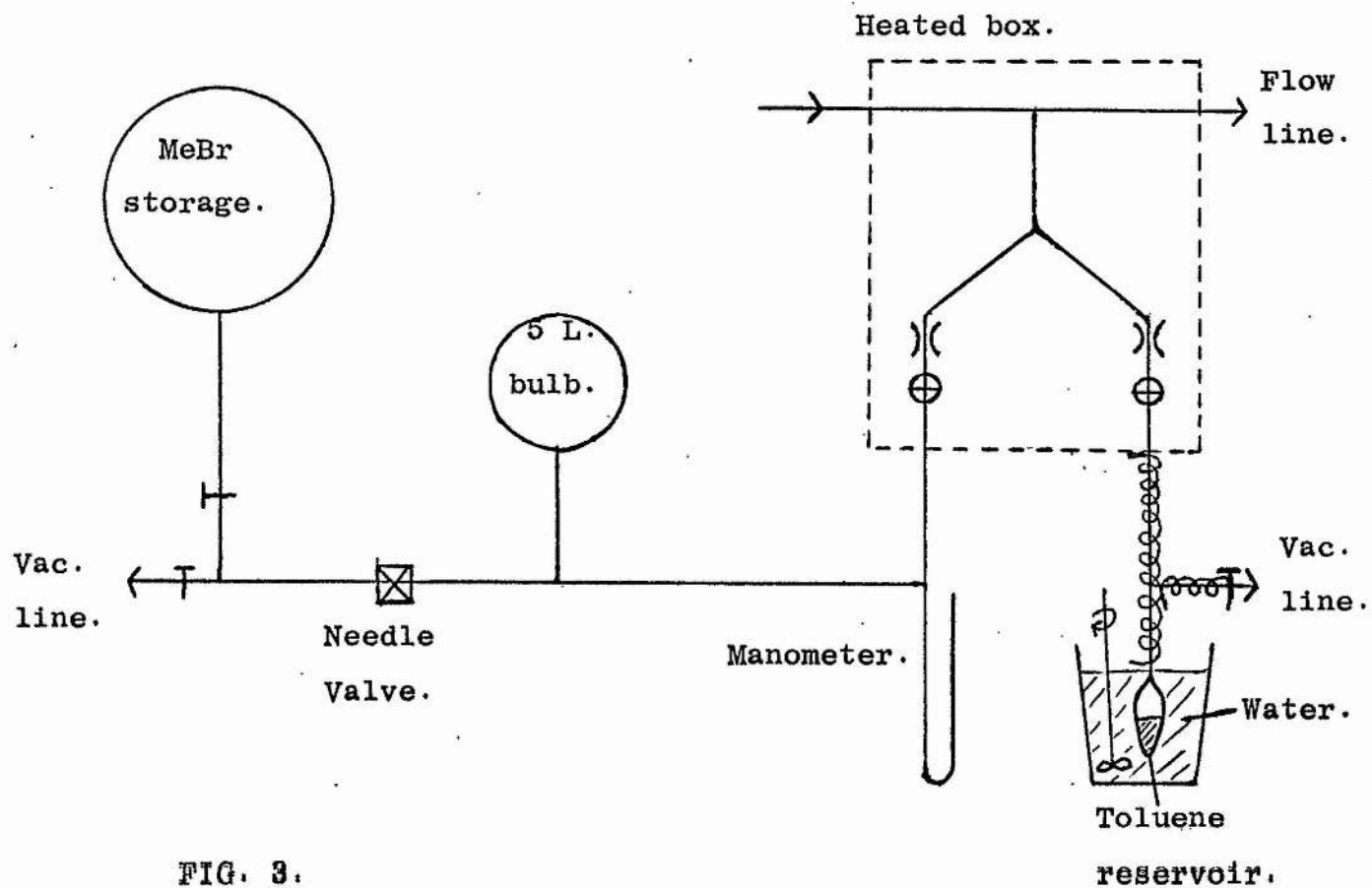


FIG. 3.

DIAPHRAGM VALVE..

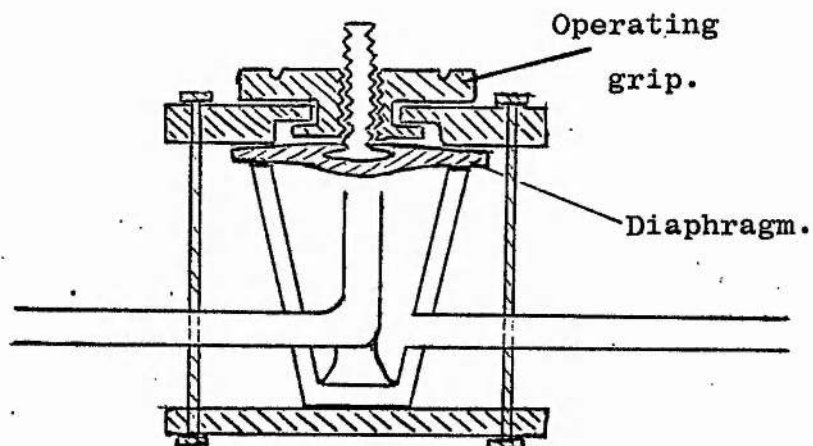


FIG.4.

FLOW SYSTEM GAS CALIBRATION.

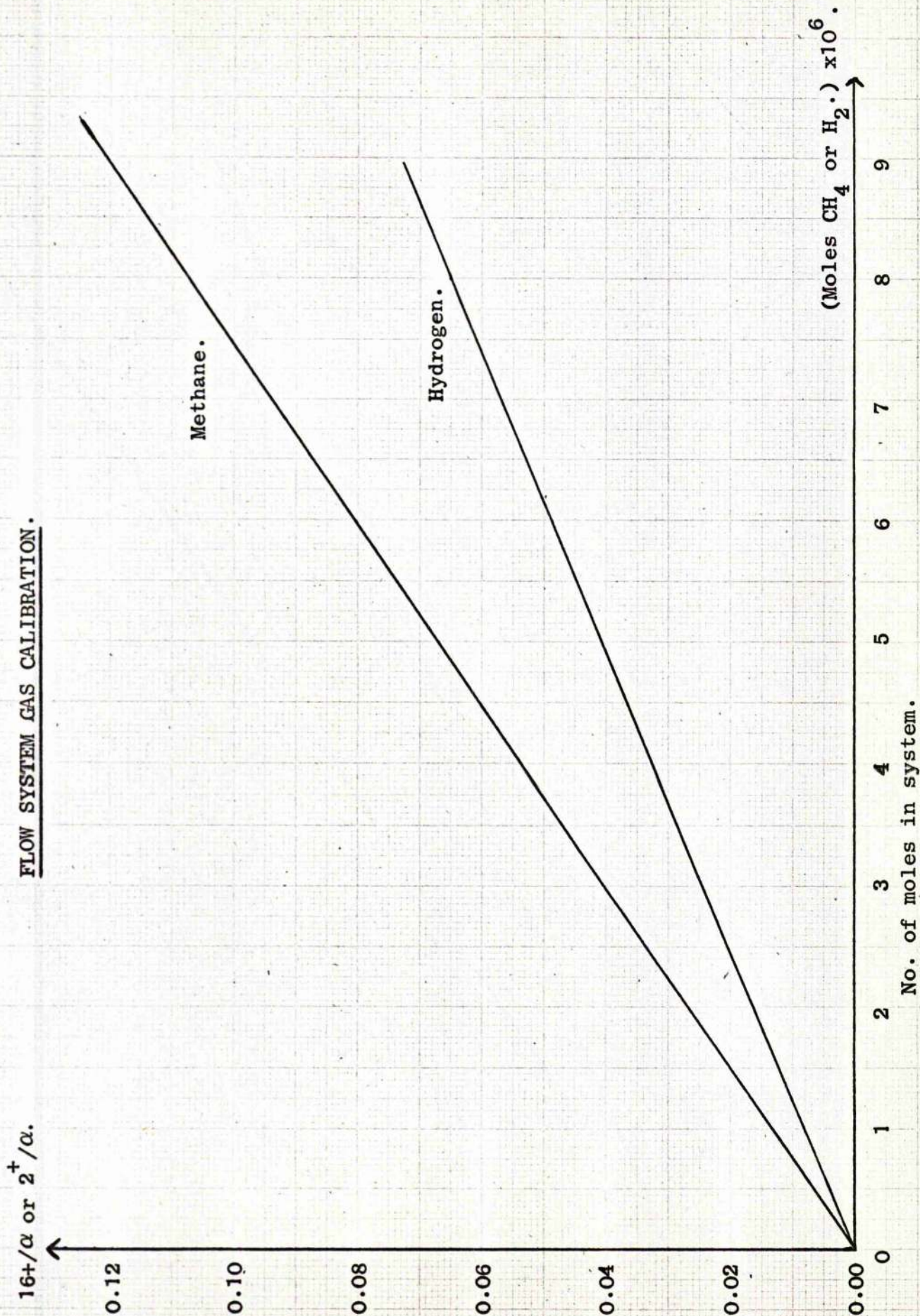


FIG. 5.

control being obtained by a needle valve between the reservoir and injection capillary (see fig. 3).

The argon was stored in three 5 litre bulbs and reproducible quantities could be admitted to the flow system by means of a manostat.

For mass spectrometer calibrations, admission of methane and hydrogen to the flow system could be gained from a gas burette. For such calibrations calculable amounts of hydrogen or methane could be admitted to the flow system into a known pressure of argon. The whole was allowed to circulate for some time, until a homogeneous gas mixture was obtained, before readings were taken. The gas burette was emptied by means of a Toepler pump injecting straight into the flow system. The pressures on the flow McLeods gave the argon pressure since the dilution of methane or hydrogen was high. Such a calibration is shown in figure 5, the readings being based on a measured argon sensitivity as is usual. The flow system argon was used as the reference. Reading of any subsequently measured peak heights was always done with an immediate reference to the argon sensitivity since this could vary from day to day and during the day.

3. Purification of reactants.

Methyl Bromide supplied by B.D.H. in 100 ml. ampoules was distilled twice from -80°C to a liquid air trap (-180°C). It was

stored in a blackened 5 litre bulb attached to the needle valve of the injection system. Its purity was checked on the mass spectrometer.

Toluene. It is known that purification of toluene by shaking with sulphuric acid, distillation and crystallisation still leads to irreproducible gas kinetic data (Szwarc (2)).

Partial pyrolysis twice at 850°C followed by fractional distillation from sodium yields toluene which gives reliable kinetic data. Toluene purified in this way was used - the details are described fully by Barraclough (1).

Argon. The carrier gas obtained from a cylinder was purified by slow passage through a -80°C trap to remove water and then through two successive sodium traps heated to 300°C to remove traces of oxygen. A mass spectrum of the purified argon was taken to check the final purity.

Hydrogen Bromide was prepared by dropping concentrated aqueous hydrobromic acid onto P_2O_5 , drawing the resulting vapour through a trap at -20°C to remove water and then collecting the HBr in a liquid air cooled trap. The HBr was distilled from a -80°C bath to a -180°C bath on the vacuum system and stored in a blackened bulb.

Methane. A sample of pure methane was available from N.C.L., Teddington. This was stored adjacent to a gas burette for injection into the flow system as required.

TOLUENE INJECTION CALIBRATION.

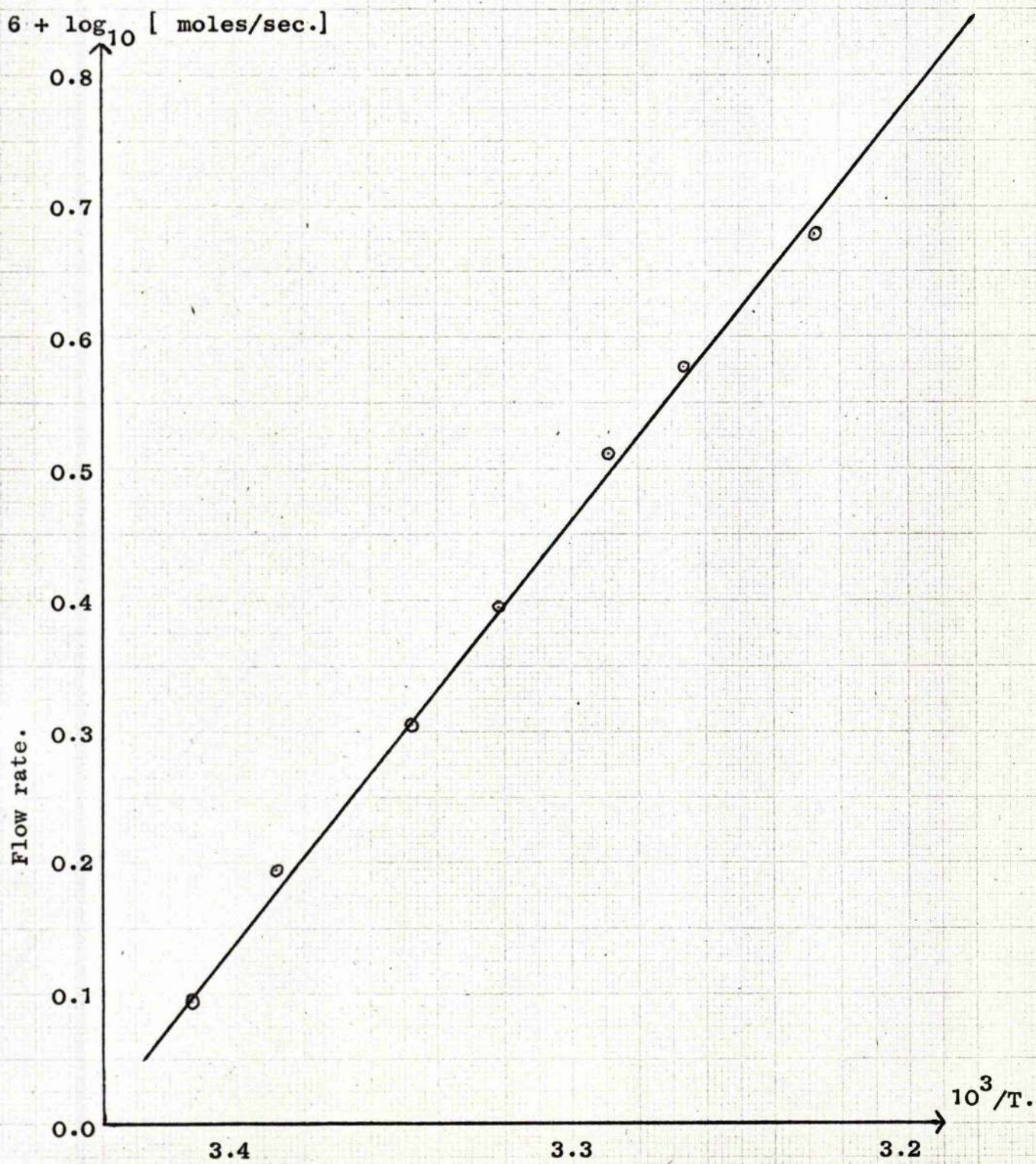


FIG. 6.

Reciprocal temperature.

Hydrogen was purified by passing it over platinised asbestos at 200°C to remove oxygen and subsequent water was removed by a liquid air trap.

Fresh samples of all reactants were always used for experiments.

4. Reactant injection calibration.

Toluene injection. The calibration was carried out as follows. A thermostatically controlled water bath which was thoroughly stirred acted as a constant temperature bath for injection. The bath was used in the temperature range from 15°C to 35°C and temperatures were measured to within $\pm 0.1^{\circ}\text{C}$. The line carrying the toluene vapour from the level of the water bath surface to the injection point was heated to about 100°C to ensure that the water bath controlled the injection rate. With about 1 mm argon in the flow system, toluene was injected for a recorded time through the cold furnace and collected in liquid air cooled traps situated after the furnace. The flow system was then evacuated and the toluene distilled over into previously weighed collection vessels. After reweighing, the injection rate in moles per second could be calculated.

A graph could then be drawn of bath temperature against moles per second of toluene injected. Under the conditions of injection the vapour pressure of toluene is between about

METHYL BROMIDE INJECTION CALIBRATION.

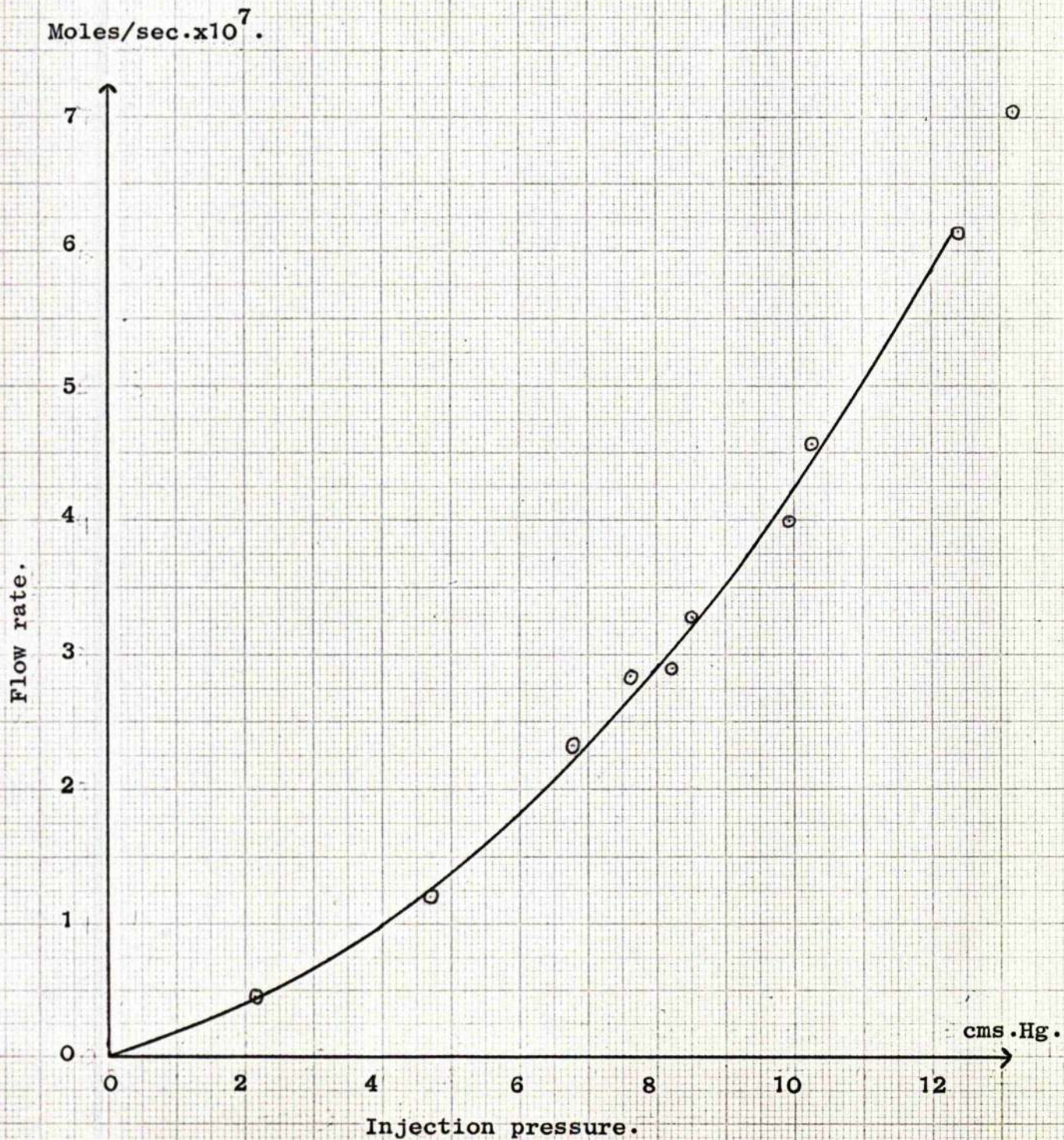


FIG. 7.

15 mm and 45 mm Hg.; the rate of flow through a capillary is proportional to the difference of the squares of the pressures on either side, and, since the pressure in the flow system is small compared with the vapour pressure of toluene, the injection rate will be determined by the toluene vapour pressure in the reservoir. Reference to the Clausius-Clapeyron equation, $\log p = -L/RT + \text{constant}$, would thus suggest that a plot of \log (moles/second) against the reciprocal of the bath temperature would be a straight line. This is the case and the toluene injection calibration is shown in figure 6.

Methyl Bromide injection. Storage was in a 5 litre bulb and up to 1 atmosphere pressure since the substance is gaseous at room temperature. Injection was via a stainless steel needle valve. A mercury manometer gave an indication of the injection pressure which was variable from 0 to 30 cms Hg. A backing volume of 5 litres before the capillary buffered any small fluctuations in pressure through the needle valve. As in the case of toluene, the methyl bromide was passed for a given time and collected in liquid air traps. Since methyl bromide boils at $+4^{\circ}\text{C}$ at normal pressure it was, after evacuation of the system, distilled over and dissolved in a weighed quantity of ethanol in which it is very soluble. Reweighing allowed a graph of moles per second injected against injection pressure to be drawn (see fig. 7).

FLOW CAPILLARY CALIBRATION.

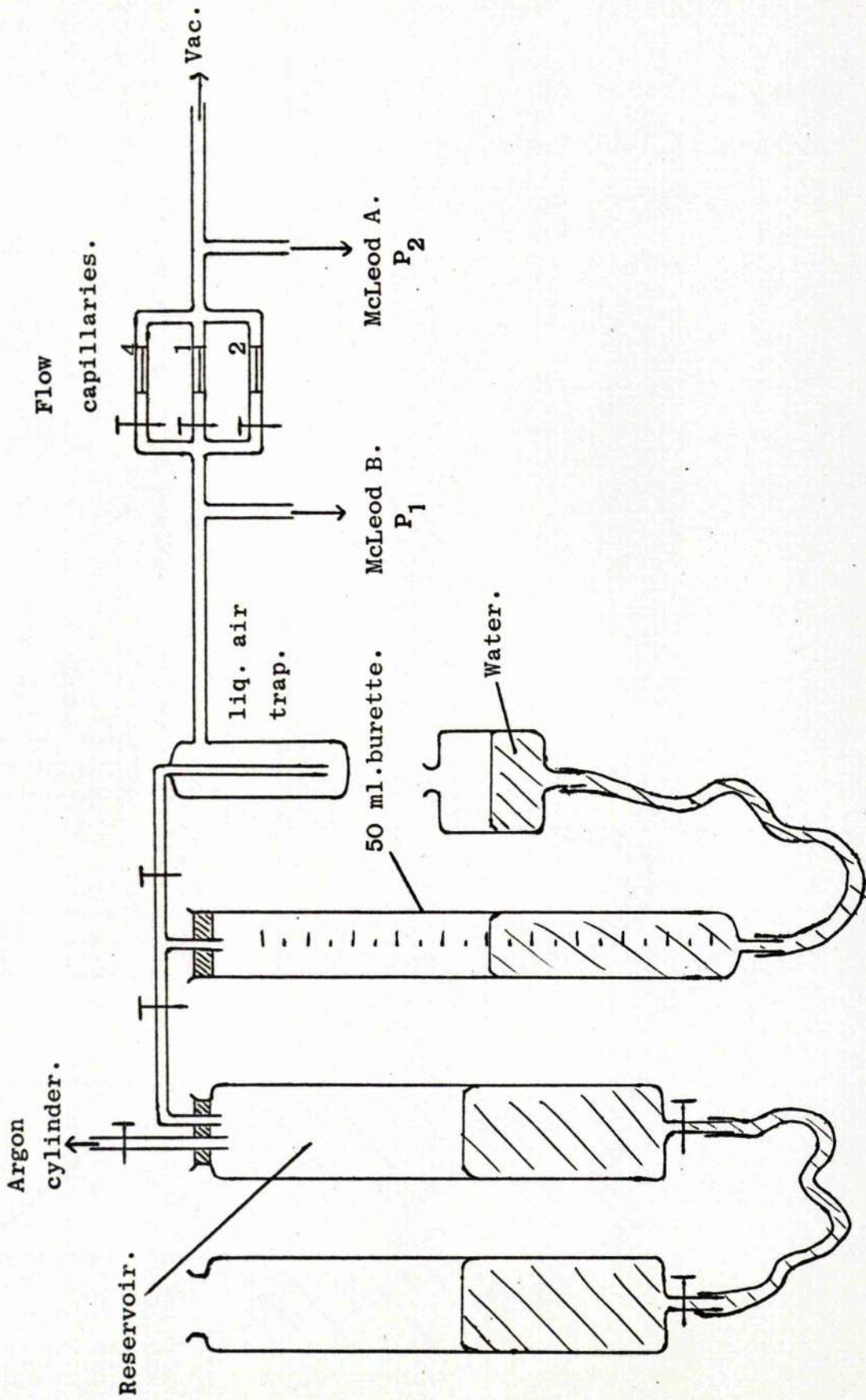


FIG. 8.

5. Calibration of flow capillaries.

Although Barraclough (1) had calibrated the flow capillaries for his work, it was thought desirable to recalibrate them in the pressure range to be used in this research since he had used somewhat higher pressures.

The section of the flow system containing the capillaries was isolated and argon was passed through it in the same direction as under experimental conditions and the flow pressures measured by means of the McLeod gauges. The apparatus is shown in figure 8. Delivery of argon was from a 50 ml. burette. The liquid air trap removed any water present in the argon and the flow rate was adjustable by tap T. The time taken (t secs.) to pass X ml. of argon gas at a known temperature and pressure through a particular capillary with pressures P_1 and P_2 (in mm Hg.) across the capillary then enables the flow rate to be calculated.

$$\text{Argon flow rate} = \frac{X \times 273 \times P}{22400 \times T \times 760 \times t} \quad \text{moles/sec.}$$

where P = pressure of argon in burette

= atmospheric pressure - w.v.p. at $T^\circ\text{K}$,

T = room temperature in $^\circ\text{K}$.

Water vapour pressure data was taken from standard tables (3).

By Meyer's modification of Poiseuille's formula, the rate of flow through a capillary is given by:

Moles/sec. $\times 10^6$.

FLOW CAPILLARY CALIBRATION.

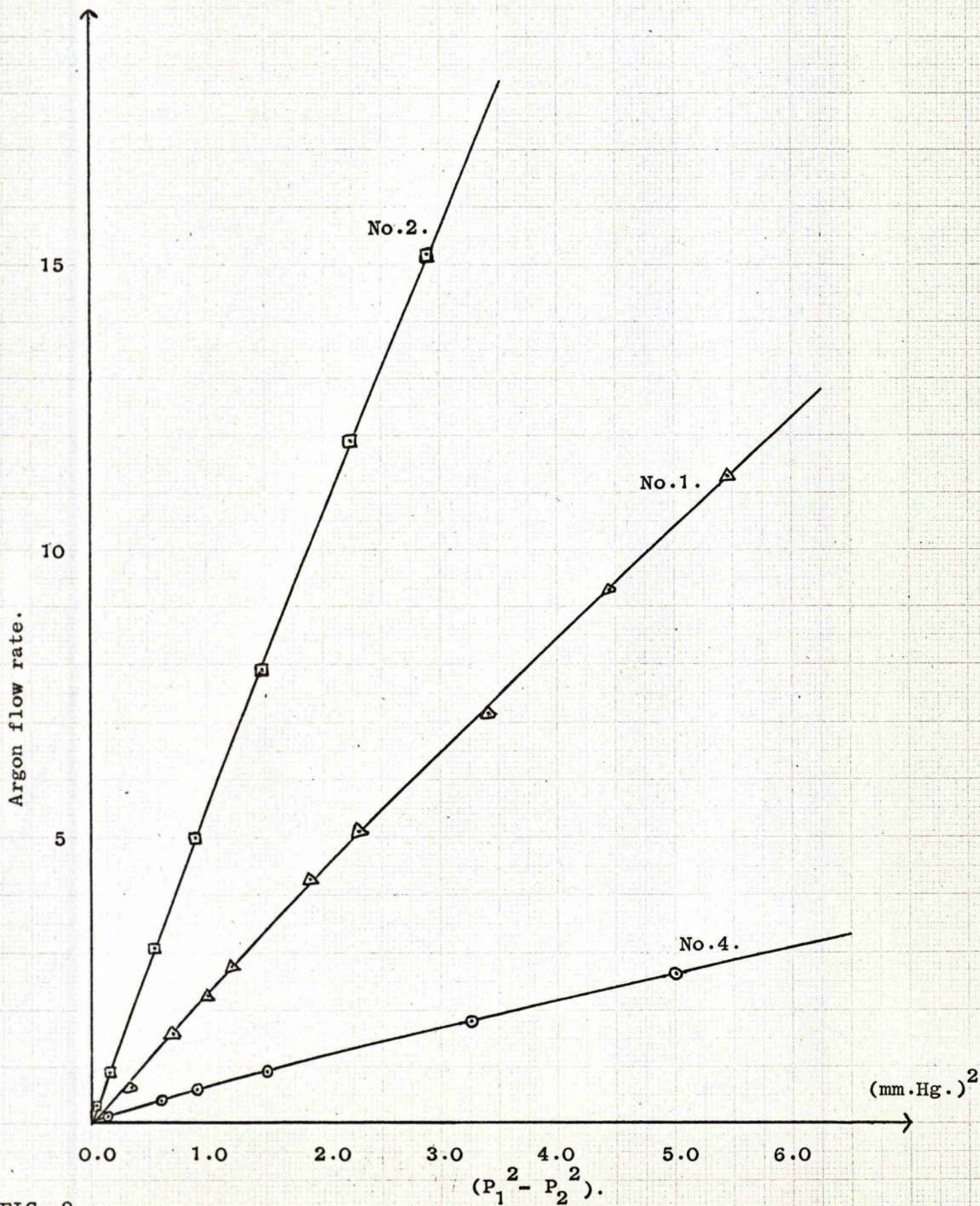


FIG. 9.

CIRCULATION PUMP FLOW RATE.

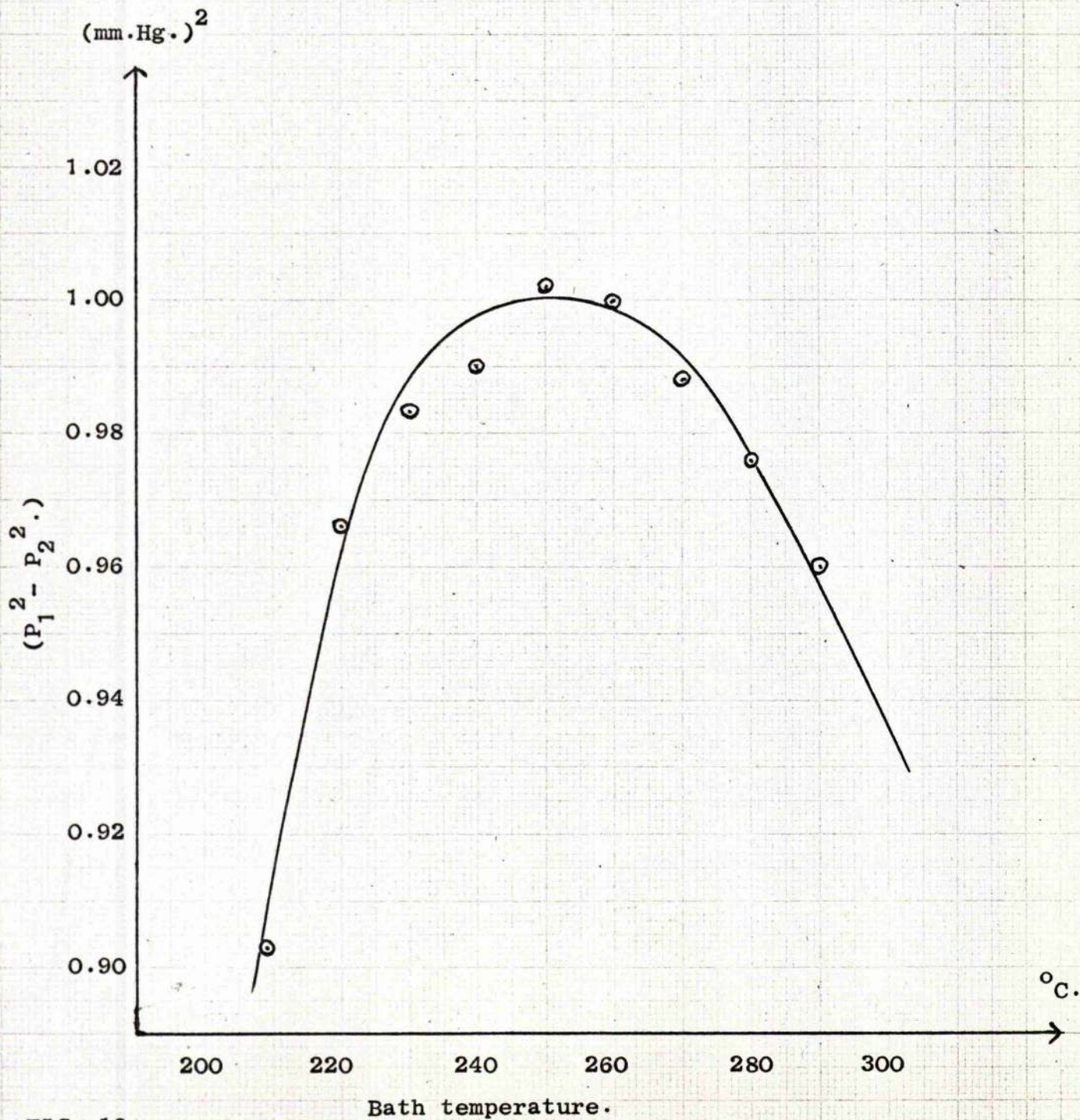


FIG. 10.

CIRCULATION PUMP EFFICIENCY.

Capillary 1.
Capillary 4.
Capillary 2.

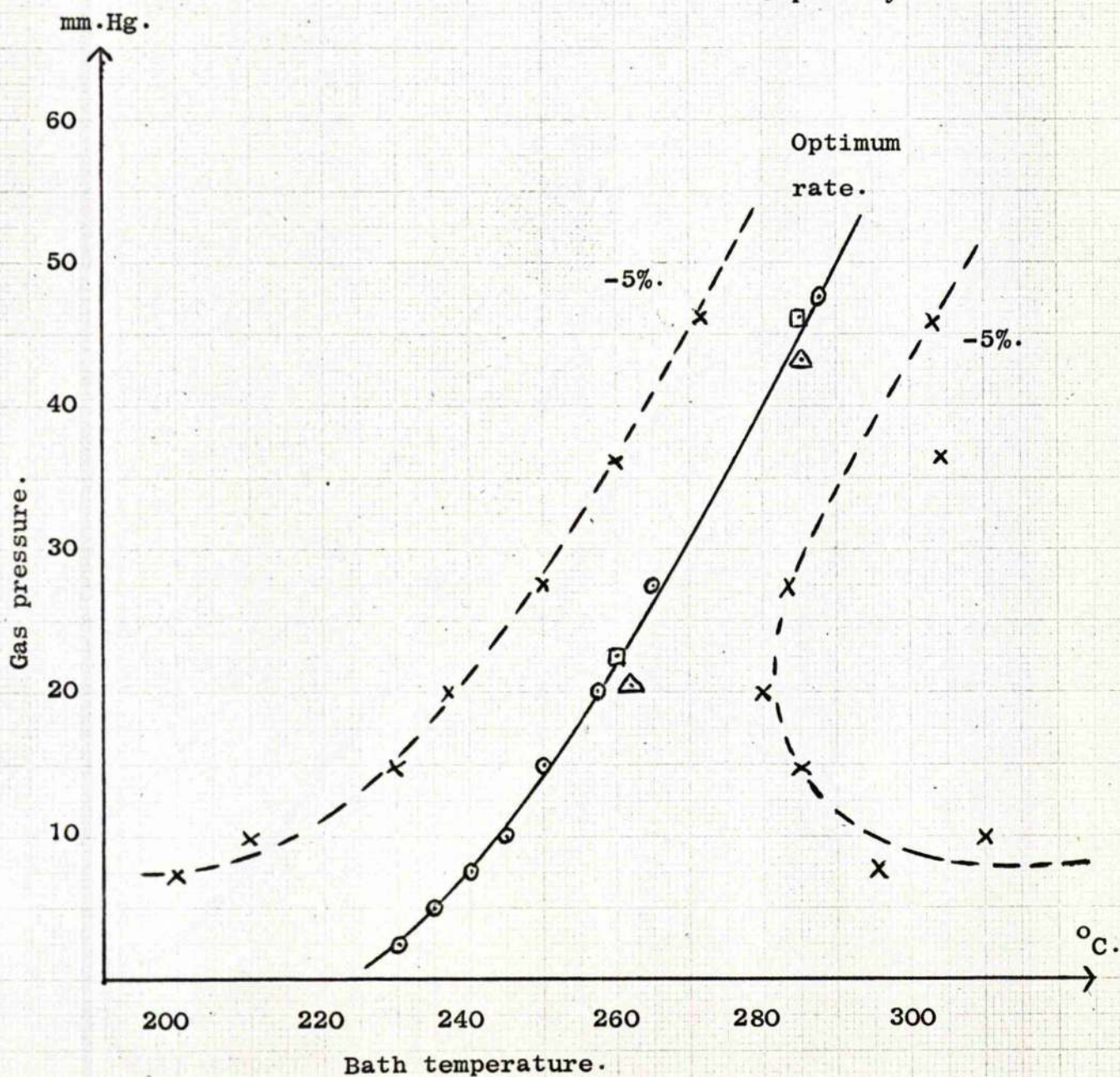


FIG. 11.

$$\text{Flow rate} = \frac{\pi r^4}{16\eta LRT} [P_1^2 - P_2^2] = k [P_1^2 - P_2^2]$$

where k will be constant for a given capillary. Other letters have their usual significance.

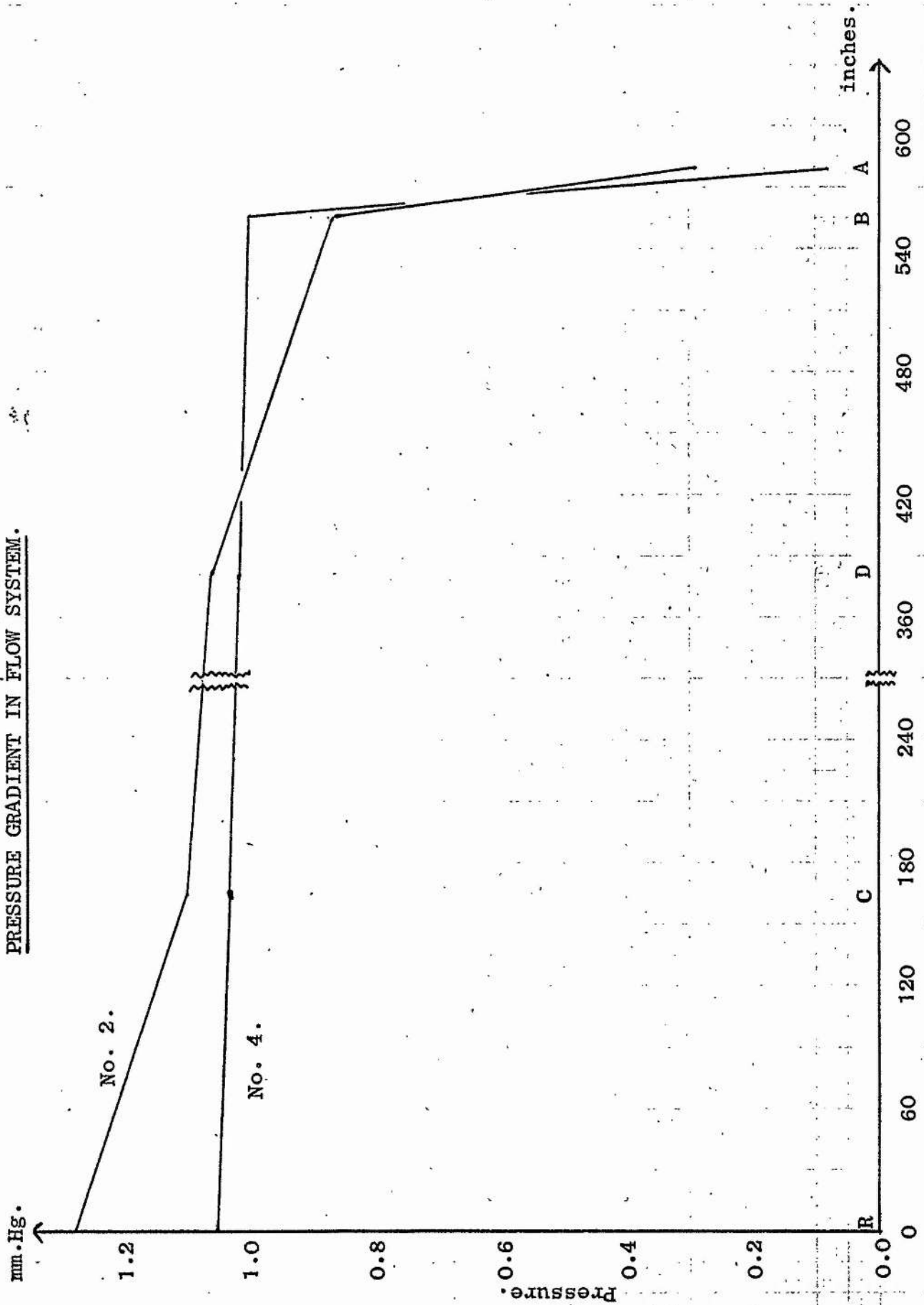
Then a plot of $(P_1^2 - P_2^2) = \Delta P^2$ against the flow rate as calculated above will serve as a capillary calibration. The results of these experiments are shown in figure 9.

When more than one capillary is used the total flow rate is the sum of the flow rates for each capillary.

6. Circulation Pump Flow Rate.

The mercury diffusion pump for circulation of the gas through the flow system was heated by a molten metal bath at 200 - 300°C. The efficiency of such a pump varies with both the bath temperature and the pressure in the system (4). A typical variation is shown in figure 10. By plotting such graphs at different pressures of argon it is possible to construct figure 11 which shows the variation in metal bath temperature allowable before the rate of the flow falls by 5%. It was found that changing the flow capillaries had little or no effect on the maximum flow rate temperature. Under experimental conditions the maximum flow rate was always used as only under these conditions is the flow rate stable.

PRESSURE GRADIENT IN FLOW SYSTEM.



Distance along flow line.

FIG. 12a.

PRESSURE GRADIENT IN FLOW SYSTEM.

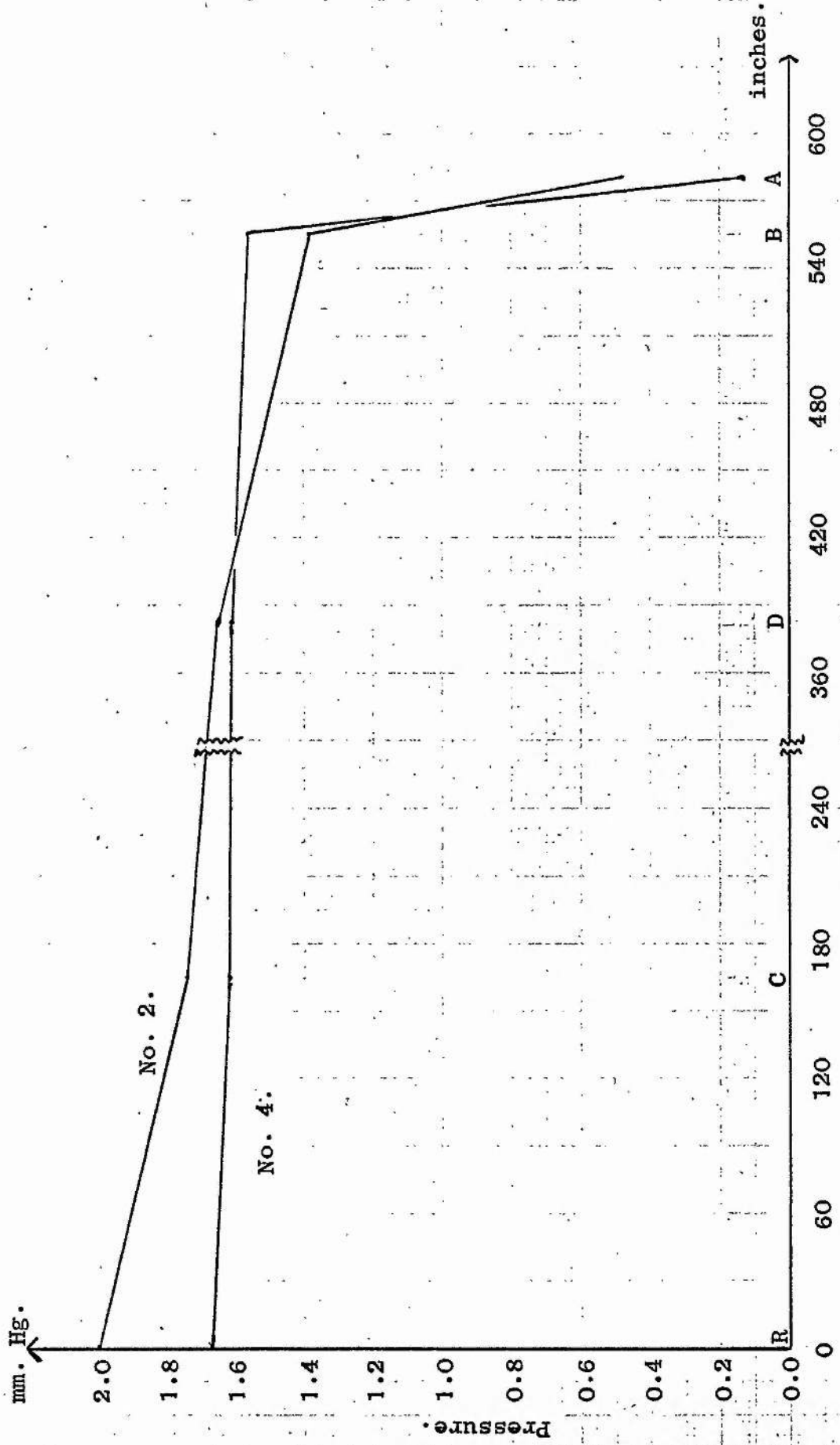


FIG. 12b. Distance along flow line.

7. Pressure gradient in the flow system.

The flow rate was determined as described above and, since it was intended to use for subsequent calculations the high pressure reading of the flow capillaries as a measure of the pressure within the furnace, a determination of the pressure gradient within the flow system was desirable. McLeod gauge attachments were therefore made at points C and D (fig. 21) and at points R, A and B (fig. 1). Readings on the furnace and bypass lines were also obtained.

The data for about 1 mm (and 2 mm) total pressure is shown in graphical form in figures 12a and 12b. To avoid confusion on the diagram only the data for flow capillaries 2 and 4 are shown.

The McLeod reading points are marked along the abscissa.

The results indicated that a constant percentage increase for each capillary applied to the high pressure side reading of the flow capillary would give the pressure within the furnace. The percentage increase was independent of the total pressure within the limits used. The average values used in calculations were as follows:-

<u>Flow Capillary</u>	<u>% Increase Required</u>
No. 1	14.0
No. 2	25.0
No. 4	3.0
Nos. 1 + 2 + 4	32.0

MASS SPECTROMETER ELECTRICAL REQUIREMENTS.

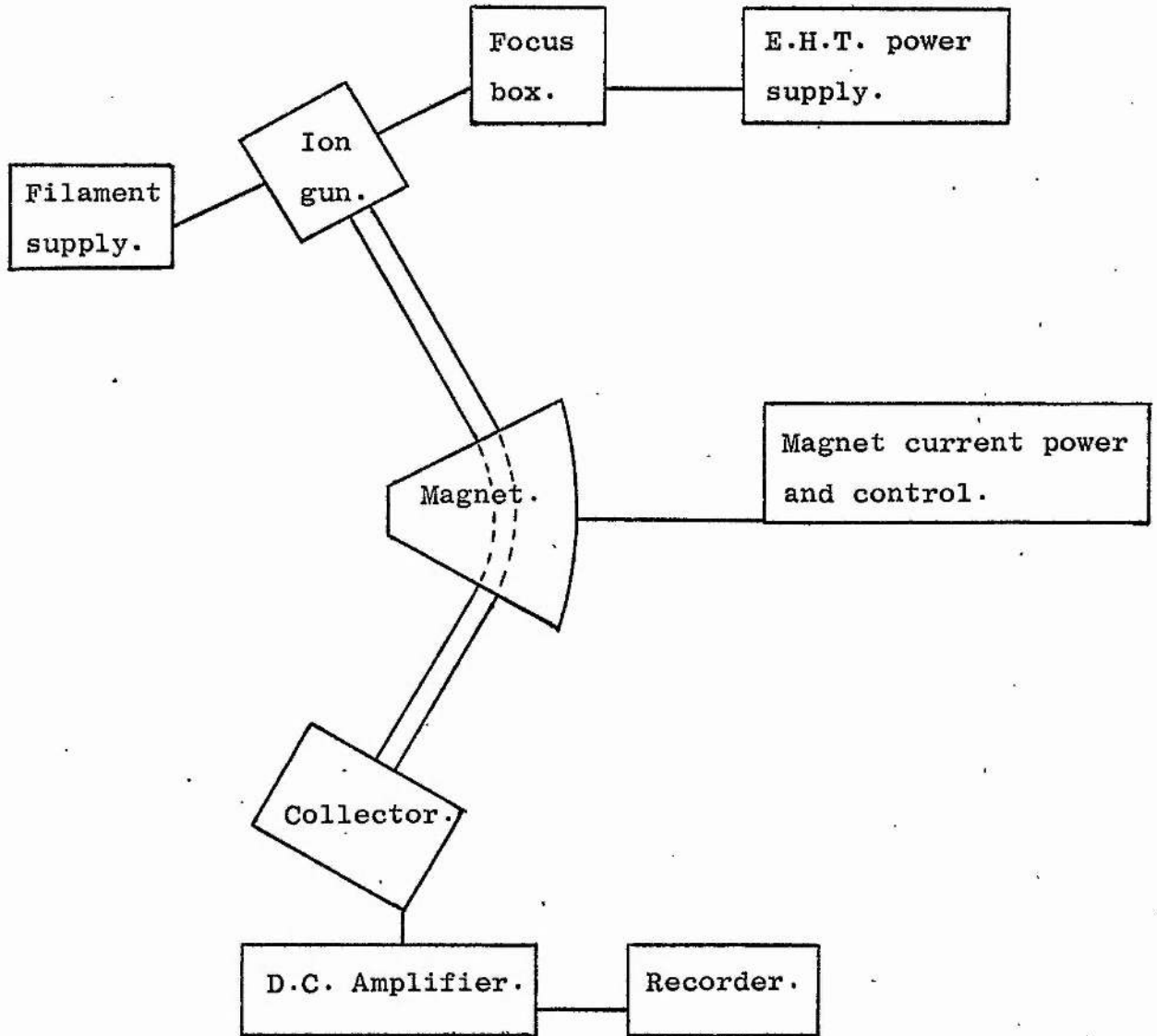


FIG. 13.

The results also showed that the pressure gradient within the furnace was small; this is a desirable feature for accuracy of calculations.

Experiments performed with the furnace hot showed the same pressure distribution, identical plots being obtained for the furnace cold and at a typical working temperature.

In later experiments where a lined furnace was used for heterogeneity tests the same pressure distribution was experimentally observed.

8. The Mass Spectrometer.

The instrument, a conventional 60° Nier (5) design, was constructed in this department. Full details are given by Davidson (6). The electronic power supplies however had aged and become unstable and were reconstructed, care being taken in the redesign to ensure maximum stability and reliability. A box diagram of the electrical requirements of a mass spectrometer is shown in figure 13.

The E.H.T. power supply to the ion gun and the magnet current power supply were basically of the same design as previously. The emphasis in reconstruction was on the under-running of component parts and the incorporation of a large number of readily accessible test points on the side of the unit. After

construction, when the unit was functioning correctly, notes were taken of the potentials of all important reference points on the circuit, particularly constant voltage lines and grid-cathode potentials on the valves. Where possible the circuit parameters had been arranged such that the valves were operating near to the middle of the straight line part of the valve characteristic.

The focus box was a voltage divider to supply various potentials to the ion gun plates. The magnet current control was either manual or automatic. The previous automatic control had been by an electric motor driving a 10 turn potentiometer at varying speeds and in varying ranges. The new circuit was an entirely electronic Miller Sweep circuit with various scanning speeds as required. The magnet current was variable from about 6 mA up to about 150 mA, the latter corresponding to mass/charge ratios of about 250 for the normally used accelerating potential of 1840 volts.

A new power supply was constructed to feed the control valve heater in the Miller Sweep circuit, three valve heaters in the D.C. amplifier and the DBM 8A electrometer valve heater. These five valve heaters were fed in series from this highly stabilized power supply which also fed one or two reference potentials to the amplifier and magnet feed circuits. The D.C. amplifier (7) was a 100% negative feedback type with amplification stages incorporating the electrometer and two 12 SC 7 valves. The circuit, when correctly adjusted

(which was a delicate operation), gave an output which was linear up to about 15 volts and it could be used on one of three high value input resistors of 2×10^{11} , 3×10^{10} or 5×10^9 ohms. The amplifier fed the collector signal to a 1 second Honeywell-Brown Elektronik recorder via an automatic range change device which was tripped by microswitches fitted to the recorder.

For the major part of the research however the D.C. amplifier was replaced by an Ekco vibrating reed Electrometer type N616B. This unit with its associated decade voltage unit N659A was ideally suited to observing a backed off output signal from the mass spectrometer (this was a later requirement of the research and is described under run procedure). The electrometer consists of a head unit which is sealed and desiccated and contains three input resistors of 10^8 , 10^{10} and 10^{12} ohms selectable by push button. This unit also contains a vibrating reed type dynamic capacitor operating at a frequency of about 450 c.p.s. The resultant A.C. signal is amplified and rectified and displayed on a meter on the indicator unit and fed to the recorder.

The electrometer has, in its most sensitive condition, a full scale reading for a current of 3.0×10^{-15} amp. When properly mounted (and considerable care is necessary) the stability observed on the instrument was 0.03 mV. variation on the 10^{10} ohm input resistor with the input switch at "ion chamber fast" operation position.

OUTLINE OF TRAP CURRENT STABILISED FILAMENT SUPPLY.

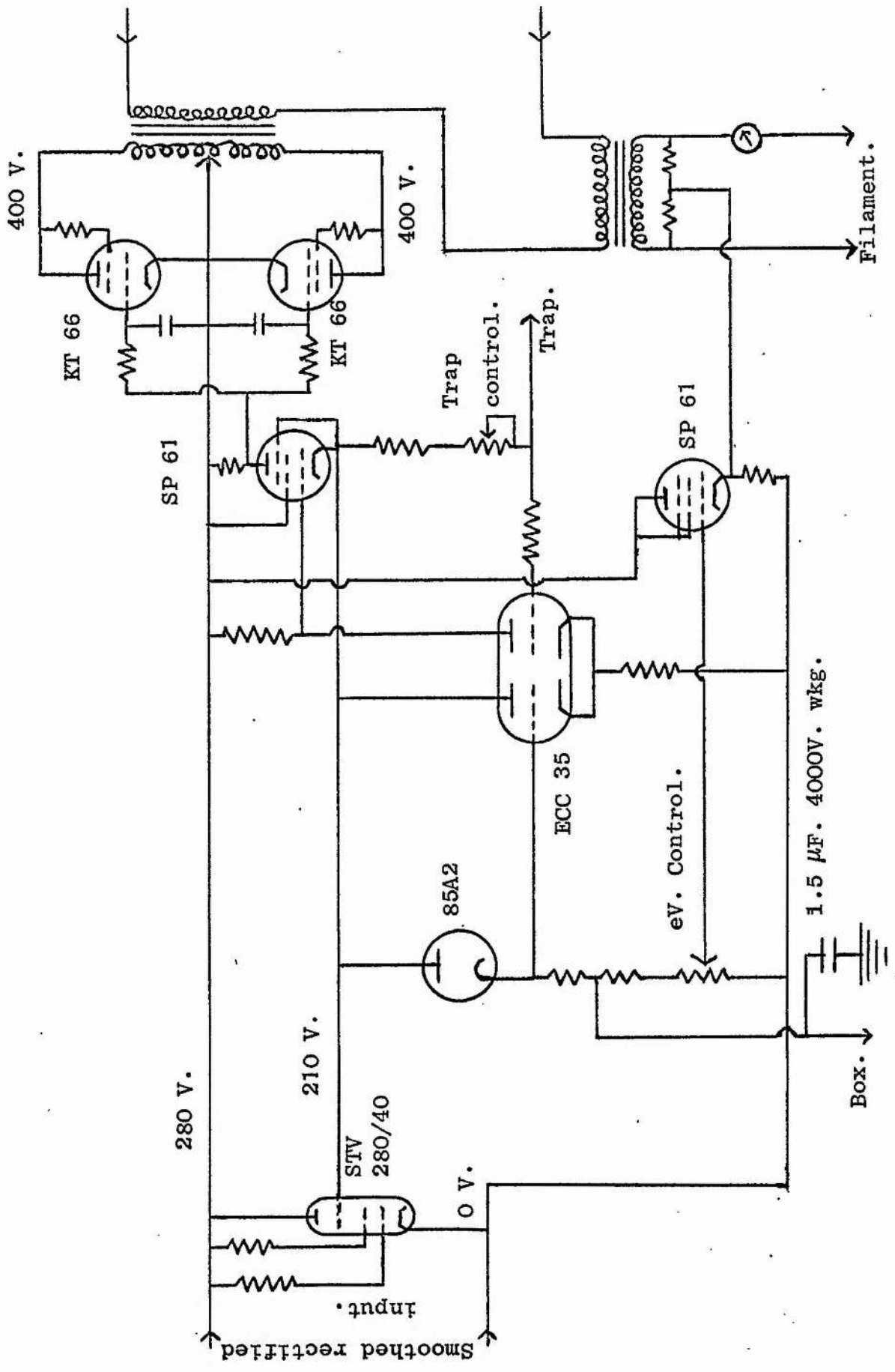


FIG. 14.

The head unit in the present set-up was fixed rigidly to the bottom of the mass spectrometer tube with no possibility of flexing between the collection system and the unit. Greater stability was available on the "voltage" position but at the expense of response time. The instrument was found to be most useful on the 10^{10} ohm resistor for this experimental arrangement.

The filament supply was a conventional circuit operating the filament on A.C. at about 6 volts and 5 amps and was stabilized on the total electron emission current from the filament. The circuit was floating at about 2000 volts fed from the E.H.T. supply via the box.

The early experiments described in the following sections were performed with the circuits as described above but without the Ekco electrometer. For the later and major part of the research however where it was necessary to back off a peak and record small changes in this peak height, considerable improvements were first of all necessary.

Backed off peaks at first showed marked instability and quite pronounced drift with time. This was suspected to be electrical trouble and one early observation was a correlation of the fluctuations with trap current (the ionizing electron beam current) instabilities.

A new circuit, based on trap current stabilization, was constructed to eliminate the problem. The essential details are shown in the circuit diagram in figure 14. The whole circuit again floats at about 2000 volts, fed in from the box line which is raised

E.H.T. VARIATION CONTROLS.

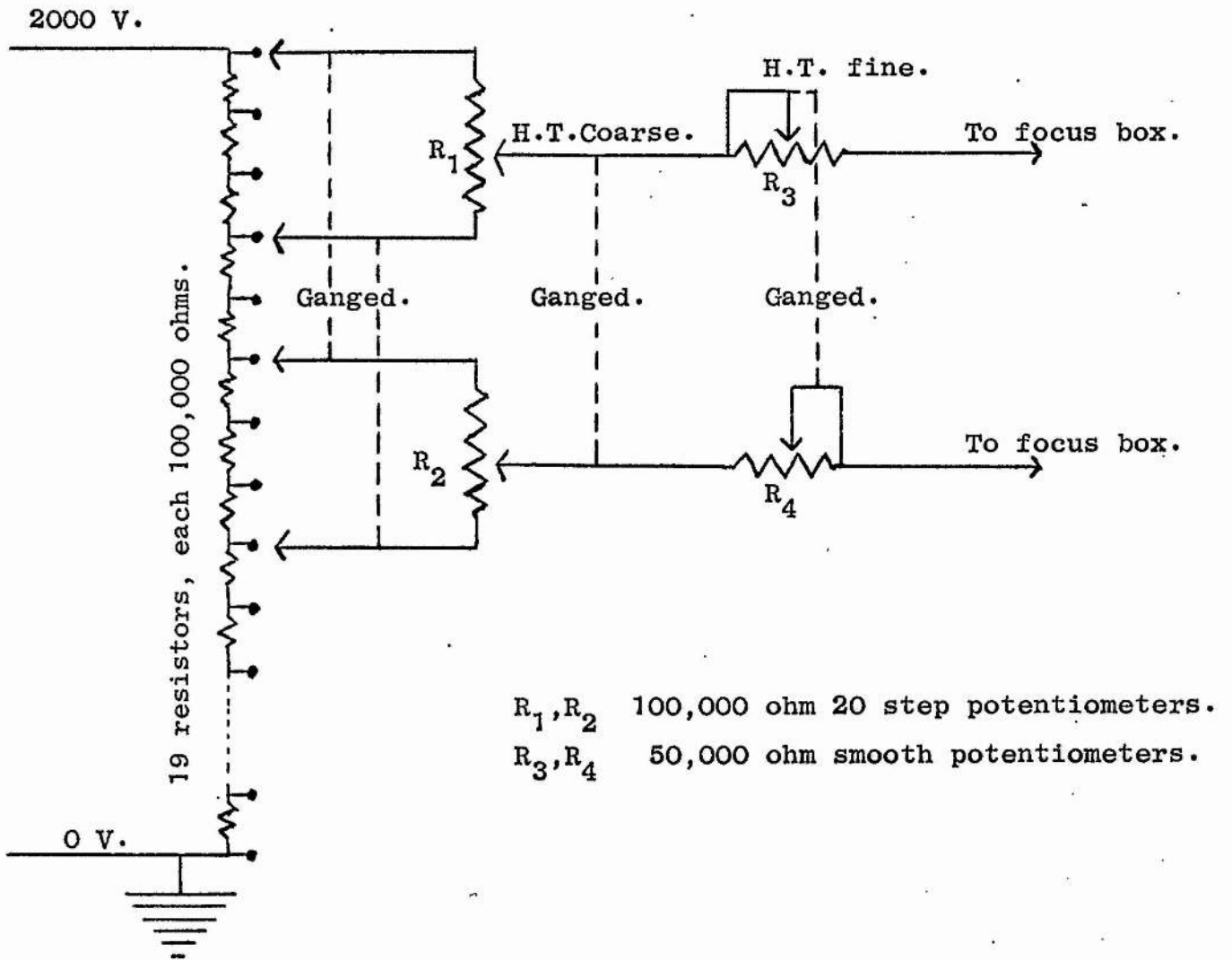



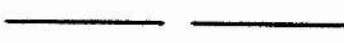



FIG. 15.

to this value by the E.H.T. power supply. Voltages marked on the diagram are relative to the zero voltage reference line shown. Facilities were available also for reading trap current (on two ranges of 400 and 200 microamps F.S.D.) and total emission current (400 microamps and 2mA F.S.D.). The energy of the ionizing electron beam was adjustable from about 8 to 70 eV by varying the box to filament voltage. A trap current of 20 microamps was available for appearance potential work if required.

The resulting peak stability was markedly improved over the older circuit but was still not good. The magnet and E.H.T. circuits were examined for A.C. ripple with an oscilloscope. The magnet in particular showed the presence of considerable R.F. which was traced to one of the power supplies. This along with ripple on the ion gun plates was reduced by judiciously placed capacitors. A modification which further reduced ripple in the ion gun is next described.

The original method of varying the H.T. was to move the earth point up from the bottom of a chain of resistors across which was the 2000 volt output -- departure from earthing the bottom introduced ripples at the top. Further, the variation in the H.T. adjustment resulted in a variation of the current through the chain of resistors. This was felt to be undesirable so far as good stability was concerned. The circuit was therefore modified to that shown in figure 15. The ganging of all controls was for the purpose of

POTENTIALS ON THE ION GUN PLATES.

Earth	E		E	$\begin{cases} 0 \text{ V.} \\ G_1 = 0 \text{ V.}, G_2 = 0 \rightarrow 120 \text{ V.} \\ G_2 = 0 \text{ V.}, G_1 = 0 \rightarrow 120 \text{ V.} \end{cases}$
Beam centre	G_1		G_2	
Earth	E		E	
Focus	J_1		J_2	$J_1 = 150 \text{ V.}, J_2 = 0 \rightarrow 250 \text{ V.}$
Draw-out	J_3			1750 \rightarrow 2000 V.

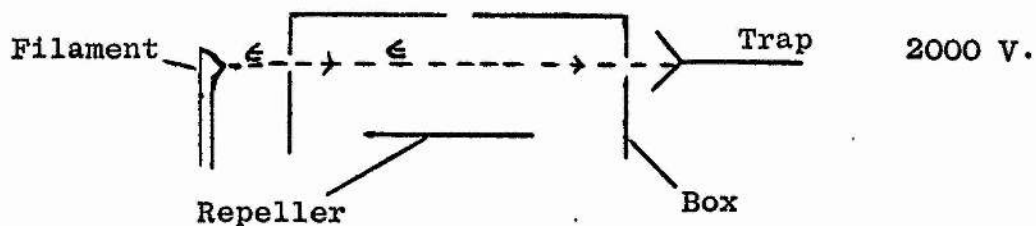


FIG. 16.

VARIATION OF PEAK HEIGHT WITH
REPELLER-BOX VOLTAGE.

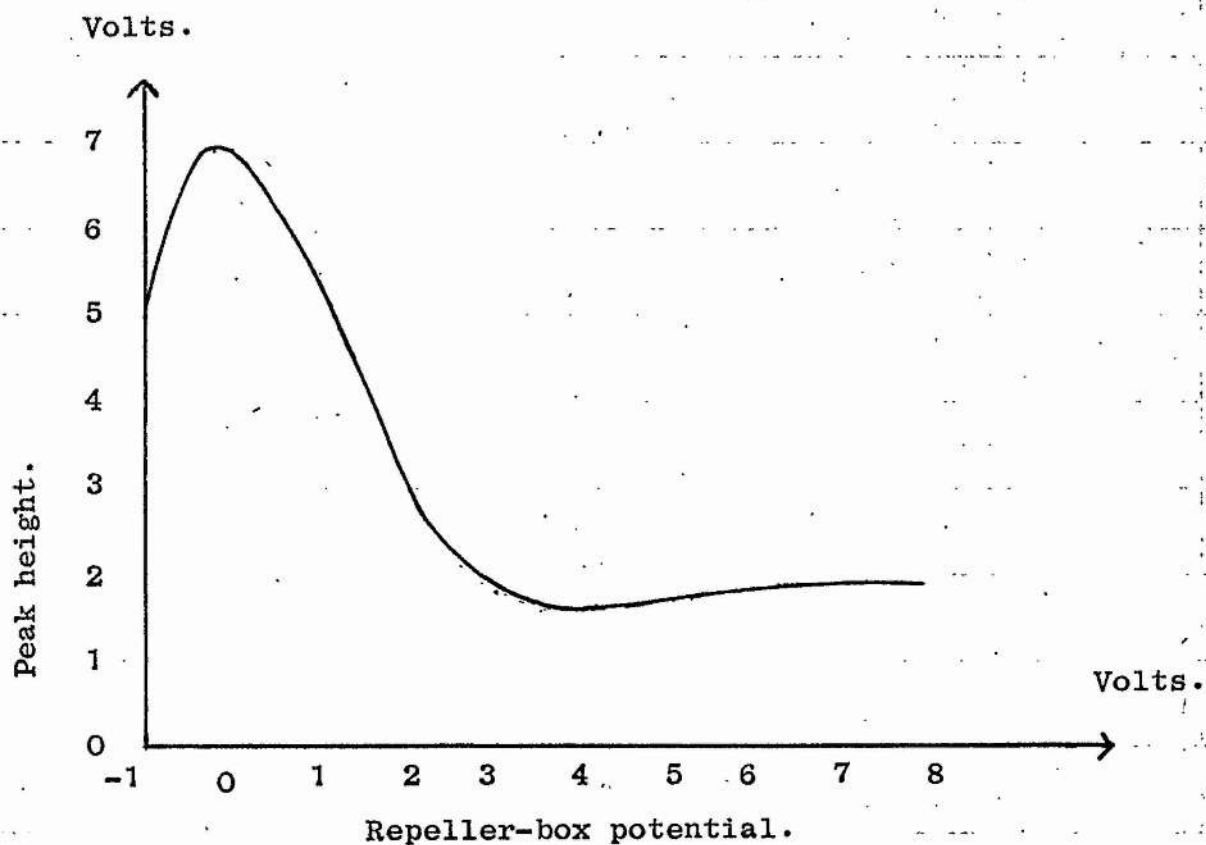


FIG. 17.

Mass Spectrometer resolution in $m/e = 100^+$ region.

Doubly ionised mercury isotope peaks.

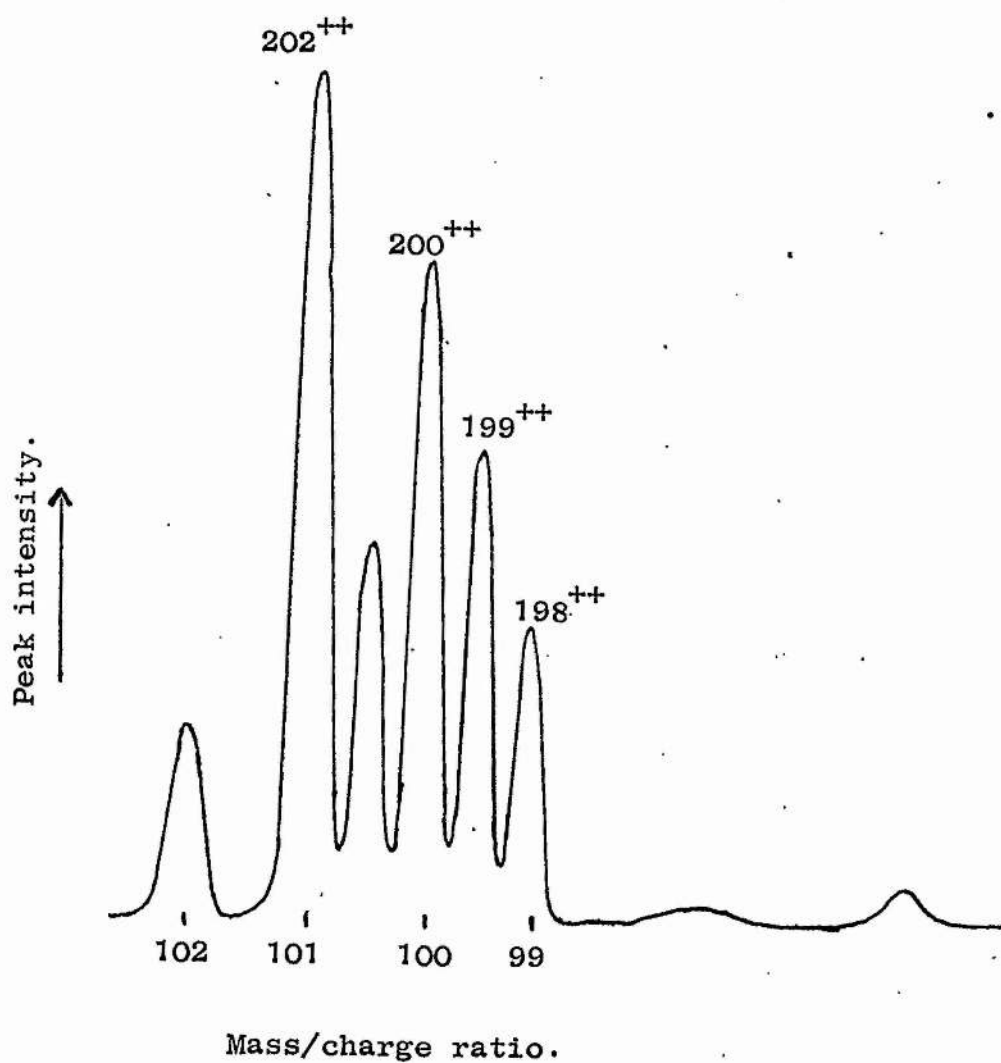


FIG. 18.

PEAK SHAPE. ($m/e = 40^+$.)

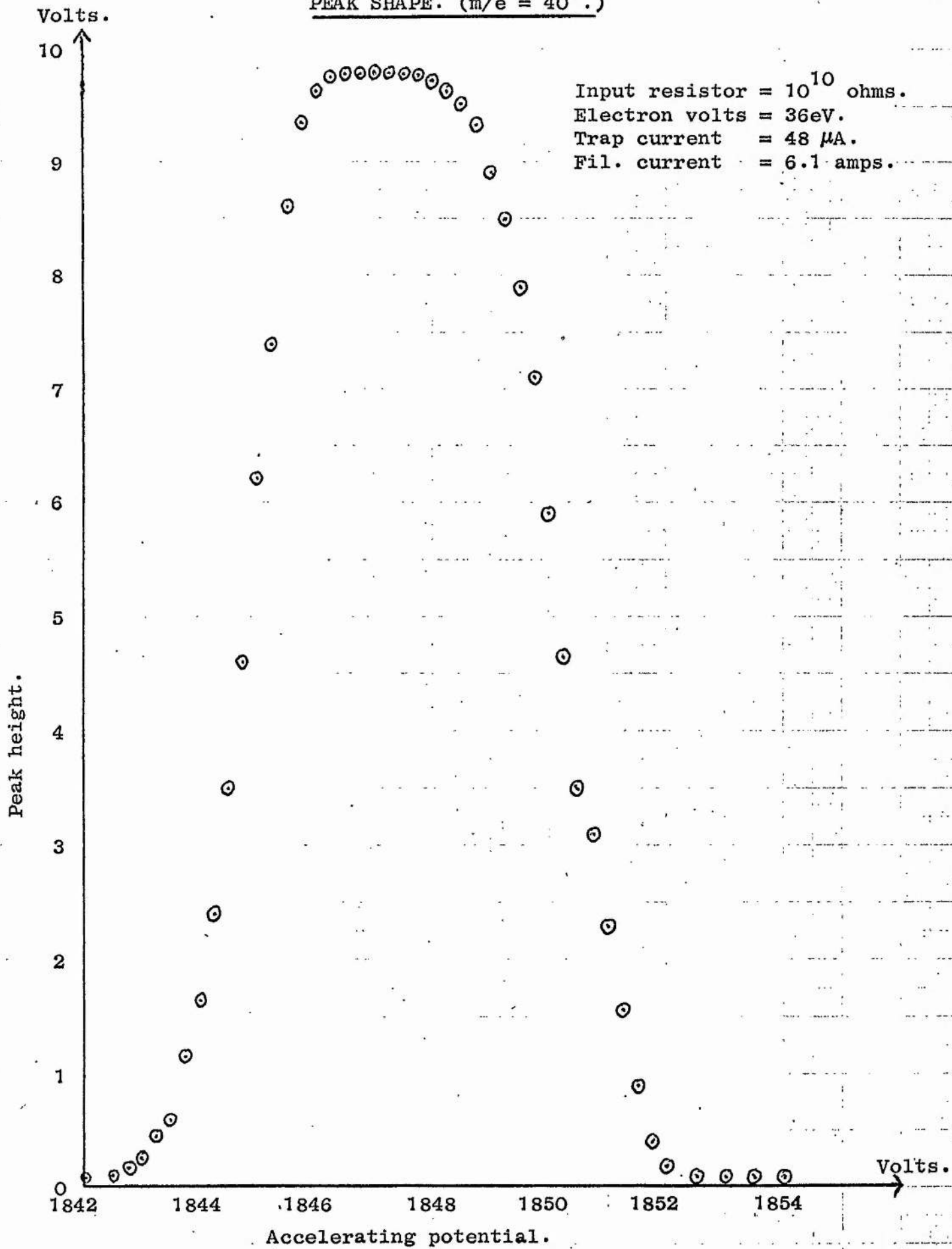


FIG. 19.

leaving a constant voltage across the focus box at all times but allowing the level to be adjusted. This meant that peaks could be observed at other voltages without resetting all the focus box controls.

Modifications were also made to the ion gun and the voltages to the various plates. The final arrangement is shown with relative potentials in figure 16. Although the repeller voltage adjustment gave marked changes in stability and sensitivity (see fig. 17) it was found that good stability on our instrument was obtained with the repeller at box voltage. The exit slits and collector slits were maintained at 0.008 inches.

The overall stability of the magnet and E.H.T. power supplies was measured at about 1 part in 10^5 .

One final improvement in stability was found by adjusting the heater volts on the main mass spectrometer three stage mercury diffusion pump. The use of liquid air on the main trap also gave improved stability when the signals from "condensable" substances were being observed.

When finally tuned by the standard procedure the performance of the mass spectrometer was checked for resolution by scanning the Hg^{++} region of the mass spectrum and by a plot of the peak shape. The final resolution was about $\overset{1 \text{ in}}{\underset{\text{A}}{200}}$. Typical results are shown in figures 18 and 19.

9. Early experiments.

A preliminary investigation into the pyrolysis of methyl bromide in the presence of toluene was performed as follows. After the mass spectrometer power supplies had been allowed to warm up and the reactants had flowed for some time to season the furnace wall, some data on the rate of decomposition was obtained. The mixture of methyl bromide and toluene with about a 20 fold excess of the latter were flowed through the furnace in about 1 mm pressure of argon carrier gas. Condensable products and unused reactants were frozen out in liquid air traps placed at a point in the flow line after the furnace. During the reaction readings were taken at regular intervals of the 16^+ , 2^+ and 40^+ peak heights on an appropriate grid input resistor, the latter always being accompanied by a pressure reading to give the mass spectrometer sensitivity. It was assumed that the methane and hydrogen as "non-condensable" gases contributed negligibly to the pressure within the flow system and so the carrier gas pressure could be used as the sensitivity reference. These data after subtracting the mass spectrum background and after reference to the calibration graphs (fig. 5) could be converted to values of moles of methane or moles of hydrogen produced per second during the reaction. An average value over the time of the run of the rate of production of the above gases was used. The run was allowed to proceed for about 15 to 60 minutes depending upon the temperature being used.

TYPICAL EARLY RUN DATA.

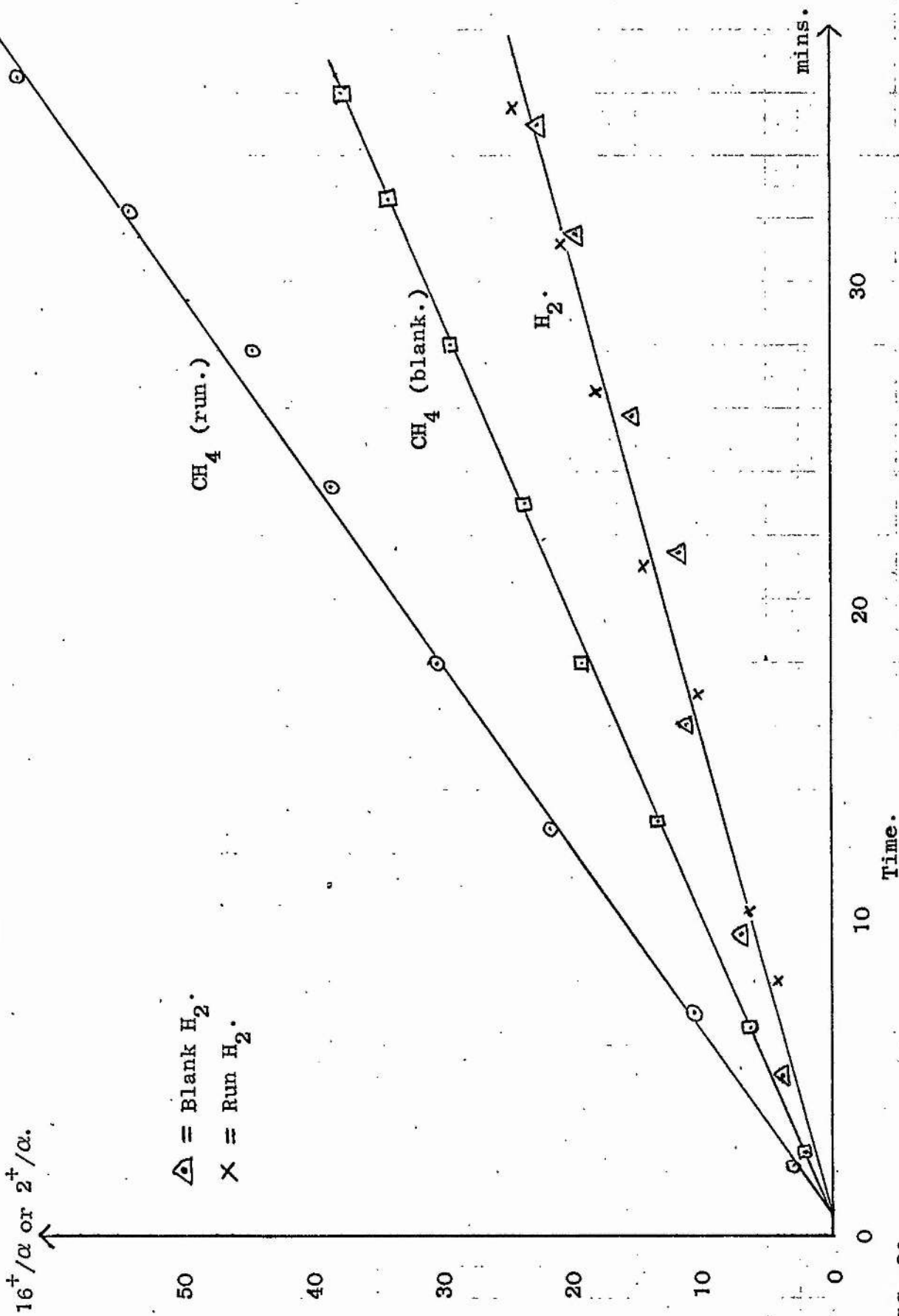
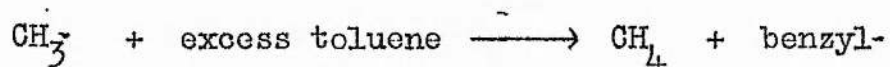


FIG. 20.

A blank run carried out identically and immediately after the above, was next performed with toluene alone flowing through the furnace. Again both hydrogen and methane were recorded at regular intervals. A typical result is shown in figure 20.

The difference in the rate of methane production between a blank and the corresponding run should give the amount of methane derived from the CH_3Br reaction i.e. from the reaction:



This methane production rate may then be converted into a percentage decomposition and an appropriate first order rate constant determined. The contact time was calculated by the formula given at the beginning of Appendix 1. In these experiments all the gases flowed down either the bypass line or the furnace line so no corrections were necessary for the fractions passing down the two lines as in the later part of the research.

Several runs were performed in the range 700 to 800°C. Contact times were of the order of 2 secs. and partial pressures were about 0.2 mm toluene and 0.01 mm methyl bromide.

However because toluene decomposes at these temperatures and is in excess then the difference in CH_4 production between a blank and a run is necessarily small. Toluene pyrolysis data is available from Smith (8). The rate of decomposition of toluene is based on the total number of moles of gaseous products. Thus the blank data may

be used to obtain toluene pyrolysis data and compare it with other workers. This would also to some extent act as a check on the method being used. Such results were in fair agreement with, for example, Smith.

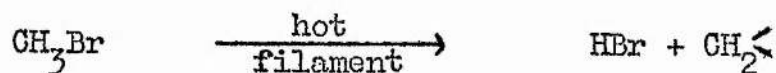
It was found that the reproducibility of a percentage decomposition for methyl bromide was poor, resulting in large spreads of any calculated rate constants. The order of magnitude of the rate constants was, however, in approximate agreement with published data (9). It was felt that one difficulty in obtaining reliable and reproducible behaviour was the fact that the CH_4 or H_2 produced were not measured when homogeneously distributed throughout the flow system, although one would not expect this to account completely for the spread observed.

No difference in rate of hydrogen production between a blank and a run was found and frequently the blank gave a slightly higher rate of production than the run. This was contrary to the observations of Szwarc who suggested that an observed increase in hydrogen production in his experiments when methyl bromide was present was due to subsidiary side reactions.

It was the above difficulties which prompted the devotion of some time to the possibility of following the reaction by measuring production of HBr ($m/e = 80^+$) on the mass spectrometer. The CH_4 and HBr produced by the radicals CH_3^- and Br^- reacting with the toluene should be present in equivalent amount. A metrosil leak

leading directly into the ionization box was inserted close to the furnace exit such that either bypass or furnace gas could be flowed over it. It was necessary to place a -80°C bath before the leak in order to suppress the large toluene peaks which spread into the 80^{+} region of the mass spectrum. There was subsequently no change in the 80^{+} peak height on switching from the furnace to the bypass. It could only be concluded at this point that mass number 80^{+} produced by the pyrolysis was balanced by loss of 80^{+} due to drop of methyl bromide concentration on the furnace line (CH_3Br alone gives peaks in the $79^{+} \rightarrow 82^{+}$ region of the spectrum (10)).

Attempts to separate HBr^{+} due to HBr , and HBr^{+} due to CH_3Br , by adjustment of the energy of the ionizing electron beam in the ion gun were unsuccessful. Measurements of the appearance potential of HBr^{+} from CH_3Br and of HBr^{+} from HBr gave values on our instrument within less than 0.5 eV of one another. The literature (11) suggested that the two should differ by some 3.4 eV. One could only assume that in our ion gun the CH_3Br was diffusing to the hot filament where,



This HBr produced would then give the same appearance potential as any HBr admitted from outside. The fact that the ratio $\text{HBr}^{+}/\text{CH}_3\text{Br}^{+}$, with both ions coming from CH_3Br , was reduced when a -180°C bath replaced the -80°C bath on the mass spectrometer

main trap, supported the above conclusion.

Various cold baths (12) were made up to give a temperature of about -120°C to -140°C in an attempt to freeze down the CH_3Br but let the HBr pass through. It was found that the methyl bromide was completely suppressed at -125°C but at this temperature the HBr^+ peak was extremely small and no change could be observed in its magnitude by further reduction in temperature. It would be a reasonable deduction that the relatively small amount of HBr produced would be soluble in the large excess of toluene condensing in the cold trap.

It was these difficulties which prompted the development of the method which was finally used to follow the reaction. This is described in the following sections.

10. Apparatus modifications.

It is advantageous to follow a reaction by observing the fall in concentration of the reactants. In this way one readily obtains a percentage decomposition without relying on a certain reaction stoichiometry, and the importance of any side reactions is eliminated. The inherent difficulties however are in measuring a small change in a relatively large concentration of reactant and in switching from a "bypass" to a "furnace" reading without upsetting the flow conditions.

Some time was devoted to trying to use two metrosil leaks, one in the furnace line and the other in the bypass line. Since it

VARIATION OF LEAK RATIO WITH INCREASING ARGON PRESSURE.

Bypass/furnace leak ratio.

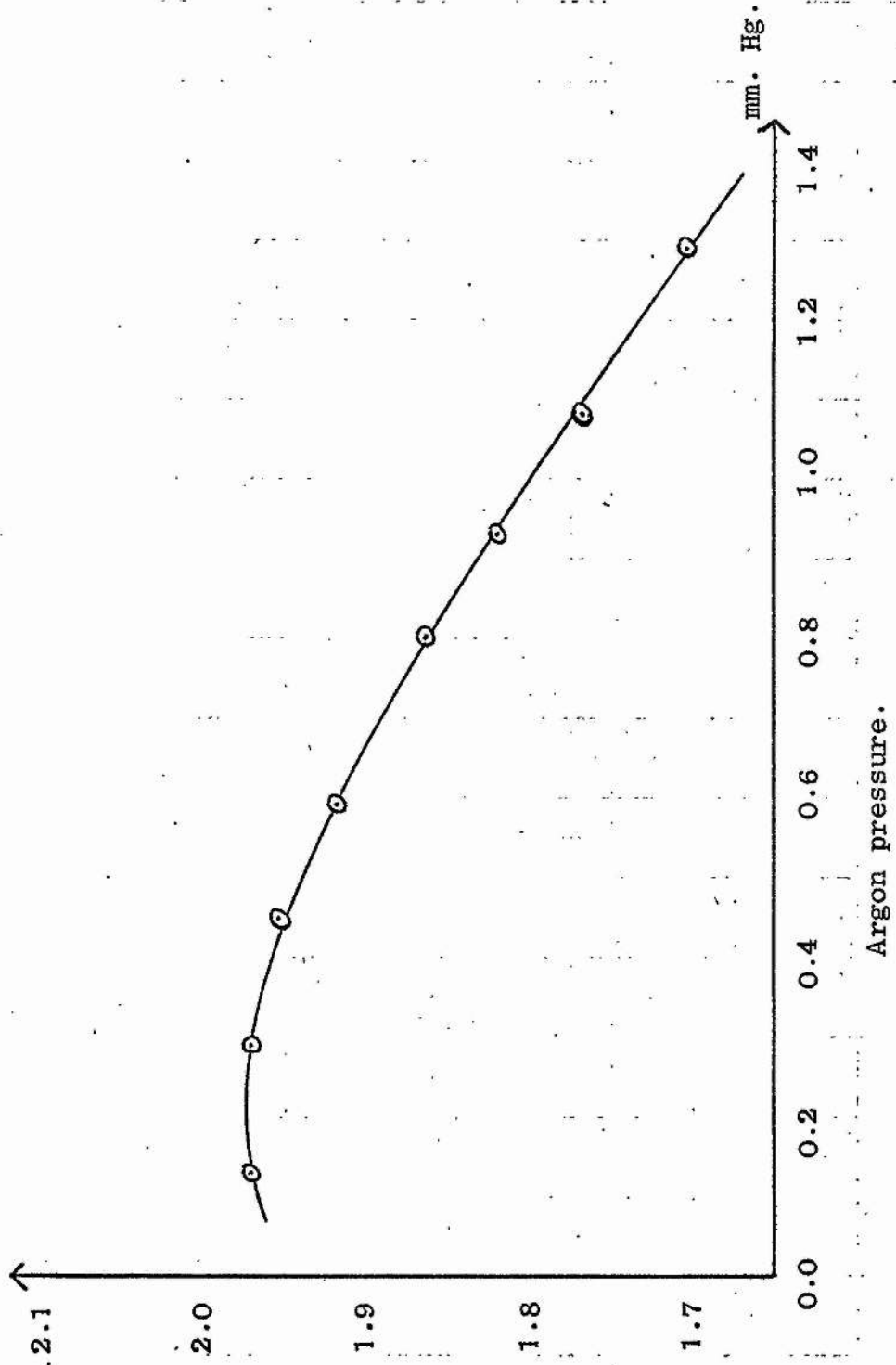


FIG. 21.

SAMPLING SYSTEM.

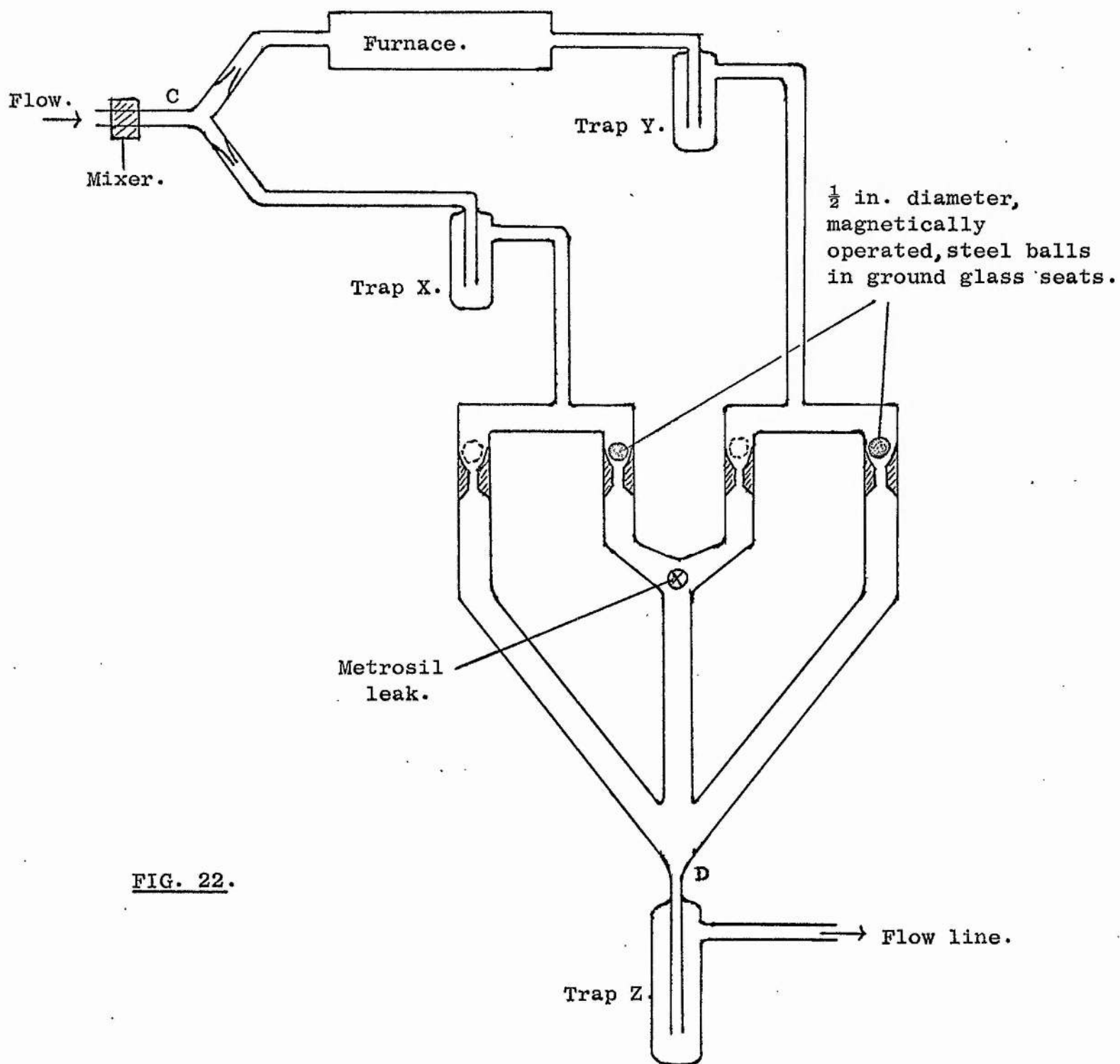


FIG. 22.

was impossible to arrange equal leakage rates the higher reading on the output recorder was reduced electrically to be equal to the lower.

Experiments, using argon, to determine the leak ratio led to the finding that the ratio varied with the pressure of gas over the leaks, (see fig. 21). The method of Halsted and Nier (13) was used to base a calculation on flow behaviour through two mass spectrometer viscous leaks. This leads to the ratio of the ion currents being represented by an equation

$$\frac{i}{i'} = \frac{(k + k''')}{(k + k')} \cdot \frac{[2\eta k' P_3 + k'' M^{\frac{1}{2}} P_3^2]}{[2\eta k''' P_3 + k'''' M^{\frac{1}{2}} P_3^2]}$$

where P_3 is the pressure in the flow system, η is the viscosity of the gas of molecular weight, M . The various k 's are flow constants which depend upon several factors e.g. geometry and temperature. These difficulties led to a design of apparatus incorporating a single leak. The apparatus in its final form is shown in figure 22. The remainder of the flow system is as shown in figure 1. The gases are allowed to flow down both routes simultaneously. Sampling of furnace gas or bypass gas is done by simply moving the steel balls to their other seatings with a magnet.

The mass spectrometer was at first very slow to respond to changes, but this difficulty was overcome by the use of wide bore glass tubing from the sampling point to the mass spectrometer head. This alteration brought about the need for a specially designed

LARGE BORE STAINLESS STEEL VALVE.

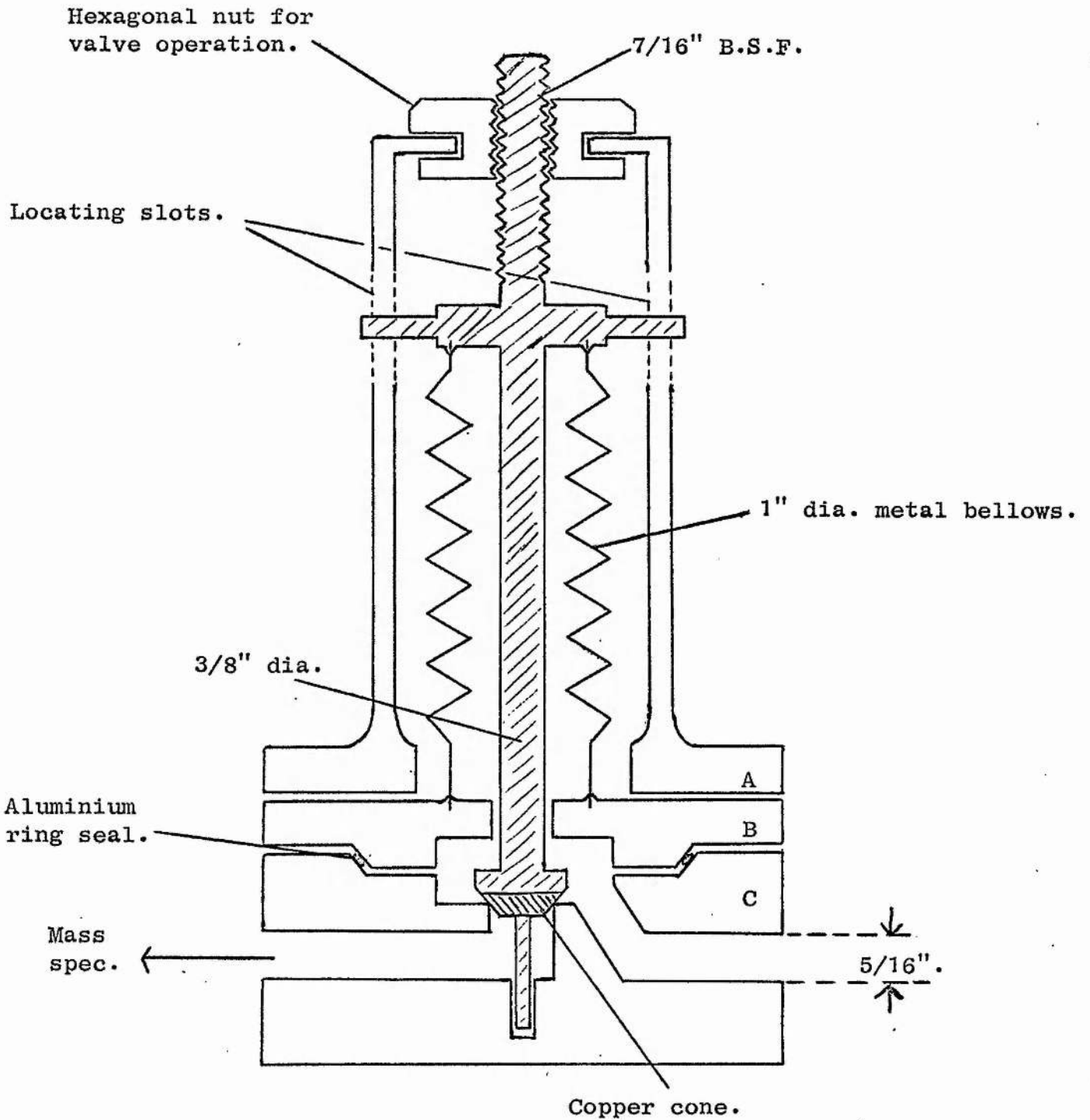


FIG. 23.

Units A,B,C clamped together by six 1 1/2"x1/4" socket bolts.

large bore stainless steel valve in this line for use in isolating the mass spectrometer when admitting air to the flow system. The valve construction is shown in figure 23. The diagram is not to scale but the main constructional details are noted in the figure. The sampling line was also led right into the box of the ion gun. After these modifications the response was almost immediate and successive readings of a particular peak could be quickly obtained. The change in reading between the bypass and furnace lines divided by the bypass reading gives the fraction decomposed.

In order to observe the small change in the reactant parent peak at $m/e = 96^+$, the output signal to the recorder was backed off by the Ekco voltage decade unit. For example, if the peak height of 96^+ for a particular input resistor was 3.0 volts, insertion of 2.970 volts backing off from the above unit then leaves the recorder pen at the top of a 0 \rightarrow 30 mV scale. A change in reading of the full scale length (10 inches) then represents a 1% decomposition of that substance.

The traps X and Y were initially held at -80°C to suppress the toluene peaks in the mass spectrometer but under these conditions apparent percentage decompositions were indicated when the furnace was at room temperature. This was proved to be due to either (a) small different amounts of methyl bromide dissolving in the molten toluene in the traps or (b) relative differences in the efficiencies of the two -80°C baths or a combination of the two. It was thus

found necessary to run with no traps at all between the furnace and the metrosil and allow everything to flow over the metrosil leak, M. A more efficient way of mixing the gases before they reached the furnace was also introduced.

Subsequent examination of the 96^+ peak showed zero decomposition with the furnace at room temperature. A scan in $88^+ \rightarrow 96^+$ region of the mass spectrum showed that the large toluene peaks, although tending to spread, did not interfere with 96^+ , the parent peak of methyl bromide.

The backed off stability of the argon peak was better than 0.1%.

Under experimental conditions a liquid air trap on the mass spectrometer increased the short term stability of 96^+ to 0.05%.

11. Further calibrations.

A certain pressure gradient exists from C to D (fig. 22) and there should (if M is relatively near to D, though not near enough to allow any significant back diffusion) be virtually the same gas pressure over M whether the gas arrives there via the furnace line or via the bypass line. Assuming good mixing at C then, although different numbers of moles of gas flow via the different routes, the partial pressures of each reactant should be the same for both paths for a cold furnace whilst in the case of a hot furnace it will give a lower reading than the bypass and thus allow

COLLECTION TRAP.

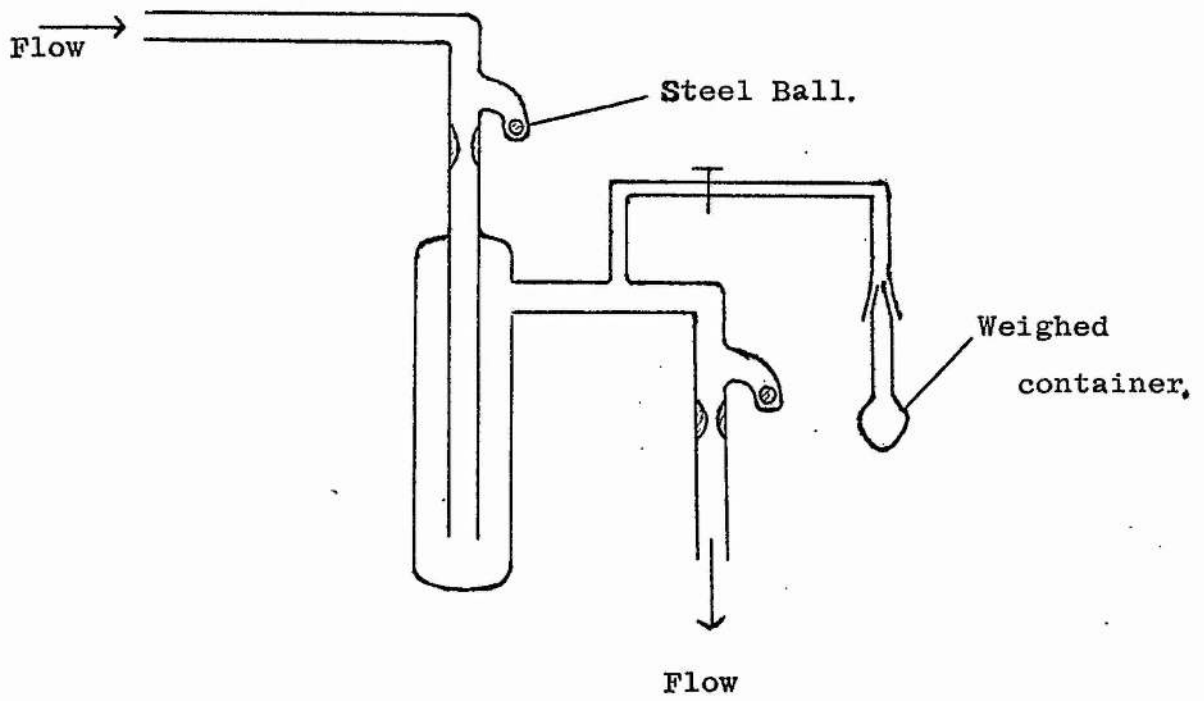


FIG. 242.

the extent of the decomposition to be calculated.

The initial calibrations of toluene and methyl bromide injection were for total moles per second injected. Since we allow the gas to distribute freely between the two routes, then it is necessary to know the ratio in which it distributes in order to calculate the moles per second of reactant passing through the furnace. This latter figure is needed for the calculation of contact times (see Appendix 1).

Toluene injected into argon was collected in traps X and Y (fig. 22) from which it could be distilled over into weighed containers (fig. 24). Greased taps were avoided where possible and magnetically operated steel balls were used instead. One would expect the ratio of furnace to bypass gas to vary with furnace temperature and this in fact was the case, but because slightly inconsistent results were at first being obtained, the presence of a pressure effect was discovered; namely that at constant temperature the fraction passing through the furnace varied with both the pressure in the flow system and with the flow capillary in use. The latter effect can only be attributed to some change in flow characteristics of the gas. The ratios, obtained for furnace temperatures of from 700 - 800°C, were then calculated at 1 mm pressure and also at varying pressures at a constant temperature of 1018°K. At the higher temperatures the toluene decomposes to some extent so allowance was made for the loss. Percentage decomposition data on toluene was available from Smith (8), and corrections were applied. These corrections were

GAS DISTRIBUTION.

Effect of variation of temperature. (Unpacked furnace.)

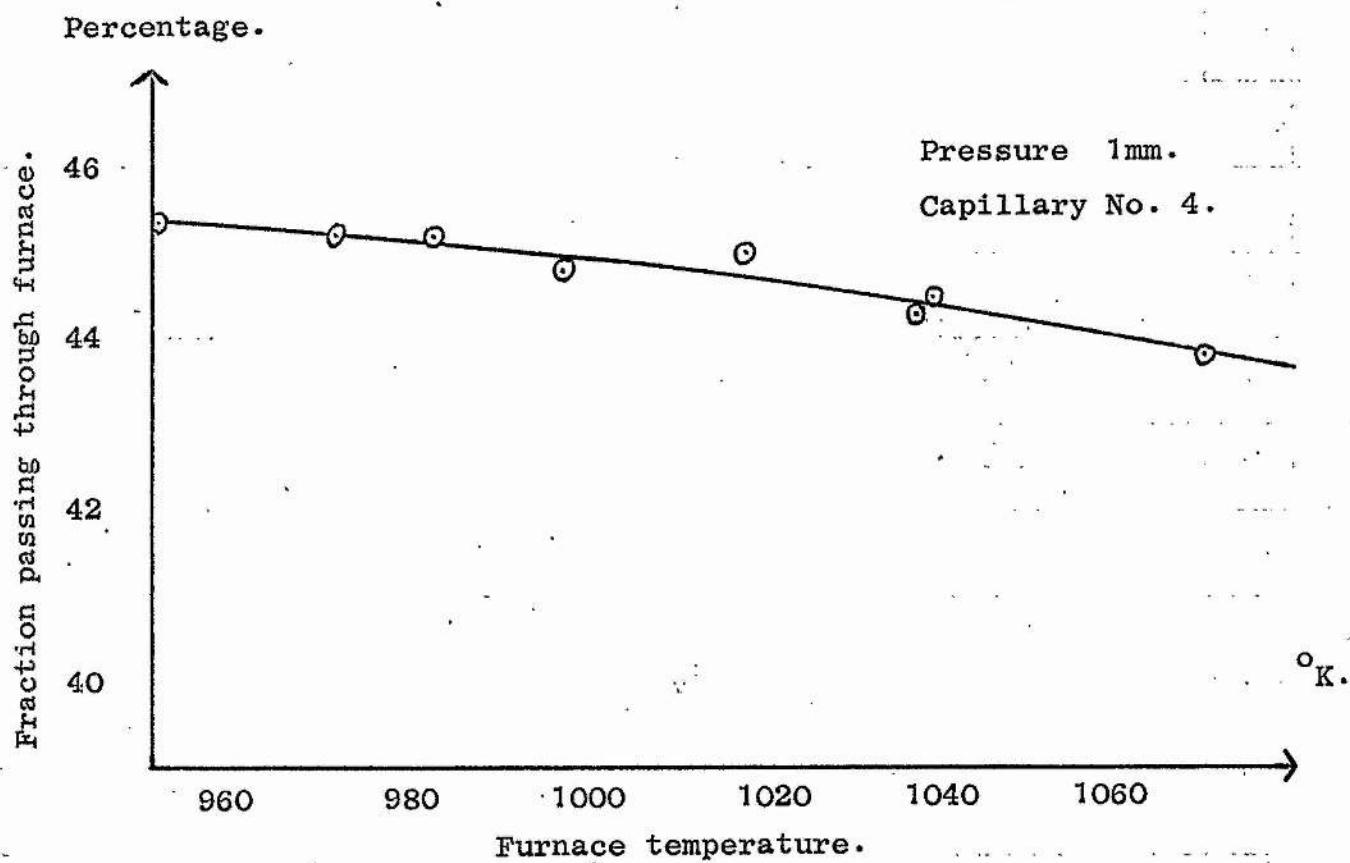


FIG. 25.

GAS DISTRIBUTION.

Effect of variation of pressure. (Unpacked furnace.)

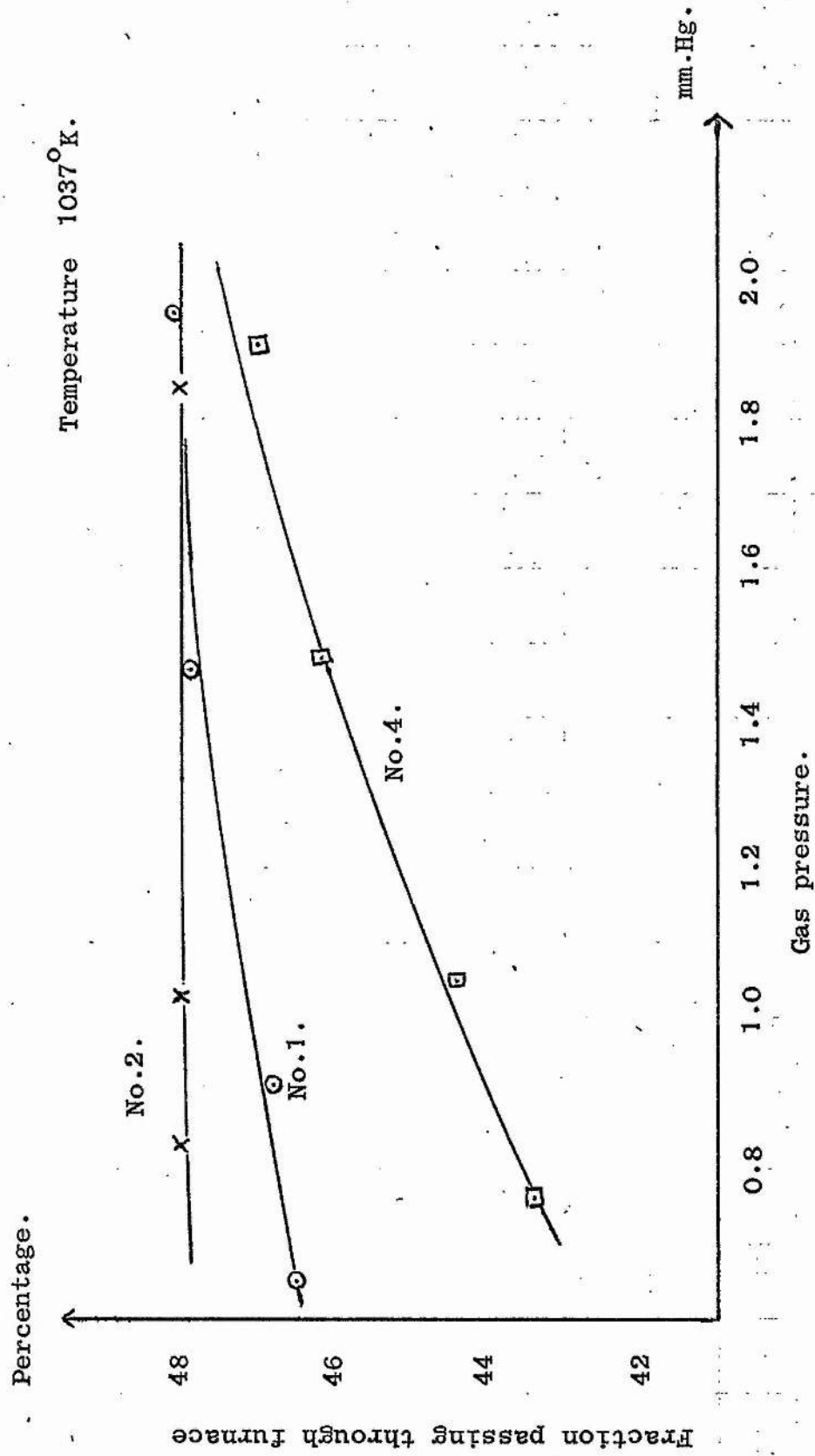


FIG. 26.

MASS SPECTROMETER RESPONSE TO METHYL BROMIDE.

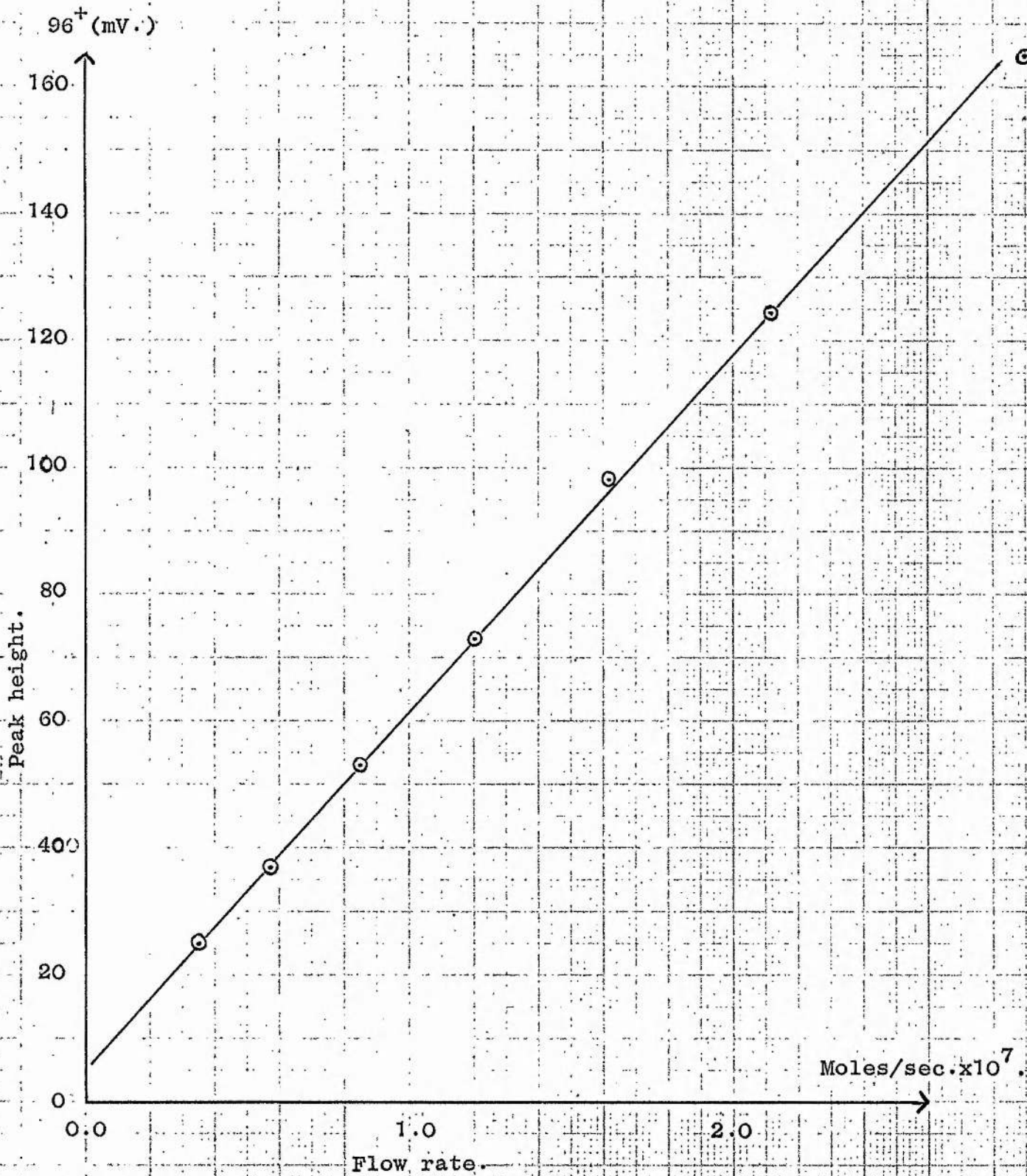


FIG. 27.

well within the limits of any experimental error at all but the highest temperatures.

The graphical results are shown in figures 25 and 26. Tabulated results are in Appendix II. Reference to both of these graphs is therefore needed in order to calculate the required fraction of total gas passing through the furnace.

In order that the difference between the furnace and bypass readings divided by the bypass reading should be equal to the fraction decomposed, it is essential that a plot of volts 96^+ against the partial pressure of methyl bromide should be a straight line, assuming that the mass spectrometer sensitivity does not vary over the duration of the run. This graph is shown in figure 27 which exhibits good linearity. All parameters were held constant with the exception of the methyl bromide injection pressure. Argon peak was recorded on the 10^8 ohm input resistor, methyl bromide was on the 10^{10} ohm resistor.

The injection rate most commonly used was between 1.0×10^{-7} and 2.0×10^{-7} moles per second.

12. Typical run procedure.

The mass spectrometer power supplies were switched on and allowed to warm up. Solid CO_2 and acetone were the coolant on the mass spectrometer trap or, for greater stability of peak, liquid air was used.

The flow system was fully evacuated to about 10^{-5} mm Hg., the toluene degassed and its water bath set to the required temperature and allowed to equilibrate. The furnace would have been arranged to switch on by a time switch and to come up to the required temperature. Three fillings of argon were released into the flow system from the manostat giving approximately 1 mm pressure.

The circulation pump metal bath was then adjusted to its optimum operating temperature, and it was then set running with its three associated liquid air traps and a liquid air cooled collection trap, (of large dimensions to allow a run to proceed for some time without a blockage occurring due to frozen toluene), was placed after the metrosil leak (trap Z in fig. 22).

The reactants were then injected. Firstly the methyl bromide injection valve was opened and the mass spectrometer tuned to the higher of the two methyl bromide parent peaks at $m/e = 96^+$. Next the toluene valve was opened and the run allowed to settle for up to half an hour (3 hours were allowed if the furnace had been previously let down to atmospheric pressure - see section on furnace seasoning p. 69). The steadiness of the peak was observed by staying tuned to 96^+ and continually backing off to a more sensitive range on the recorder. When steady conditions were attained and the peak showed no tendency to drift, the values of furnace temperature T, pressures on the flow McLeod gauges P_1 and P_2 , toluene bath temperature and methyl bromide injection

pressure were taken, a note being made also of the flow capillary being used.

With the recorder chart running the ball valves were operated alternately to read bypass and furnace line values of 96^+ . Each reading was recorded for two minutes or more depending on the stability of the instrument. After four or six readings had been taken, flow pressures, furnace temperature etc. were again recorded. These values were usually the same as at the start of the run but where any slight discrepancy occurred the average value was taken for use in subsequent calculations.

Finally, with the mass spectrometer still tuned to 96^+ , the methyl bromide valve was closed - the final position to which the 96^+ peak fell being taken as the zero - and then the toluene valve was closed and the system evacuated.

It was quite possible to perform several runs in succession at different contact times simply by changing capillaries. It should be pointed out that this is undesirable especially at the higher percentage conversions since the methane and hydrogen formed in the reaction will dilute the carrier gas and could to some extent invalidate the flow capillary constants. Although on occasions during the research up to five or six runs were performed without changing the carrier gas, no errors could be attributed to this dilution. This was probably because the total volume of the system was over 20 litres and so the dilution was insignificant.

TYPICAL EXPERIMENTAL DATA. (Run 128.)

Signal from $m/e = 96^+$ on
30 mV. range of recorder
backed off by 15mV.

10^{10} ohm input
resistor.

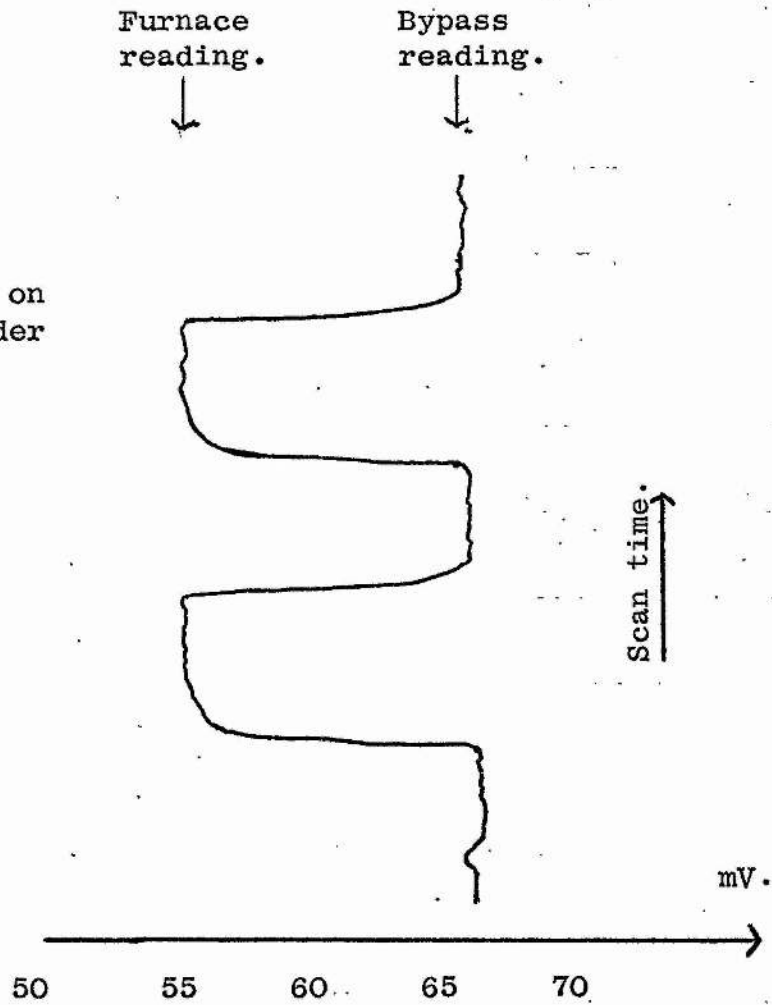


FIG. 28.

A typical result is shown in figure 28. The average of the values is taken for use in calculations.

Then

$$\% \text{ decomposition} = 100 \left[\frac{\Delta (\text{mV})}{\text{Bypass Total (mV)}} \right]$$

The contact times, partial pressures and rate constants were calculated as described in Appendix 1.

The above treatment assumes constant sensitivity of the mass spectrometer during readings. A check on 40^+ at intervals during several runs showed no variation during a run; also the constancy of the 96^+ peak suggests no sensitivity variation. The treatment also assumes that there will be no variation in 96^+ zero reading when decomposing toluene alone (the toluene peaks spread towards the 96^+ region). This was checked at the high temperatures and there was found to be less than 0.2% error in the total peak height from this cause. This correction was not applied as it was considered to be well within the limits of the experimental errors.

13. Tests for surface reaction.

A series of experiments were performed as described above in a furnace of heated volume 280 ml. The furnace had a re-entrant thermocouple well which gave a surface/volume ratio of 1.82. The normal method of evaluating or testing for a heterogeneous

contribution is by increasing the surface/volume ratio (s/v ratio). This will increase the heterogeneous reaction velocity and one can then compute the homogeneous component of the rate constant by plotting the rate constant for the whole reaction against s/v ratio and extrapolating to $s/v = 0$. This treatment holds so long as the homogeneous and heterogeneous reactions are the same order. Lapage (14) found the treatment applicable in the case of methyl iodide pyrolysis.

Design difficulties usually prevent a wide variation in s/v ratio for a particular experimental set-up. The alteration of the shape of a vessel gives a small but sometimes sufficient change, but packing the vessel with irregular pieces or tubes or glass wool of the same material as the furnace will give a much larger surface area. Probably the most convenient way of packing a reaction vessel is that used in the present work, namely the insertion of tubing within the furnace. The central tube was supported from touching the furnace over the whole length by attaching small glass lugs at the ends. Measurements on the lines and on the furnace before it was inserted allowed the new s/v ratio to be calculated at 5.2 and the new furnace volume at 215 ml. The sharp edges of the tube should be fire polished as this will have a different surface activity from broken glass (see, for example, Wood)(15).

Melville and Gowenlock (16) suggest and describe a thorough cleaning of the surface to reduce heterogeneous contribution.

GAS DISTRIBUTION.

Effect of variation of temperature. (Packed furnace.)

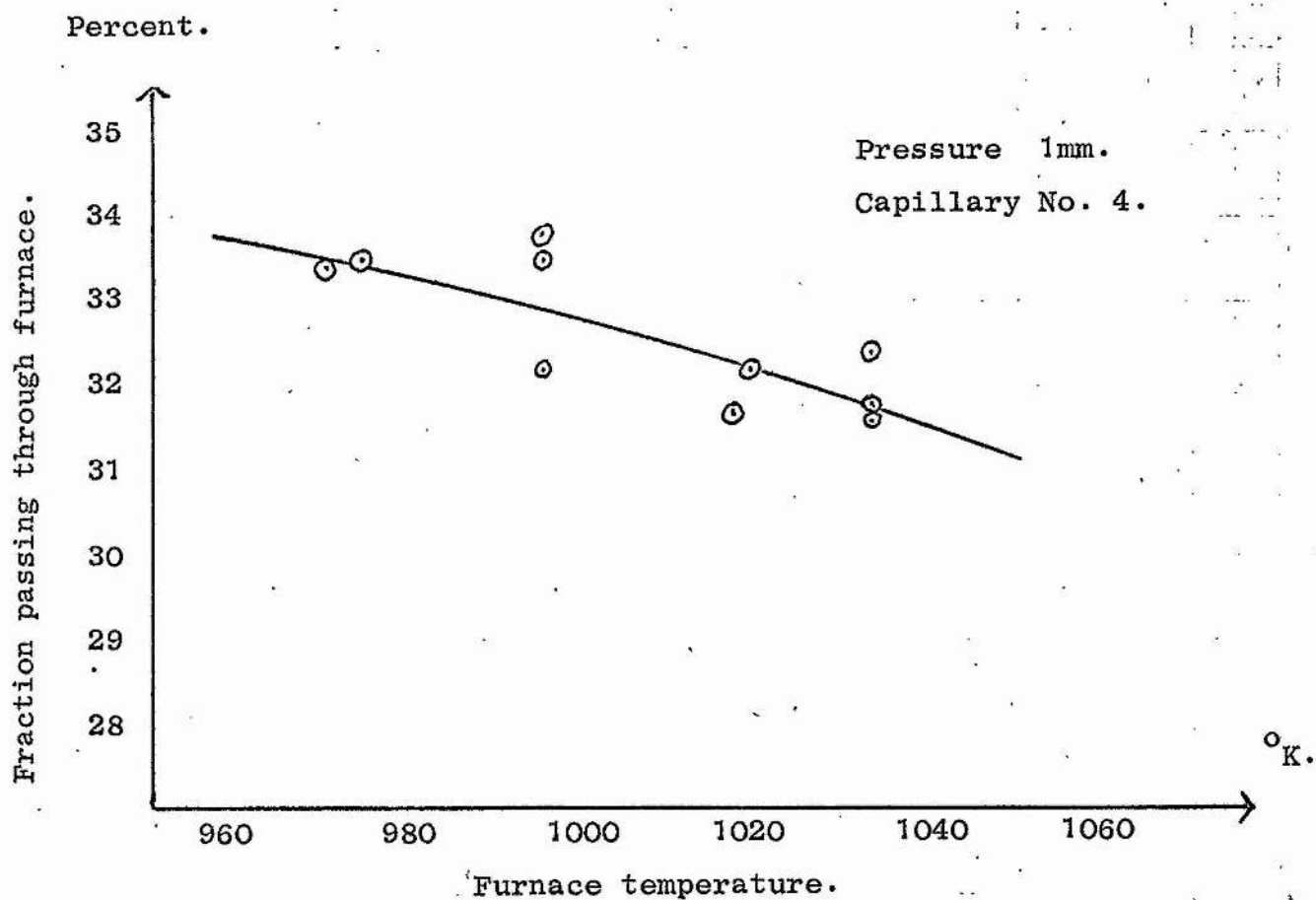


FIG. 29.

GAS DISTRIBUTION.

Effect of variation of pressure. (Packed furnace.)

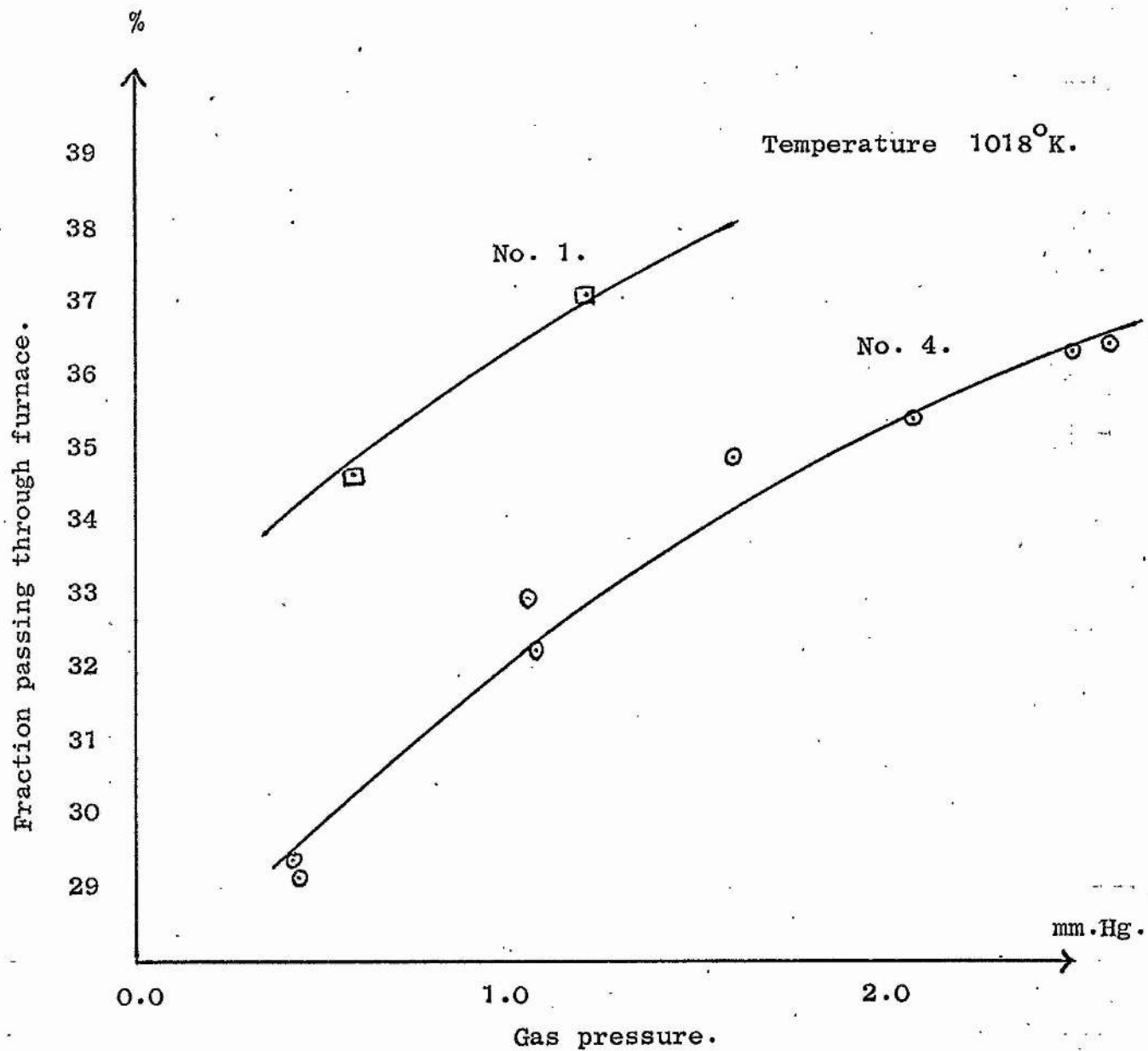


FIG. 30.

They also recommend that packing materials shall have had the same history and heat treatment as the reaction vessel.

Poisoning of the walls may also be used to further eliminate wall reactions and several treatments are described by the above authors. Trace impurities in silica as a result of "unhygienic" glassblowing can be the cause of unreliable data.

It was necessary at this stage to repeat the calibration for the percentage of gas flowing down the furnace line. As expected, since the furnace liner now presented a larger resistance to flow than before, the percentage of gas passing through the furnace was lower. The graph is shown in figure 29. Here again a pressure effect was observed and it is shown graphically in figure 30, which was obtained at a constant temperature of 1018°K . As before, reference to both figures 29 and 30 is needed to determine the percentage of the total gas passing down the furnace line.

DESCRIPTION OF EXPERIMENTS PERFORMED AND EXPERIMENTAL RESULTS.1. Introductory.

The expected behaviour of methyl bromide under pyrolytic decomposition is to produce methyl radicals and bromine atoms. Any subsequent secondary reactions of these entities should be quenched by the incorporation of an efficient radical acceptor. Toluene has been used for this purpose and for small percentage conversions one should obtain a first order decomposition the rate of which would be expected to correspond to the rate of fission of the C-Br bond in the halide. Evidence for the presence of the above radicals exists in, for example, the increased methane production when methyl bromide is added to toluene at the pyrolytic temperature.

After the final development of the apparatus a check of the first order nature of the decomposition of the halide was made at a constant temperature in the middle of the temperature range to be used. Plots of $\log \left[\frac{100}{100 - \% \text{ decomposition}} \right]$ against contact time showed straight lines through the origin. The variation of contact time was obtained by changing flow capillaries.

Having roughly and briefly established a first order character for the reaction a series of runs throughout the temperature range were quickly performed to ensure that no difficulties would occur and to check the general handling technique. A normal Arrhenius plot of the resultant $\log k_1$ against $1/T(^{\circ}\text{K})$ was a reasonable

straight line with an activation energy of about the expected order of magnitude but the A factor was lower than expected on the assumption that the C-Br bond rupture is the rate determining step.

A series of more carefully performed runs was therefore begun in order to establish the full kinetics of the reaction.

2. Seasoning of furnace.

It was found during the early experiments that if one carried out a reaction in the furnace after air had been admitted then the reaction rate was initially high but gradually fell to a constant level. This seasoning effect, which has been observed by many workers in pyrolysis kinetics, has usually been attributed to the formation of a coating on the silica furnace wall. The nature of this layer has been shown to be carbon in the case of benzil pyrolysis by Barraclough (1) who burned it off in oxygen and analysed for carbon dioxide mass spectrometrically.

Quantitative experiments to observe the seasoning rate were performed as follows. A temperature of 1000°K was chosen as being suitably near to the middle of the range. Air was then admitted to the hot furnace to 'deseason' it, the flow system was evacuated, and air was again admitted to complete the deseasoning process. The reaction was then followed as described under 'run procedure' - about five successive runs being performed before the carrier gas

SEASONING RATE OF FURNACES. (Data of Appendix III.)

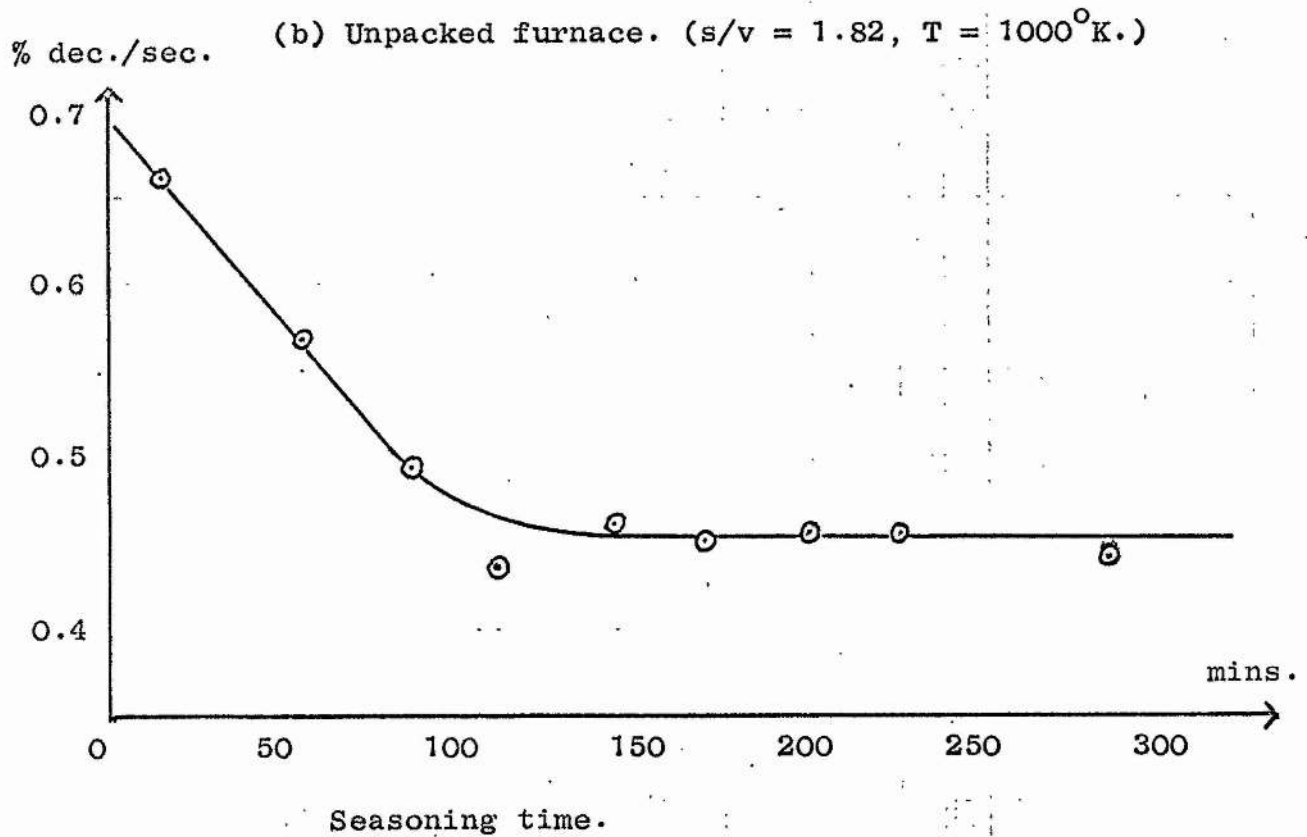
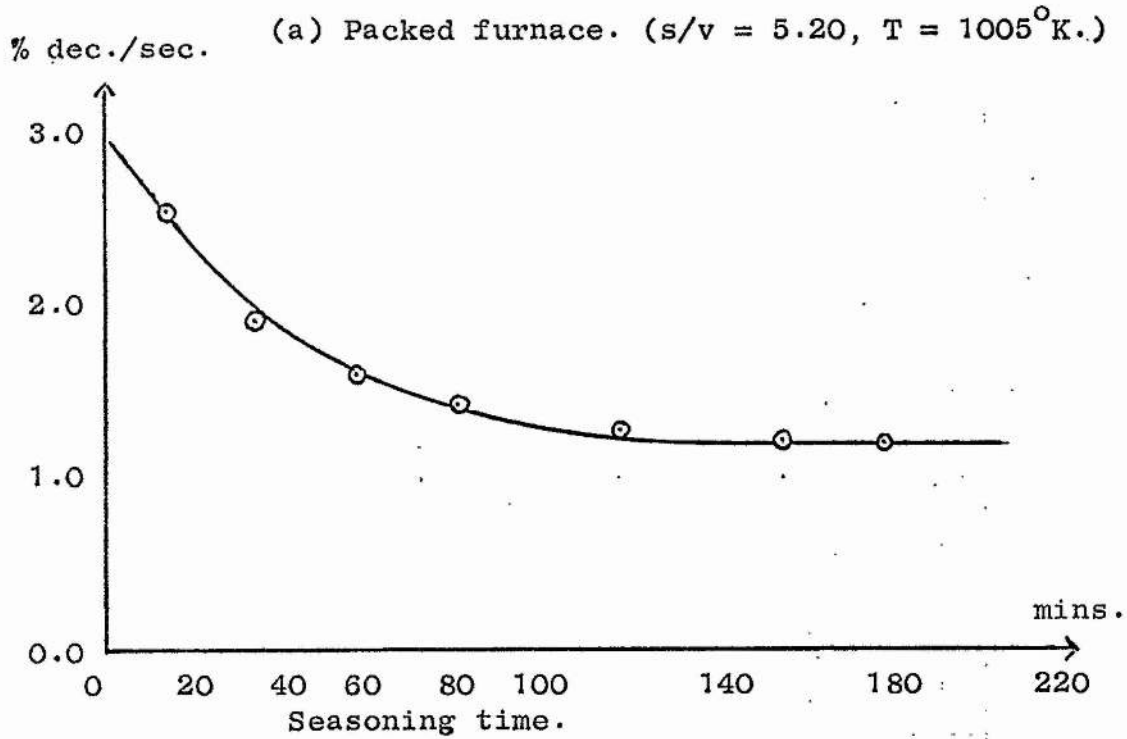


FIG. 315.

was changed. This was considered quite legitimate since the percentage conversion was not high.

Readings were taken at intervals of about 20 to 30 minutes. The data is given in Appendix III for both packed and unpacked furnaces - data for the former being obtained later in the research but inserted here for comparison. Similar behaviour was observed in each case and the results are represented graphically in figure 31. Although the contact times were maintained fairly constant there were small variations due to slightly varying partial pressures. The percentage conversion was therefore related to one second of residence time in the furnace. All other parameters of the system were maintained constant.

It will be observed from the graph that for reliable and reproducible kinetic data seasoning of the furnace by the reactants for about 2.5 hours was necessary if air had been admitted to the furnace. This recommendation was followed for all runs even if the system had not been let down to atmospheric pressure. This ensured adequate seasoning and allowed the system and the mass spectrometer to "settle down" prior to taking readings.

The nature of the coating was investigated by thoroughly seasoning the furnace and then allowing the coating to burn off slowly by introducing about 0.5 mm Hg. pressure of oxygen into the 1 mm of argon carrier gas. The experiment was performed at 953°K at which temperature the coating would burn off slowly enough to allow

EXAMINATION OF FURNACE COATING.

Argon sensitivity 5.56 volts/mm.

Furnace temperature 953°K.

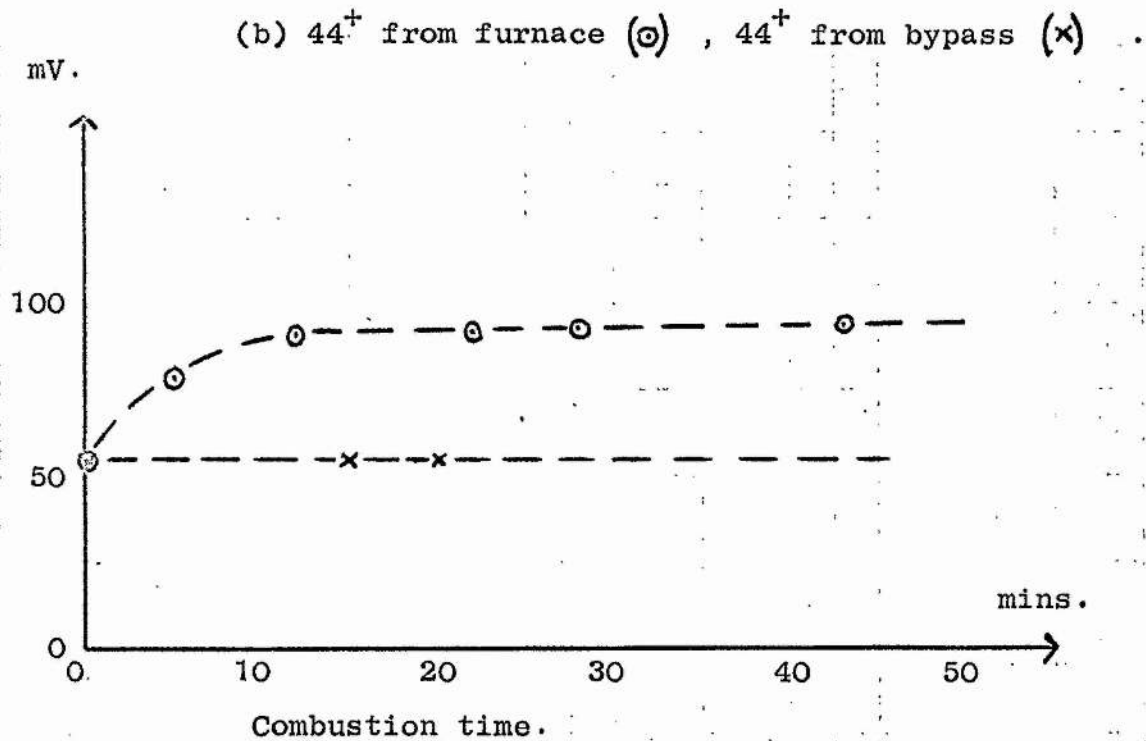
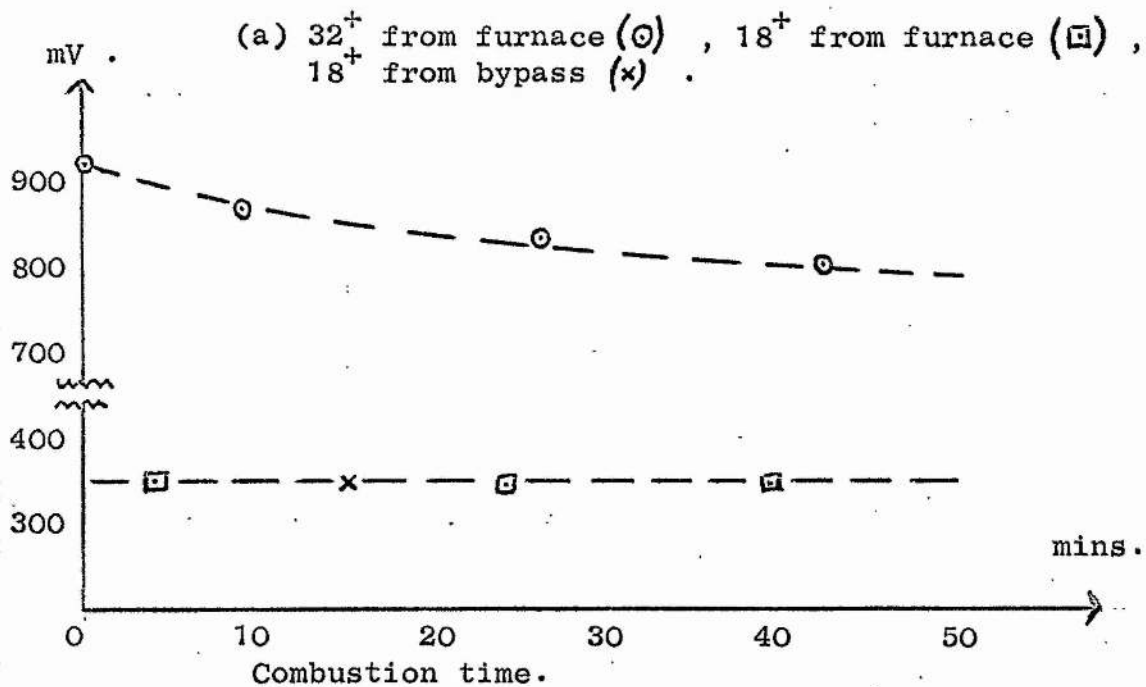


FIG. 32.

the process to be followed by mass spectrometer analysis. The peaks at $m/e = 18^+$ (water), 44^+ (carbon dioxide) and 32^+ (oxygen) were followed on the furnace and bypass lines. The results are shown graphically in figures 32a and 32b.

The nature of the variation is readily explained by the gradual burning off of a carbon coating on the walls. The bypass line shows a constant carbon dioxide peak - this is the mass spectrometer background. The furnace value of CO_2^+ rises to a maximum and then stays steady corresponding to uniform production of carbon dioxide (the CO_2 is removed by liquid air cooled traps later in the flow line so its pressure does not build up). One may presume that the 44 minutes of the experiment is not sufficient time at this temperature to burn off all of the coating. This explains why the oxygen peak at 32^+ continually falls as it is used up in the combustion reaction and why carbon dioxide from the furnace is still steady after this time. The time of 14 minutes taken for the 44^+ peak to reach a maximum may be due to the opening up of new oxidation sites on the surface. Water at $m/e = 18^+$ is constant and the same value on both furnace and bypass lines suggesting lack of any hydrogen in the coating substance.

Smith (8) also observed a seasoning effect in the pyrolysis of toluene alone. It is interesting to note that the carbon coating has a kinetic effect on the decomposition of methyl bromide and of toluene which shows the participation of the wall nature at these pressures.

EFFECT OF VARIATION OF METHYL BROMIDE PRESSURE. (Data of table I.)

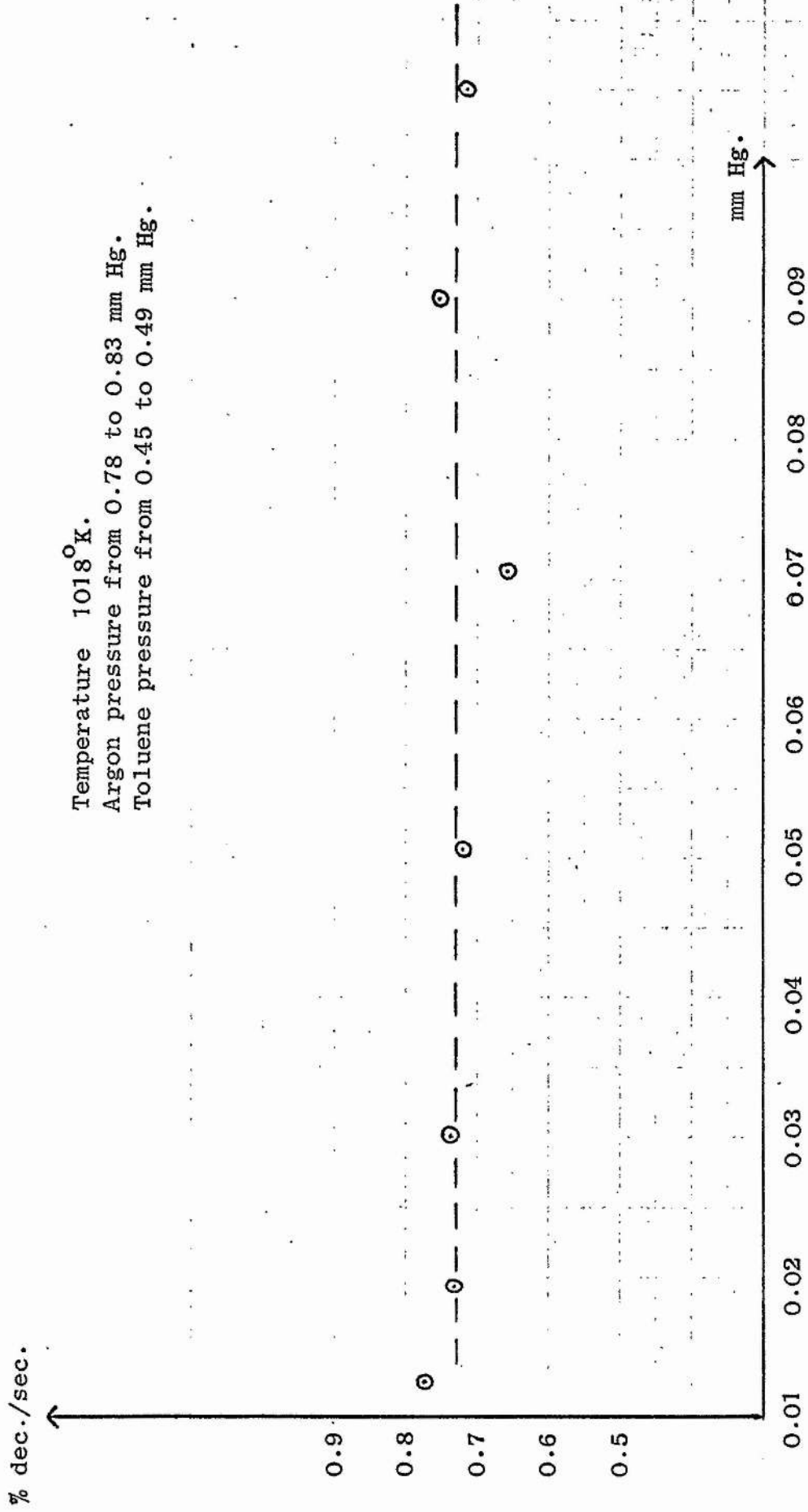


FIG. 33. Methyl bromide partial pressure.

3. Effect of variation of methyl bromide partial pressure.

To analyse the rate dependence of this parameter, all reaction and run conditions were maintained constant with the exception of the methyl bromide injection pressure which was adjusted by the needle valve control (see fig. 3). The results are shown in figure 33 and table I.

TABLE I *

Run	Partial Pressure (mm Hg)			% dec.	t_e (secs.)	% dec./sec.
	MeBr	Tol.	Argon.			
92	0.0125	0.486	0.780	2.00	2.58	0.776
93	0.0193	0.481	0.831	1.87	2.56	0.731
94	0.0301	0.476	0.835	1.87	2.53	0.739
95	0.0511	0.468	0.821	1.79	2.49	0.720
96	0.0705	0.463	0.825	1.61	2.45	0.659
97	0.0900	0.461	0.820	1.84	2.44	0.754
98	0.1050	0.446	0.818	1.68	2.36	0.713

*For an estimation of errors see Appendix VIII.

It will be observed that the percentage decomposition per second has remained virtually constant for a nine-fold increase in the partial pressure of the reactant. The experiments were performed at 1018°K using flow capillary number 1. The results

EFFECT OF VARIATION OF CONTACT TIME. (Data of table II.)

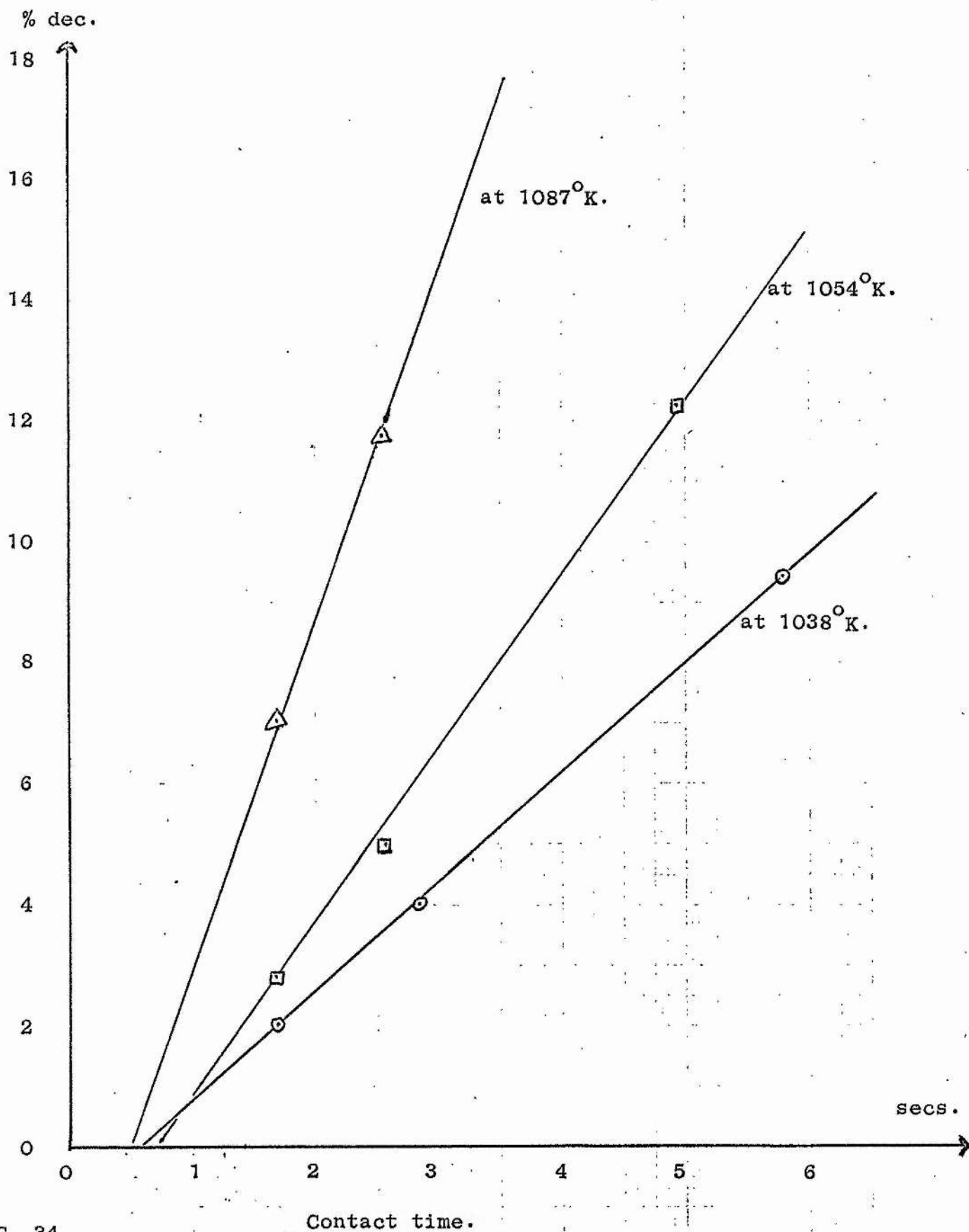


FIG. 34.

Contact time.

indicate a first order dependence on methyl bromide. The contact time varied slightly since the partial pressure was being altered and the small correction relating the percentage decomposition to one second of contact time was applied assuming direct proportionality between the two.

4. Effect of variation of contact time.

The early experiments referred to above, namely of the effect of contact time variation on the decomposition rate, indicating that first order behaviour was being observed, were performed before the full significance of the pressure distribution throughout the flow system was realized. This pressure distribution is described on page 46 . Reassessment of the decomposition rate with variation in contact time was therefore necessary. The data (for the unpacked furnace) is contained in table II and some of it is shown graphically in figure 34. Use of the more accurate first order treatment by plotting $\log [100/(100-\% \text{ decomposition})]$ rather than % decomposition against t_0 serves only to slightly increase the slope giving a similar intercept, assuming a linear relationship. Inclusion of the origin will give the graph an upward curvature. This is contrary to expected first order behaviour which would show a fall off with increasing % decomposition.

TABLE II *

<u>Run</u>	<u>% dec.</u>	<u>t₀ (secs.)</u>	<u>T (°K)</u>	<u>P¹tol. (mm Hg.)</u>
4	4.02	2.85	1038	0.327
5	9.44	5.79	"	0.650
6	2.02	1.70	"	0.196
25	3.33	5.04	1009	0.804
26	1.46	2.65	"	0.434
27	1.07	1.74	"	0.288
28	1.77	1.72	1033	0.288
29	2.72	2.59	"	0.432
30	6.71	4.97	"	0.804
31	12.24	4.94	1054	0.808
32	5.00	2.56	"	0.432
33	2.81	1.68	"	0.280
34	4.31	1.73	1069	0.295
35	7.52	2.58	"	0.437
36	16.94	4.78	"	0.792
37	7.05	1.70	1087	0.291
38	11.79	2.54	"	0.432
39	25.96	4.84	"	0.803
50	8.82	1.21	1106	0.216
51	10.57	1.61	"	0.286
52	17.73	2.42	"	0.439

*For an estimate of errors see Appendix VIII.

The runs were performed with a toluene/methyl bromide ratio of approximately 12 to 15. Variations in contact time were obtained by changing flow capillaries.

It will be observed that the reasonable straight lines pass through a positive intercept on the abscissa of about 0.5 sec. It was at first thought that this might have been the warm-up time for the gas entering the furnace. The gas would be heated by collisions with the wall or with other already heated molecules. An estimate of the time required for the former may be made from kinetic theory. The argument determines the rate of diffusion of a centrally placed molecule to the wall and is set out in Appendix VII. The calculations suggest that a warm-up time of 0.5 secs. is unexpectedly high for the conditions used in the present experiments.

For a given injection rate of reactants, changing the flow capillaries, (and hence the rate of flow of carrier gas), altered the contact time and also the absolute values of the partial pressures of reactants. The partial pressure of a reactant in the furnace under these conditions can be shown to be proportional to the contact time (see Appendix IV).

Since the variations in contact times produced above were obtained by simply changing capillaries it is not fully valid to plot contact time against percentage decomposition, while ignoring the variation in toluene pressure, since there may be a toluene dependence which could explain the intercepts. We had, therefore,

EFFECT OF VARIATION OF TOLUENE/METHYL BROMIDE RATIO. (Data of table III.)

Temperature 1018° K.
MeBr pressure from 0.039 to 0.087 mmHg.
Argon pressure from 0.71 to 0.95 mm Hg.

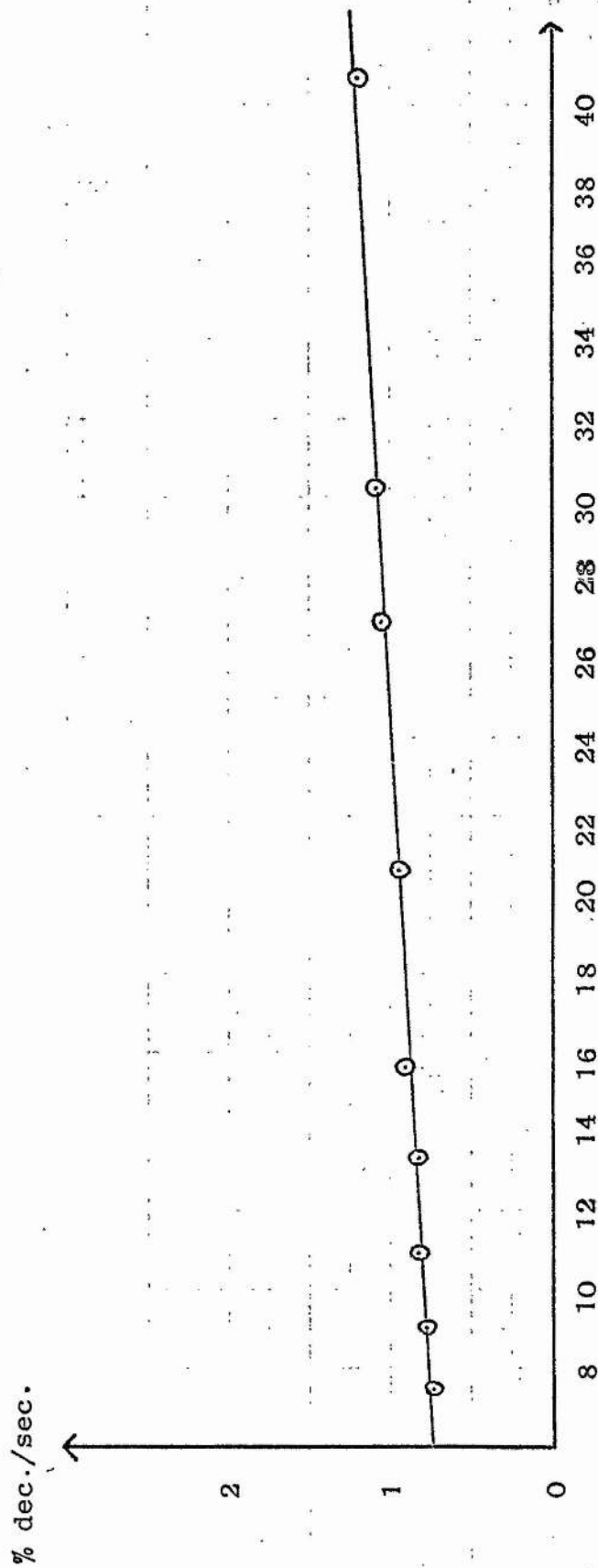


FIG. 35. Toluene/Methyl bromide ratio.

to establish whether the partial pressure of toluene affects the decomposition rate.

5. Effect of variation of toluene partial pressure.

A sequence of runs were performed to produce a variation in the toluene/methyl bromide ratio from 6 to about 40. The experiments at 1018°K were carried out by varying the reservoir temperature for toluene injection. Variations in contact time were again corrected by relating the decomposition of the methyl bromide to one second of residence time. The results are shown in Table III and figure 35. For an assessment of the errors in the measured quantities see Appendix VIII.

EFFECT OF TOLUENE PRESSURE VARIATION ON DECOMPOSITION RATE. (Data of table III.)

Temperature 1018°K.

Argon pressure from 0.71 to 0.95 mm Hg.

Methyl bromide pressure from 0.039 to 0.087 mm Hg.

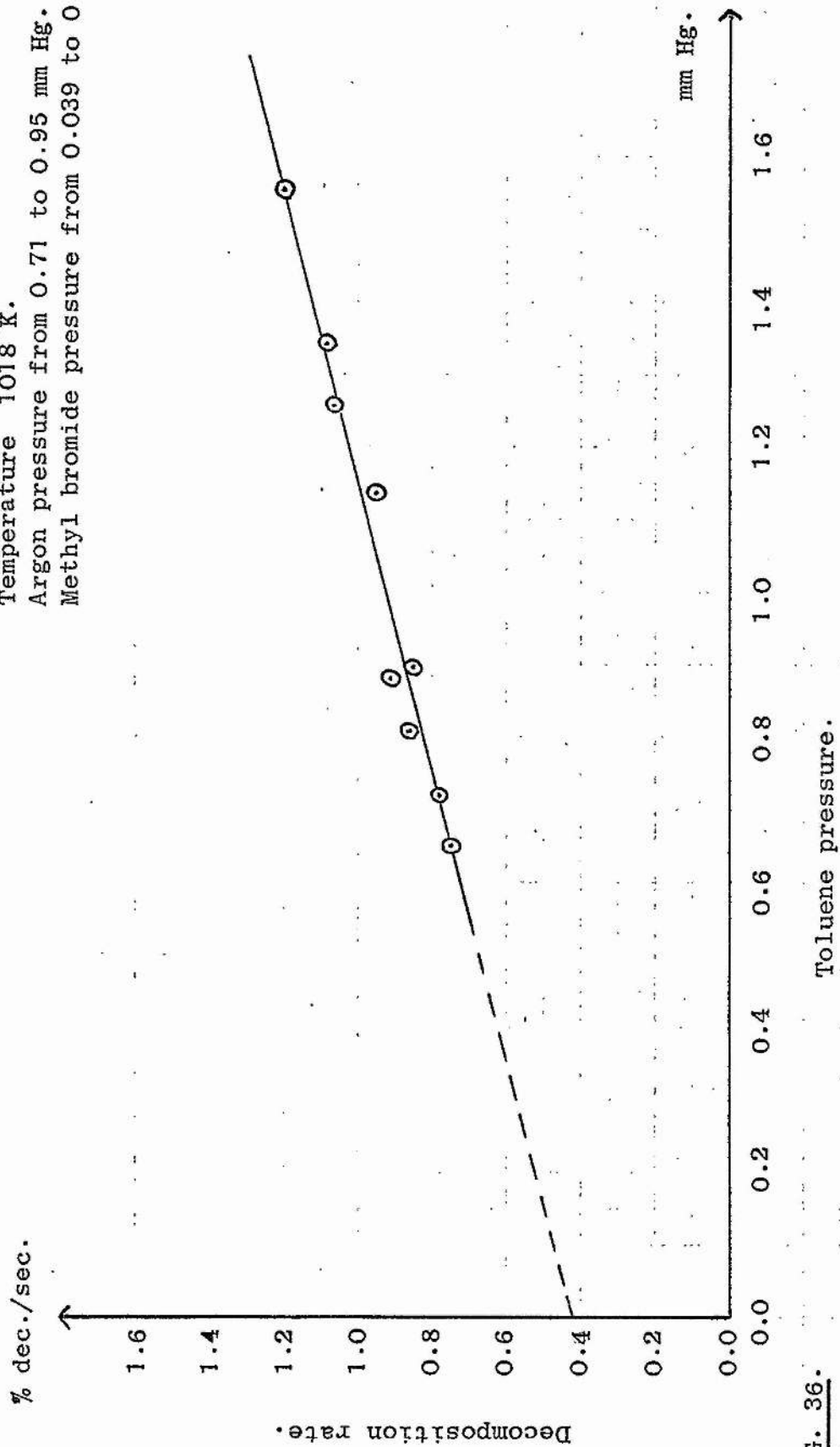


FIG. 36.

TABLE III

Partial Pressures (mm Hg.)

Run	MeBr	Tol.	Argon	% dec.	t_c (secs.)	% dec./sec.	Tol./MeBr ratio
11	0.0872	0.651	0.935	4.40	5.87	0.748	7.47
12*	0.0430	0.326	1.013	1.67	2.87	0.584	7.58
13	0.0800	0.719	0.951	4.27	5.48	0.779	9.02
14	0.0740	0.804	0.813	4.36	5.04	0.866	10.90
15	0.0676	0.896	0.836	3.94	4.61	0.855	13.30
16	0.0675	0.878	0.765	4.26	4.64	0.917	13.60
17	0.0464	1.255	0.711	3.34	3.13	1.065	26.90
18	0.0446	1.340	0.716	3.20	2.95	1.088	30.20
19	0.0552	1.135	0.866	3.55	3.74	0.952	20.60
20	0.0386	1.550	0.833	3.15	2.62	1.200	40.70

* Run 12 is omitted from the graphs since it was performed using a different flow capillary from the rest.

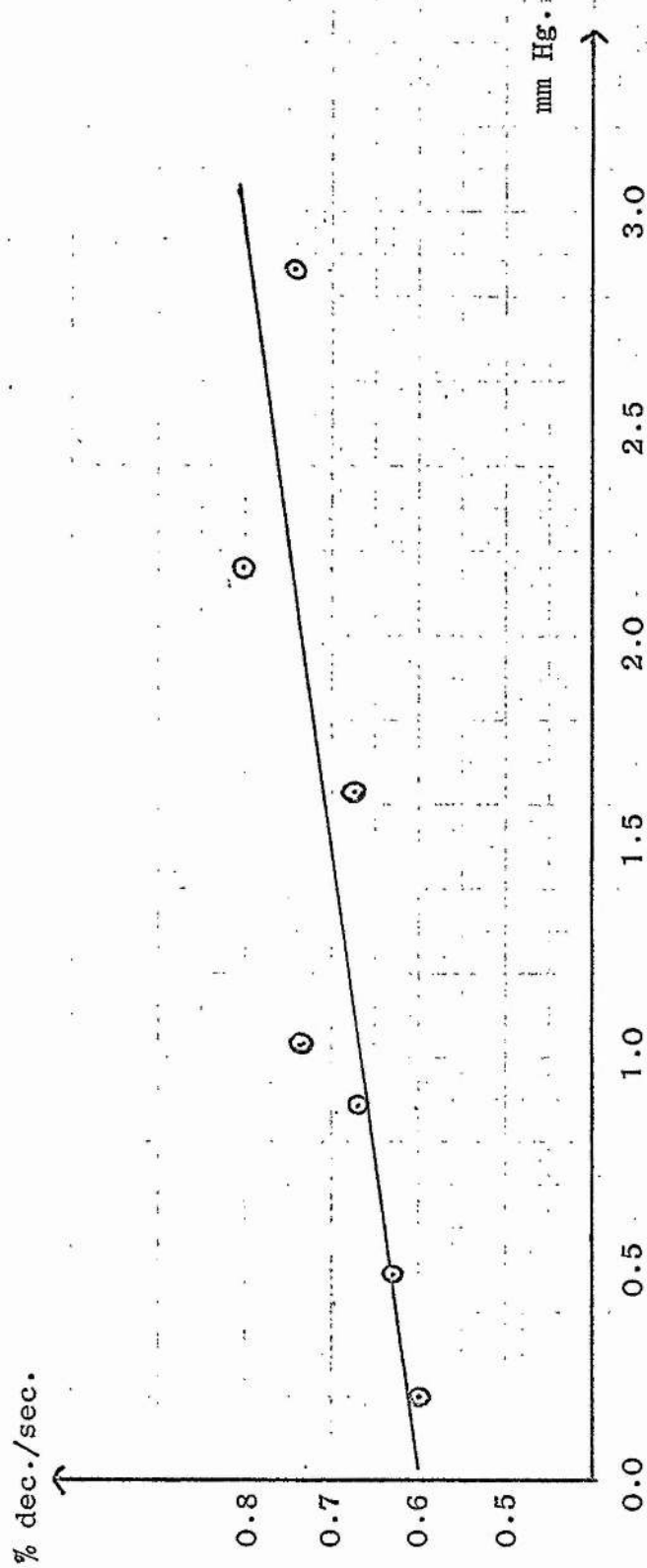
It will be seen that the percentage decomposition increases by about 50% for about a five-fold increase in the ratio of toluene/methyl bromide. For small variations in the ratio the decomposition rate varies only slightly. From such data one can estimate the dependence of the rate on toluene pressure. To do this it is better to plot the absolute partial pressure of toluene against the percentage decomposition. Such a plot is shown in figure 36.

EFFECT OF VARIATION OF ARGON PARTIAL PRESSURE ON DECOMPOSITION RATE. (Data of table IV.)

Temperature 1018° K.

Toluene pressure from 0.36 to 0.51 mm Hg.

MeBr pressure from 0.16 to 0.24 mm Hg.



Argon pressure.

FIG. 37.

Extrapolating linearly back to zero toluene pressure it is apparent that a rate law to fit such data is of the type

$$-d[\text{MeBr}]/dt = k_0[\text{MeBr}] + k_T[\text{MeBr}][\text{Tol.}]$$

It indicates that the presence of toluene aids the decomposition process at these pressures. This may be by energising collisions with the toluene or by a chemical effect of toluene or its decomposition products.

Unfortunately any toluene pressure higher than the maximum used caused the toluene mass spectrum to spread into the region under observation resulting in loss of resolution and inaccuracy in reading peak heights. It was therefore desirable for subsequent runs to keep the toluene pressure as low as practical.

6. Effect of variation of carrier gas pressure.

These experiments, at 1018°K, were performed with contact times as nearly constant as possible. Methyl bromide and toluene injection rates were maintained constant but the variation of the argon in the flow system changed the contact time slightly so the decomposition was again related to one second of residence time. The results are shown in figure 37 and Table IV.

TABLE IV *

Run	Partial pressures (mm Hg.)			% dec.	t_0 (secs.)	% dec./sec.
	MeBr	Tol.	Argon			
99	0.0225	0.461	0.200	1.42	2.36	0.60
100	0.0243	0.514	0.489	1.63	2.59	0.63
101	0.0234	0.495	0.882	1.65	2.50	0.67
102	0.0230	0.486	1.031	1.79	2.42	0.74
103	0.0207	0.436	1.615	1.44	2.15	0.67
104	0.0184	0.398	2.160	1.57	1.95	0.80
105	0.0160	0.362	2.860	1.33	1.78	0.75

* For an estimate of errors see Appendix VIII.

It will be seen that the rate of decomposition increases with increasing carrier gas pressure. The extent of the increase is not as marked as in the case of toluene pressure variation. The spread of points about the line may be due, in part at any rate, to a slight variation in toluene partial pressure between experiments.

Consideration of this graph alone suggests a rate law

$$-d[\text{MeBr}]/dt = k_0[\text{MeBr}] + k_A[\text{MeBr}][\text{Argon}]$$

An interpretation would be that collisions with argon also aid the decomposition of the methyl bromide.

$3 + \log_{10} k_1$

TEMPERATURE VARIATION OF FIRST ORDER RATE CONSTANT IN UNPACKED FURNACE.

Capillary 1. (⊙)
Capillary 4. (×)
Capillary 2 and 1+2+4. (+)

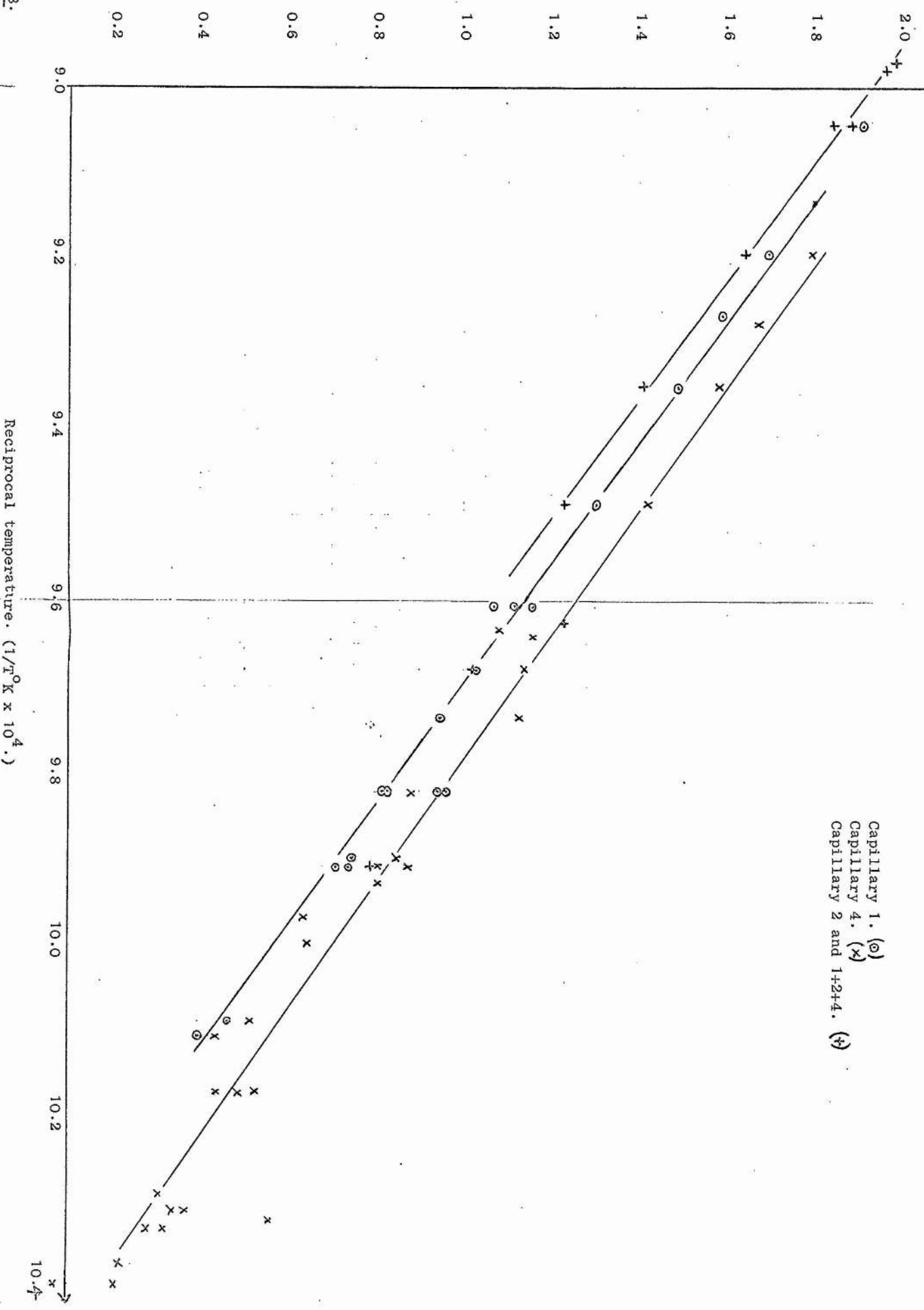


FIG. 38.

Here again experiments could not be extended beyond about 3.0 mm without changing the metrosil leak since the mass spectrometer resolution was lost as a result of the higher pressure in the box in the ion gun. Subsequent experiments were performed with the argon partial pressure at about 1 mm.

7. Effect of temperature variation on the reaction rate in the unpacked furnace.

The above formulations would suggest that at constant toluene/methyl bromide ratios and about constant toluene and argon pressures the reaction would become pseudo-first order in methyl bromide. Hence one may determine the temperature variation of the resultant first order rate constant. The latter was calculated as described in Appendix I and the results are given in figure 38 and in table V in Appendix V.

One noticeable feature is that the three sets of data obtained by the use of the three flow capillaries appear to give three separate approximately parallel lines with an activation energy of about 64 k.cals/mole and an A factor of about 7.0×10^{11} sec.⁻¹. The three lines correspond to three partial pressures of toluene since this is proportional to contact time (see Appendix IV). The data is shown in the composite graph figure 38. There appears to be a larger spread of values of k_1 at the lower temperature end of the

scale. This may be explained by the fact that here very small decompositions are being measured with consequently greater relative experimental error. Comparison of this with published first order rate data will be left to the discussion.

8. Effect of variation of surface/volume ratio of reaction vessel.

The reaction was studied in two furnaces of basically identical design and size. The unpacked furnace had a surface/volume ratio of 1.82 and the other a ratio of 5.2 - this latter will be referred to as the packed or lined furnace. The method of obtaining the increased s/v ratio is fully described on p 66 . The introduction of a liner was felt to be more desirable than the use of silica wool or solid silica spheres. It is difficult to produce a homogeneous packing density with the wool and the use of spheres is open to some doubt if the furnace is not filled completely, and if it is filled then the resistance to flow becomes high and one does not know exactly how much wall area is blanked off.

The study of the rate of seasoning of the packed furnace has been described above on page 69 , and was very similar to the unpacked case. It was apparent however that the increased surface had brought about a higher decomposition rate signifying a fair extent of wall participation in the reaction rate.

Runs were performed as described above to ascertain the temperature dependence of the overall first order rate constant in

$3 + \log_{10} k_1$ ↑

TEMPERATURE COEFFICIENT OF FIRST ORDER RATE CONSTANT IN PACKED FURNACE.

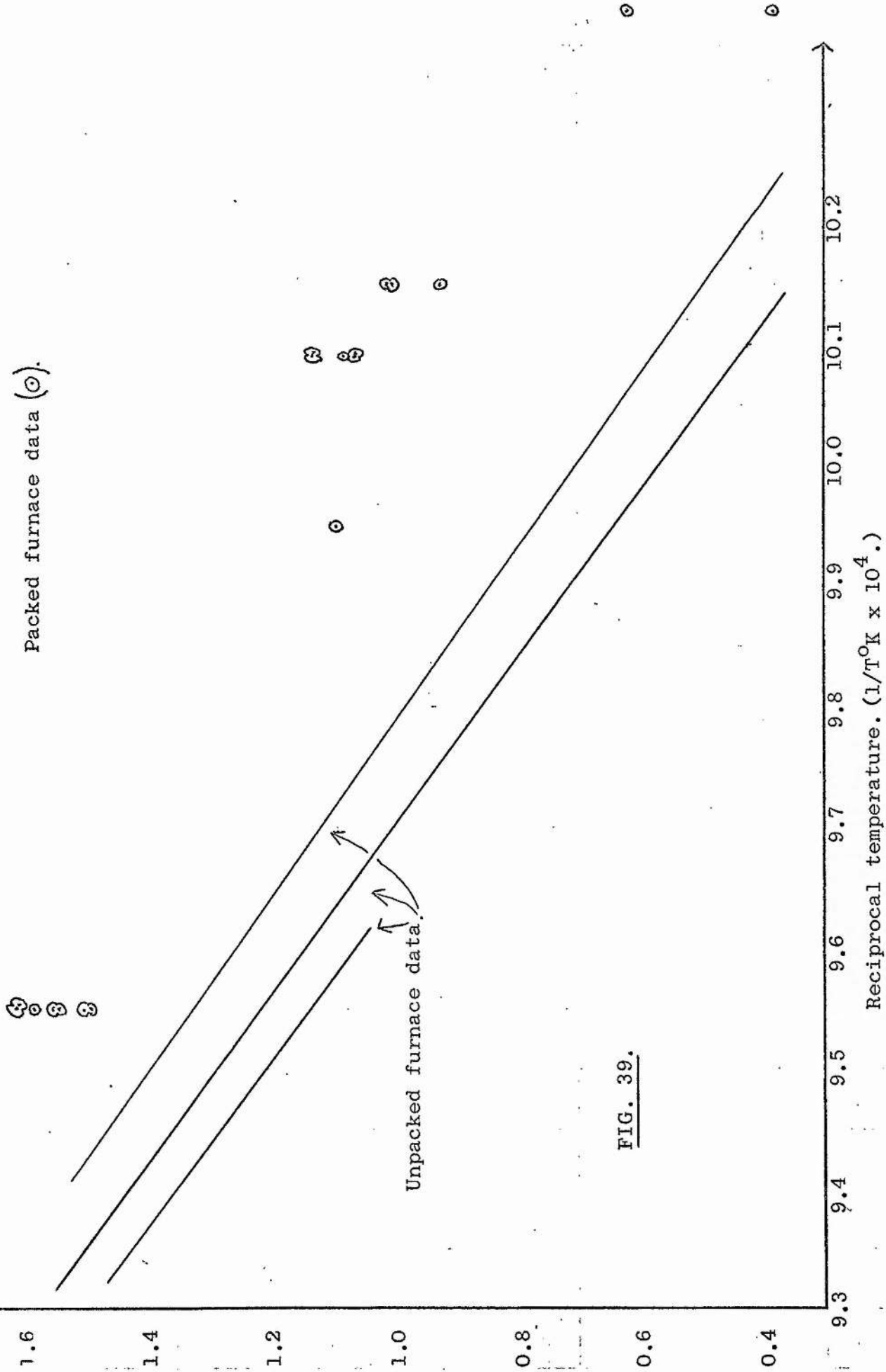


FIG. 39.

the lined furnace. The data is given in Table VI in Appendix VI and is presented in figure 39 in comparison with the equivalent data from the unpacked furnace. The values appear to have a marked spread although the general trend is apparent.

It should be pointed out that the evidence does not prove the presence of a true heterogeneous component in the reaction. Let it suffice at this stage to refer to the 'apparent heterogeneity' and note that the increase in reaction rate resulting from the increased surface may not be true heterogeneity but may be explained by surface interaction with a possible chemical effect.

Any further argument will be left to the discussion.

Variation of partial pressures of toluene and argon.

Temperature 1018°K.

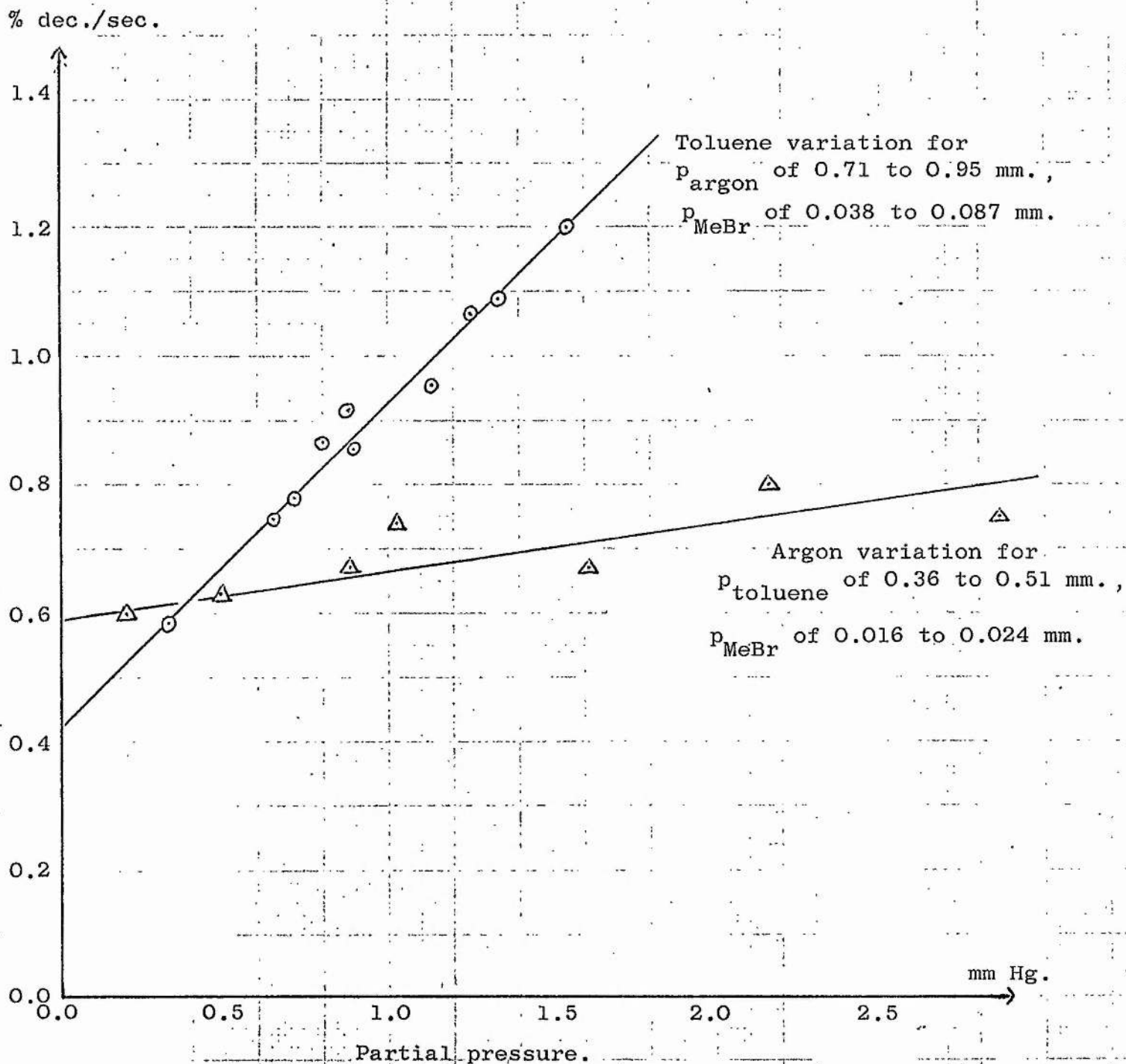


FIG. 40.

DISCUSSIONA. The empirical rate equation, evaluation of the rate constants and their temperature dependence.

The empirical analysis of the effect of variation of both toluene and argon partial pressures, taken along with a first order dependence on methyl bromide (see figures 33, 36, 37), has suggested that the decomposition of the halide in excess toluene and in argon carrier gas can be represented within the range of pressures used by the rate equation:

$$- d [\text{MeBr}]/dt = [\text{MeBr}] \left\{ k_0 + k_T [\text{Toluene}] + k_A [\text{Argon}] \right\}$$

It is the purpose of this section to justify the above analysis.

1. The rate equation

The data of figures 36 and 37 which were obtained at 1018°K are drawn together in figure 40. Also included is run 12 which was omitted in figure 36 because it was based on a very different contact time using another flow capillary. The fact that it is in accord with the other data of the graph is further support for the above treatment.

Clearly from figure 40 the toluene has a greater influence on the decomposition rate than has the argon carrier gas. The rate of activation of a molecule, M, irrespective of the mechanism must be proportional to the partial pressure of M and to the total pressure in the system since the process of activation is essentially bimolecular. If one supposed that at the pressures being used here there

is not a full equilibrium quota of activated methyl bromide molecules to give a first order decomposition, one could interpret the observations as being due to an energy transfer process from the toluene or argon to the halide. One would expect the toluene, being a larger molecule with more degrees of freedom for energy storage, to be more efficient than the argon at handing on energy to the bromide.

If such an interpretation was to be valid for this work one would expect a term $k_M[\text{MeBr}]^2$ to occur, since mutual collisions of methyl bromide molecules will also contribute to the activation process. The methyl bromide concentration, however, is small both in comparison with the toluene pressure and with the argon pressure. To analyse, therefore, for the possibility that a rate equation of the type

$$-d[\text{MeBr}]/dt = k_M[\text{MeBr}]^2 + k_T[\text{MeBr}][\text{Tol}] + k_A[\text{MeBr}][\text{Argon}]$$

might have been confused with the deduced empirical equation, we must re-examine our findings (figure 33) of the nature of the dependence on methyl bromide pressure.

The data was obtained with toluene and argon both held reasonably constant at 0.5 and 0.8 mm Hg respectively, while the methyl bromide pressure was varied from 0.01 to 0.1 mm Hg. The question at issue is whether an empirical equation

$$-d[\text{MeBr}]/dt = [\text{MeBr}] \{ k_0 + k_T[\text{Tol.}] + k_A[\text{Argon}] \}$$

is distinguishable from

$$-d[\text{MeBr}]/dt = [\text{MeBr}] \{ k_M[\text{MeBr}] + k_T[\text{Tol.}] + k_A[\text{Argon}] \}$$

when using our data.

This would depend upon the importance of the terms k_0 and $k_M[\text{MeBr}]$ when compared with the remaining terms. The maximum pressure of methyl bromide was only one fifth of the toluene pressure but we would expect k_M to be larger than k_T if they represent rate constants for energisation. In fact these first terms are represented by the intercepts on the axis in figures 36 and 37, (for [Toluene] and [Argon] equal to zero), and they have substantial values. Misinterpretation might have occurred if the first terms were very small but since a ten fold variation of [MeBr] showed no effect under the conditions of figure 33, it has to be concluded that the empirical equation is well founded. This conclusion argues against an energisation process being involved as the major factor explaining this rate equation.

The two different intercepts on the ordinate of figure 40 may be explained. The intercept on the toluene variation graph corresponds to a residual rate arising from a k_0 for the first order decomposition component of the rate law plus a component $k_A[\text{Argon}]$. Similarly the intercept on the argon variation graph corresponds to the k_0 and $k_T[\text{Toluene}]$ terms.

From the two graphs it is possible to deduce a value of k_0 and at the same time show the mutual consistency of the data. Thus, taking an average value for p_{Argon} at 0.82 mm Hg for graph A (figure 40) one can refer to the slope of graph B to deduce the lowering required to replot A for zero contribution from argon.

CORRELATION BETWEEN GRAPHS OF FIGURE 40.

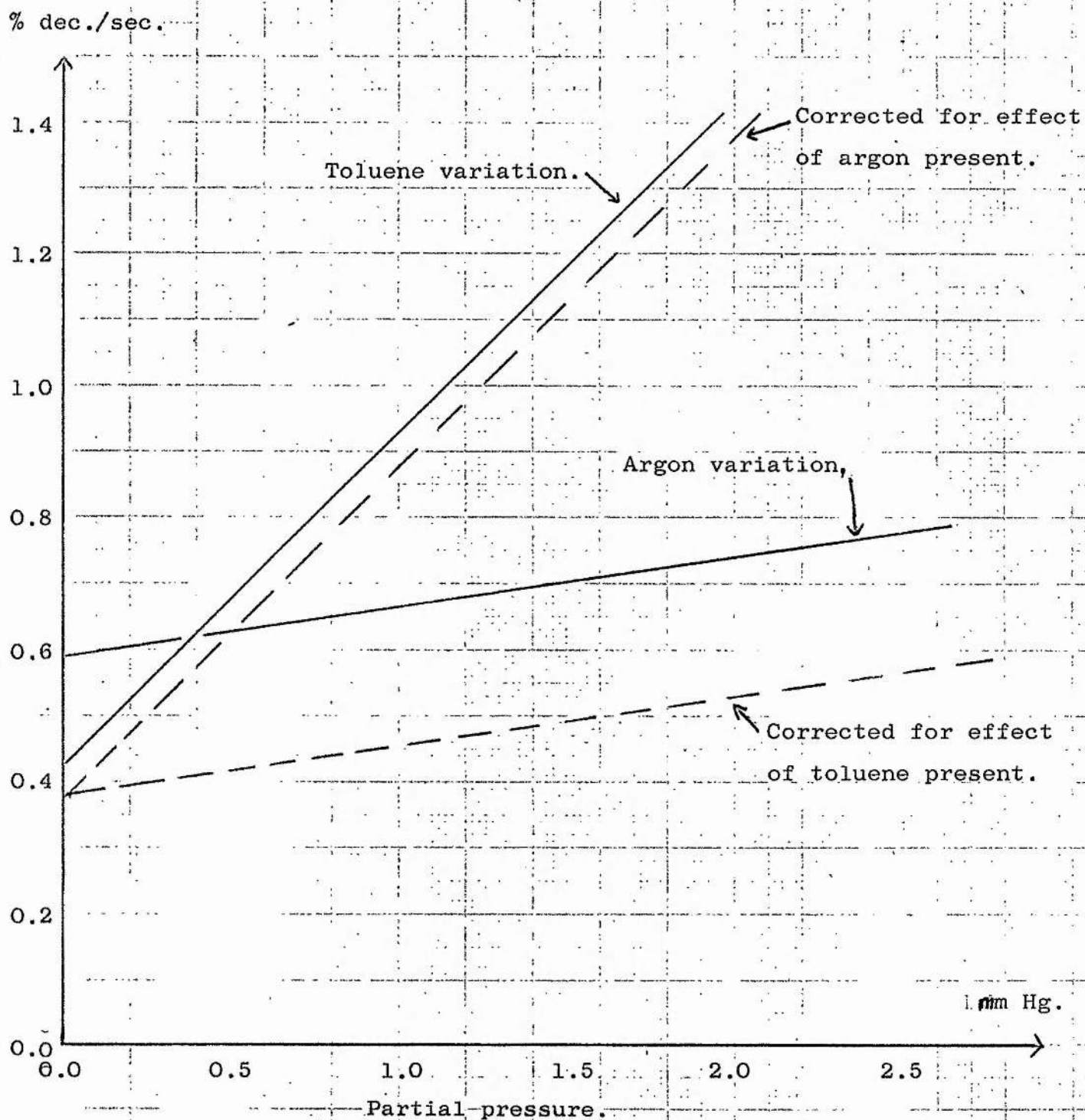


FIG. 41.

COMBINED DATA FOR VARIATION OF TOLUENE AND
METHYL BROMIDE PARTIAL PRESSURES,

Temperature $1018^{\circ}\text{K}.$

Toluene variation data. (\odot)

Methyl bromide variation data. (\triangle)

% dec./sec.

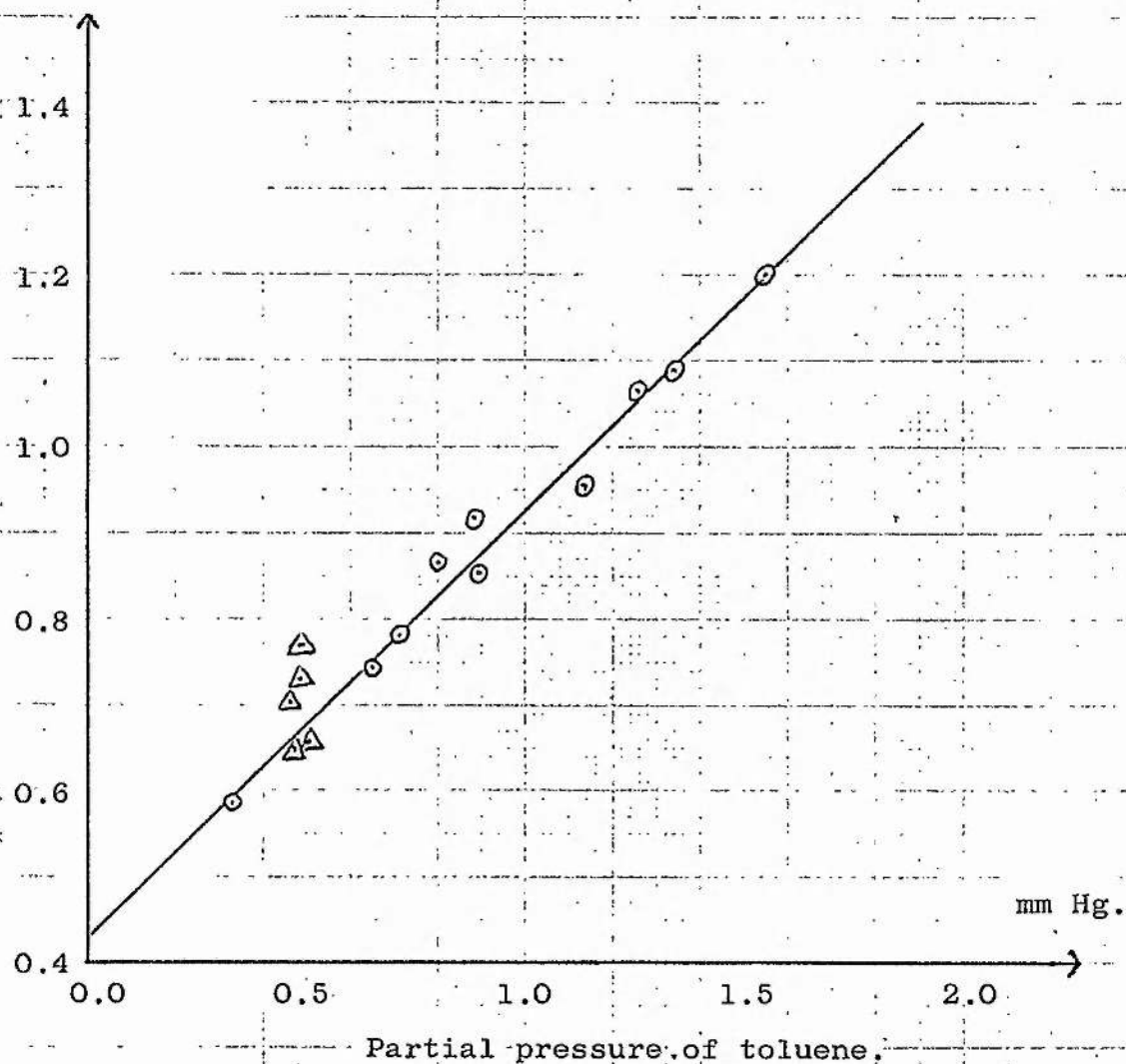


FIG. 42

Likewise an average value of 0.43 mm toluene may be taken as present for graph B and reference to the slope of A will yield the lowering required to replot B for zero toluene contribution. The corrections are drawn in figure 41 and it will be seen that the two lines pass through the same point on the vertical axis. This corresponds to a value with no contribution from toluene or from argon. Such a consistency between the two is good evidence for the validity of the above suggested rate law.

One further point we can make is that the methyl bromide pressure variation data which was obtained at the same temperature may be shown to fit the above graphs. Since the argon pressures for this were about the same as in the toluene variation the points are seen in figure 42 where the data of runs 92, 93, 96, 98 and 101 have been incorporated. They are seen to lie about the same line which is again in agreement with the devised rate law. It is also evidence for the absence of the term in $[\text{MeBr}]^2$ discussed above since the intercept of the line would, if this were the case, be proportional to the methyl bromide pressure. Widely differing methyl bromide pressures give data falling about the one line.

2. Toluene dependence of rate law

When the effect of variation of toluene partial pressure was studied the data (figure 36) were described by the relationship

$$-d[\text{CH}_3\text{Br}] / dt = \{ \text{Constant} + k_T[\text{Toluene}] \} [\text{CH}_3\text{Br}]$$

COMBINED DATA OF SZWARC AND THIS WORK TO SHOW TOLUENE
DEPENDENCE OF FIRST ORDER RATE CONSTANT.

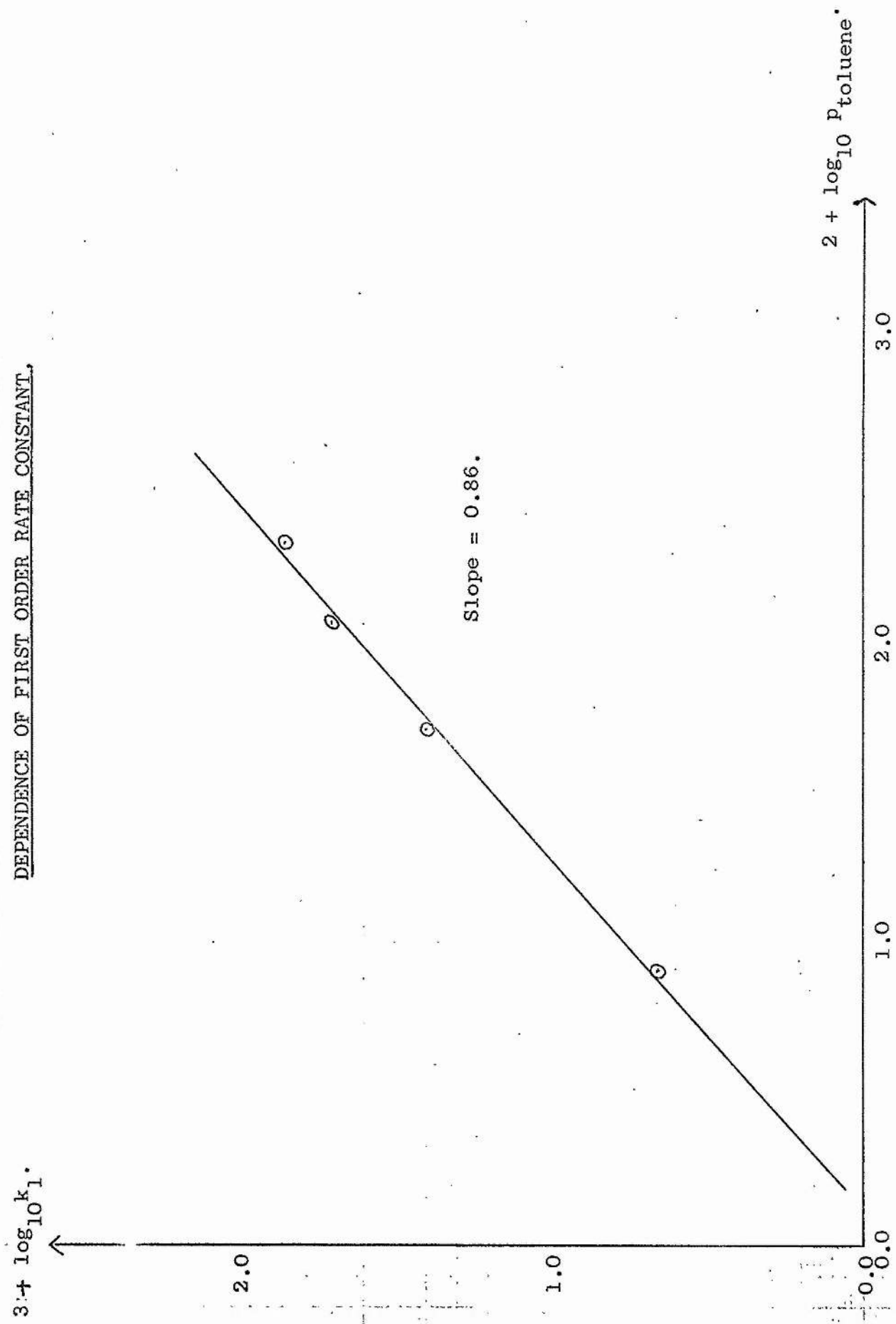


FIG. 43.

It must be said, however, that, with the range of toluene concentrations achievable, it would not be possible to assert that the dependence involved precisely the first power of the toluene concentration. If we consider a formula of the type

$$-d[\text{CH}_3\text{Br}]/dt = \left\{ \alpha + \beta[\text{Toluene}]^n \right\} [\text{CH}_3\text{Br}]$$

the process of evaluating α , β and n cannot be facilitated by setting the toluene concentration equal to zero in an experiment, in order to find α . The chemical reason for including toluene in the reaction mixture requires that it shall be in excess concentration to the methyl bromide, and the assessment of α depends, therefore, on the decision on the values of n and β , followed by an extrapolation. If we take a given set of data for rates of decomposition at varying toluene pressures, and attempt correlations with $[\text{toluene}]^n$ where n is less than unity, it is easy to verify that as n decreases so also does the value of α , while β increases. In the limit this makes the term $\beta[\text{Toluene}]^n$ the dominant one. If we could ignore α it would be easy to evaluate n by plotting $\log(\text{rate})$ against $\log[\text{Toluene}]$. The extent of our own data for the latter was limited experimentally but in figure 43 the data at higher toluene pressures from Szwarc's work (39) have been added to our own. The resultant graph gives a reasonably linear relation yielding a value of $n = 0.86$. This combination of data from two experimental sources is open to several uncertainties arising from differences of method, but it does suggest that even if we ignored the α term we would not get

a value of n much below unity. The limited extent of toluene pressures of our own data makes it insensitive to variations of n near unity and the indications of figure 36, that the rate depends on the first power of the toluene concentration have been taken to permit the evaluation of α . This term yields the plain first order rate constant (k_0) of CH_3Br decomposition.

3. The effect of variations in contact time and in the pressure of carrier gas

The dependence of the rate on argon partial pressure has been shown to be less than on the pressure of toluene. The role the argon plays is not obvious. The possibility of it acting as an energising entity has been disproved since no such energisation was observed for methyl bromide. If the decomposition were in part due to the reaction of some radical or atom with methyl bromide, then one would expect an increase in argon pressure to impede its diffusion to the wall and so to increase the stationary state concentration of the atom or radical and the rate. This may be the case and it will be discussed later. The possibility of the argon occupying wall sites and so reducing the extent of a wall reaction is unlikely since it would be a much more weakly adsorbed molecule than either the toluene or methyl bromide, and in any case such behaviour would reduce the rate.

It would seem from the experimental evidence available, that the rate equation, at first derived empirically, is well founded. One strange feature described in the experimental section may be readily explained by the equation. This was the presence of an intercept of about 0.5 secs if one treated the % decomposition/contact time graph as linear or, of an apparent accelerative effect if one made use of the zero of the graph. The possibility of a warm-up time of 0.5 secs was shown to be unacceptable (see Appendix VII). However, when one appreciates that the toluene pressure, in the experimental method used, was proportional to contact time (see Appendix IV), the relation between % decomposition and t_c becomes parabolic in nature since % dec. = $(\alpha + \beta[\text{Tol.}]) t_c$

$$= \alpha t_c + \beta' t_c^2$$

The removal of the toluene dependence is performed in Appendix IX, where it is shown that a good linear behaviour between % decomposition and contact time is obtained in the initial stages of reaction.

4. Evaluation of k_T , k_A and k_O and their temperature dependence.

It is possible to deduce values of k_T , k_O and k_A from the experimental data presented. Thus for the extensive data at 1018°K the slope of the toluene variation yields a value of k_T and the argon variation yields k_A (see figure 40). The intercepts yield k_O after correction to zero toluene and zero argon values.

GRAPHICAL EXTRAPOLATION FOR α AND α_0 .

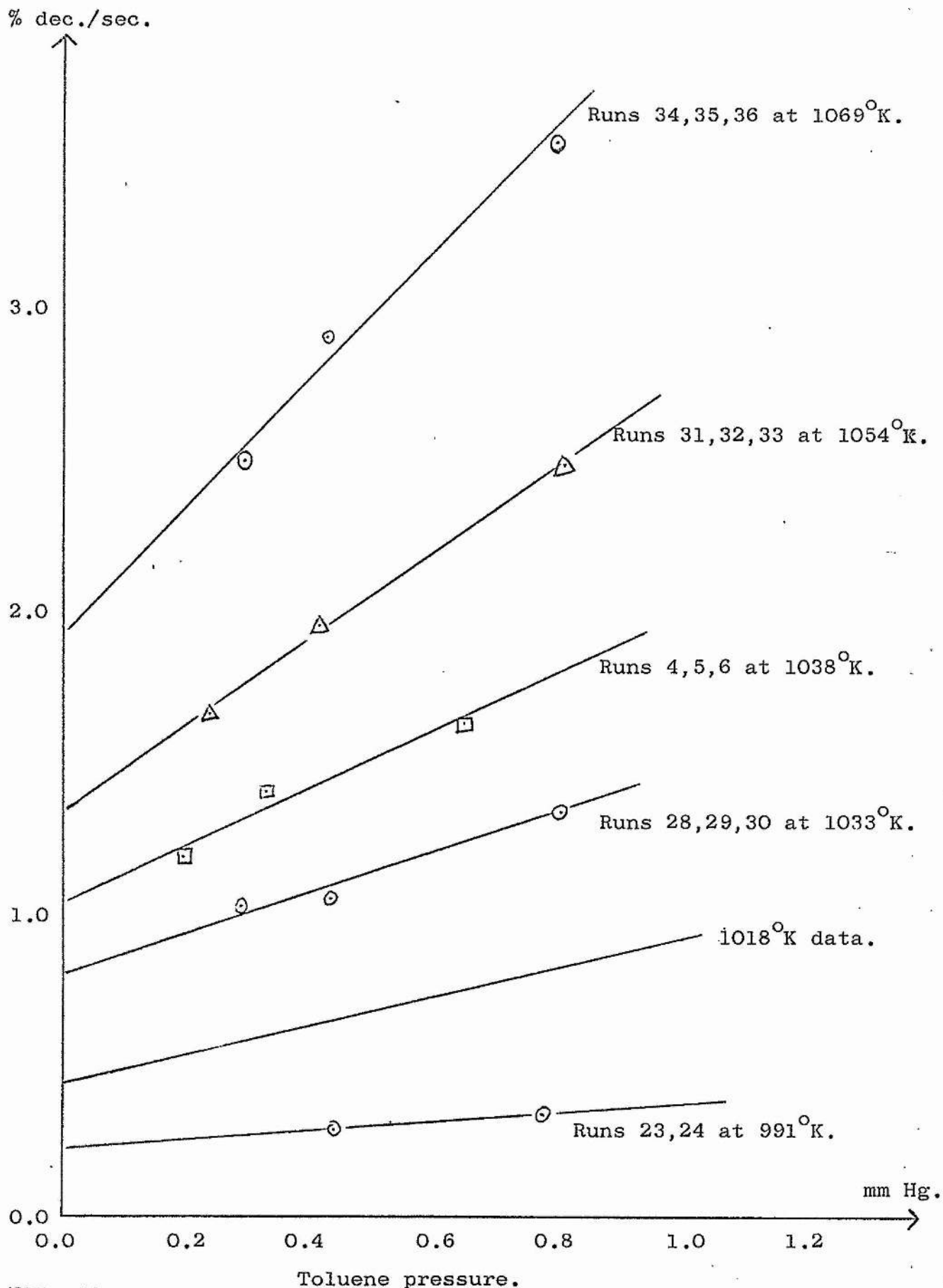


FIG. 44.

Toluene pressure.

In order to determine these slopes and intercepts for all temperatures within our range of investigation it was necessary to restrict the number of separate experiments which were undertaken. Moreover there were certain special difficulties which were a consequence of the temperature range. Thus all the flow capillaries could not be used over the full temperature range; at the lower temperatures and with the higher flow rates (lower contact times) the decompositions were too low to be measured accurately.

The data from the experiments gave values for the percentage decomposition at various temperatures for two or three values of toluene pressure, and by graphing such data in the manner of figure 40, values for the slope β (in % decomposition $\text{CH}_3\text{Br}/\text{sec. mm}$ toluene) and intercept a (in % decomposition/sec.) were obtained.

Some of the data are shown in figure 44. The extensive information at 1018°K is also graphed. The data of these and other plots are given in Table VII. It will be seen that β varies appreciably with temperature as does a_0 . The value a_0 corresponds to k_0 for the homogeneous decomposition of CH_3Br , and a is $a_0 + \alpha_A[\text{Argon}]$. a_0 was obtained from the intercept by subtraction of a quantity $\alpha_A[\text{Argon}]$ where $[\text{Argon}]$ is the argon pressure used for the group of runs. The value of α_A was estimated at $\beta/6.7$; this value being obtained from the extensive data at 1018°K . Although it is realized that the choice of ^{the} fraction $1/6.7$ is open to some doubt if used over the full temperature range, it is felt that the error

involved in using this value is small since (a) it was obtained at a representative temperature near to the middle of the range and (b) the value of α_A is not large when compared with α_o .

TABLE VII

<u>Run</u>	<u>Temp. ($^{\circ}$K)</u>	<u>α^*</u>	<u>β^+</u>	<u>α_A^+</u>	<u>[Argon] (mm)</u>	<u>α_e^*</u>
37,38,39	1087	3.48	2.42	0.362	0.82	3.18
9,10	1078	3.30	1.20	0.179	1.00	3.12
34,35,36	1069	1.92	2.10	0.313	0.74	1.69
31,32,33	1054	1.33	1.44	0.215	0.90	1.14
4,5,6	1038	1.04	0.96	0.143	1.00	0.90
28,29,30	1033	0.80	0.66	0.099	0.83	0.72
77,78	1027	0.33	1.20	0.179	0.72	0.20
Many.	1018	0.44	0.50	0.075	0.78	0.38
75,76	1009	0.25	0.60	0.089	0.73	0.18
23,24	991	0.23	0.14	0.021	0.68	0.22
21,22	981	0.20	0.18	0.027	0.90	0.18

* Units are % decomposition/sec.

+ Units are % decomposition/sec mm.

Consideration of the extrapolation procedures in figure 44 showed how sensitive to errors are the derived values of the slopes and intercepts on the axes when few points are available per graph. Indeed, attempts to derive energies of activation for the two terms showed considerable scatter in the data. It was decided, therefore, to endeavour to graph the data in a manner which would lead to the possibility of a smoothing procedure. Most of the experiments of

$1 + \log_{10} (\% \text{ dec. / sec. mm})$ DATA OF EXTENT OF DECOMPOSITION FOR 0.8 AND 0.4 mm PRESSURE OF TOLUENE.

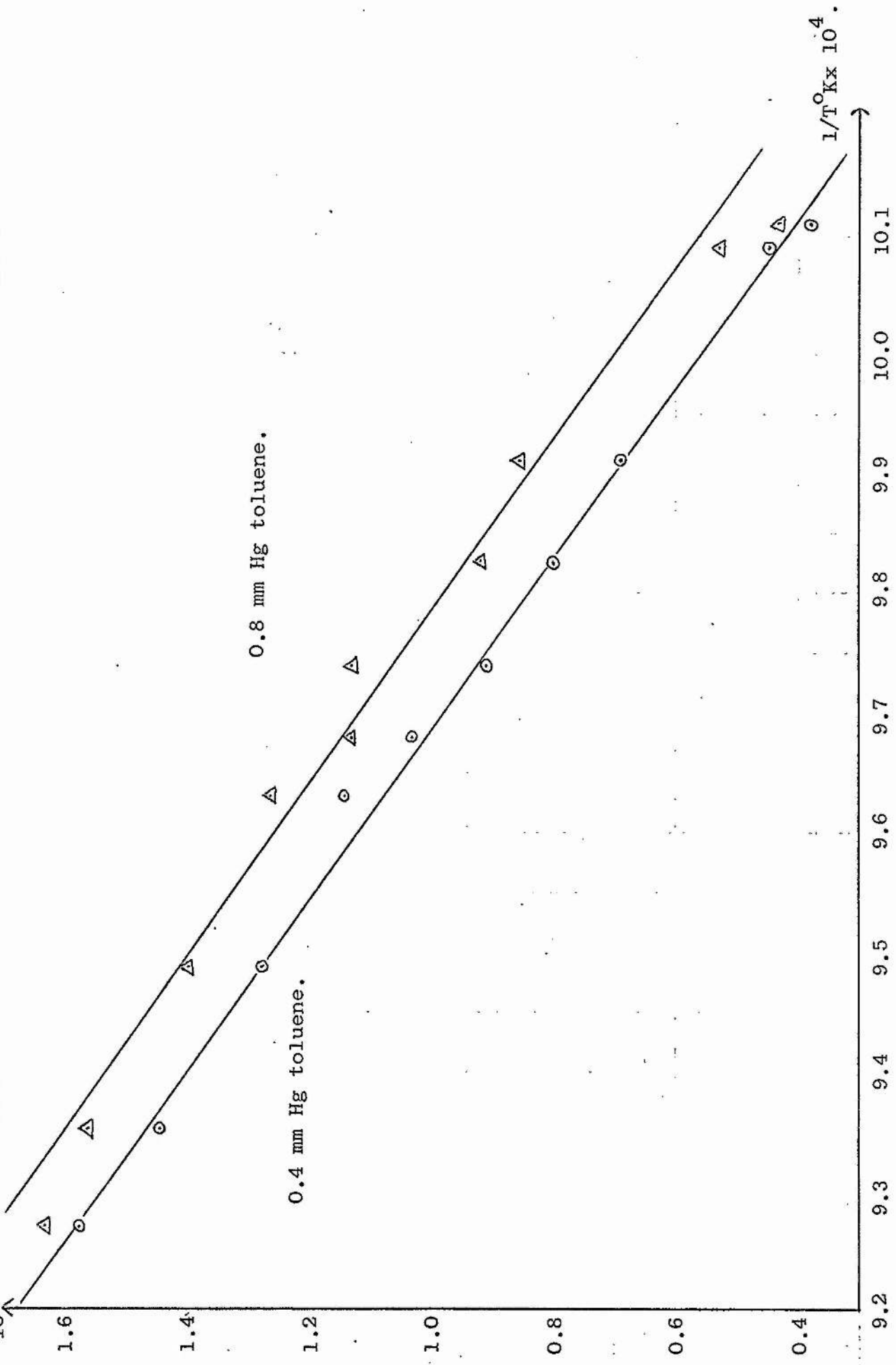
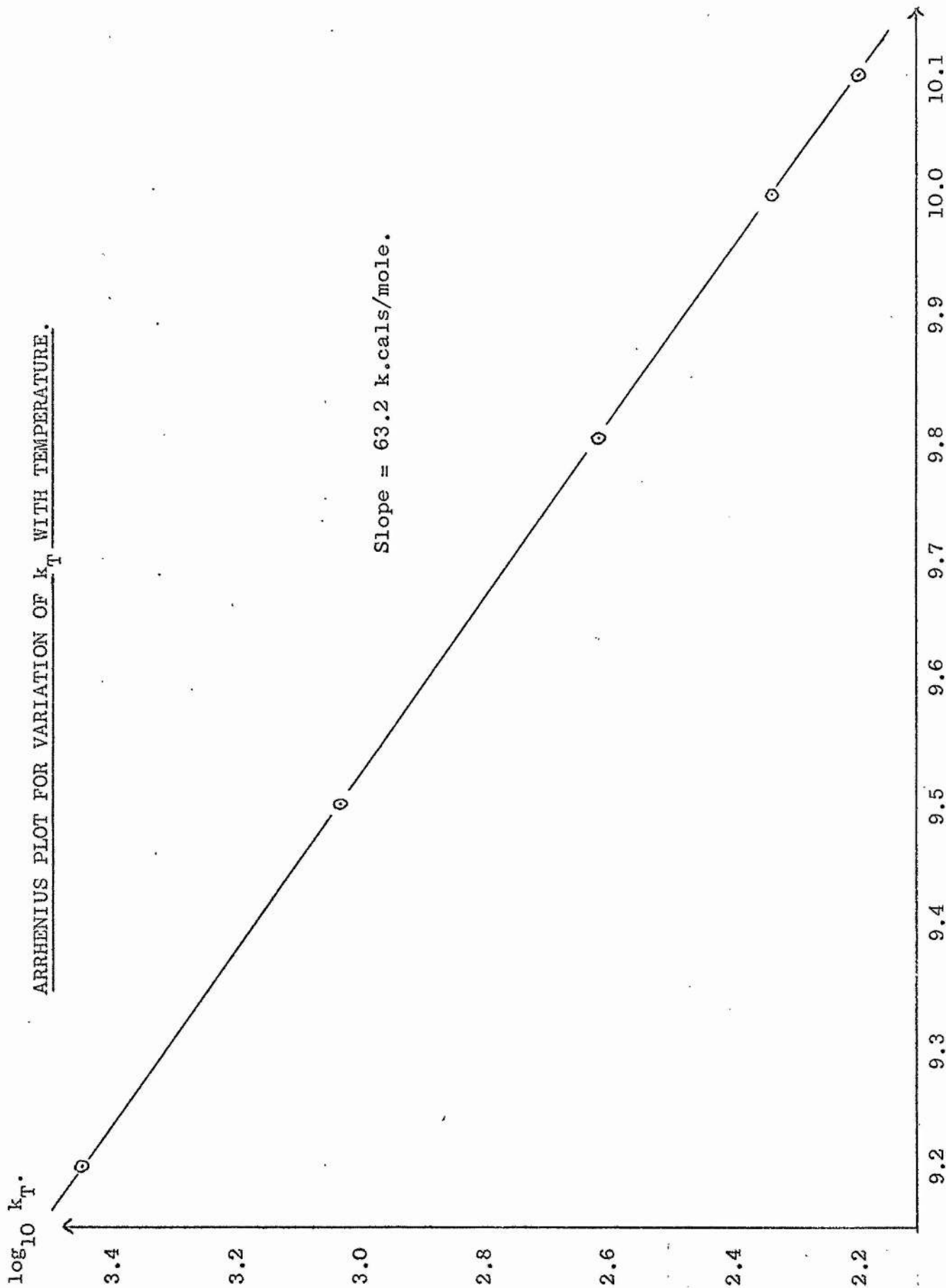


FIG. 45. Reciprocal temperature.

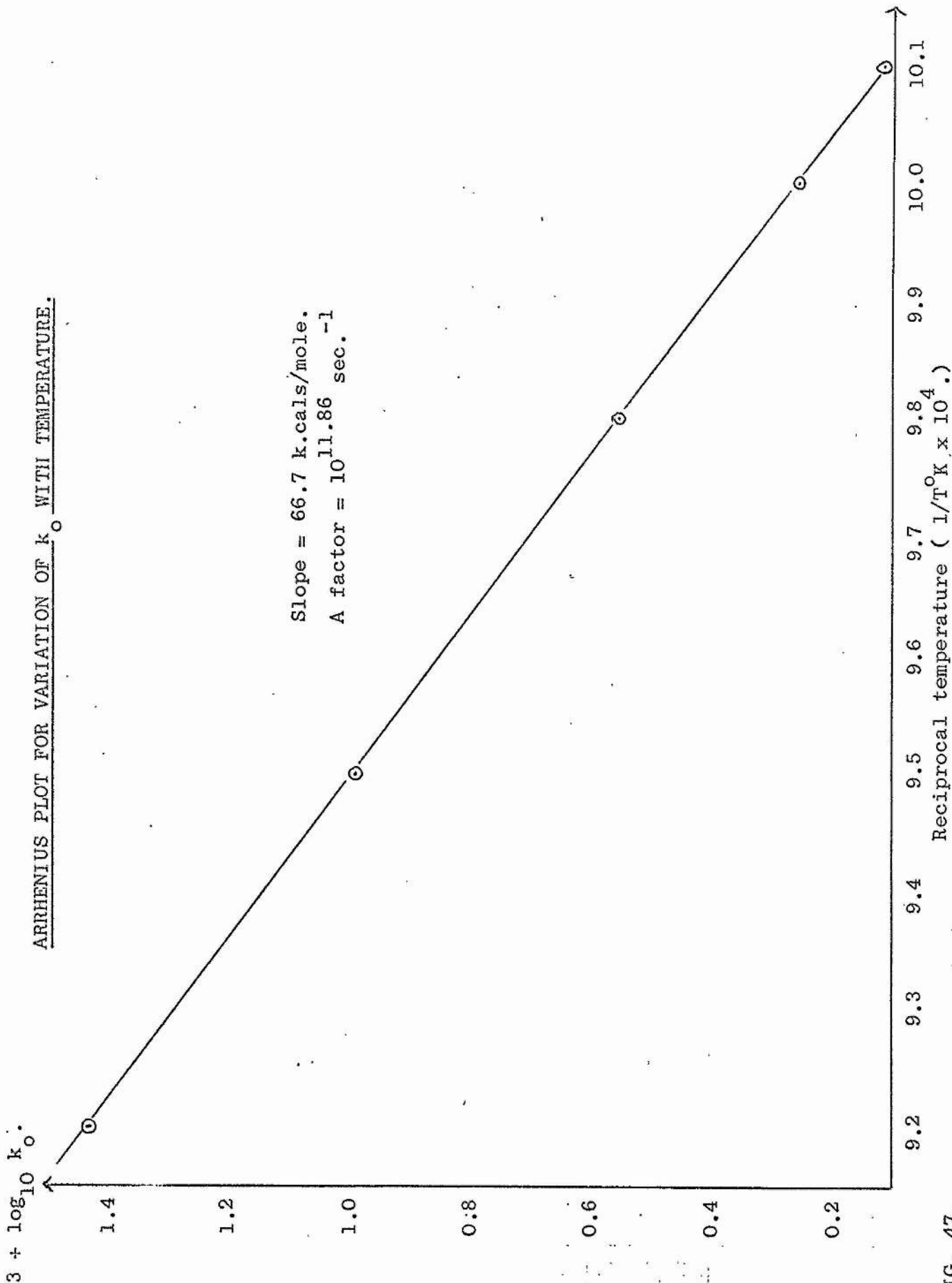
ARRHENIUS PLOT FOR VARIATION OF k_T WITH TEMPERATURE.



Reciprocal temperature ($1/T^{\circ}K \times 10^4$.)

FIG. 46.

ARRHENIUS PLOT FOR VARIATION OF k_0 WITH TEMPERATURE.



Slope = 66.7 k.cals/mole.
A factor = $10^{11.86} \text{ sec.}^{-1}$

FIG. 47.

figure 44 were conducted at pressures of toluene near to 0.8 and 0.4 mm. Using the graphs of figure 44, the values of percentage decomposition per second were read off at various temperatures for exactly 0.4 and 0.8 mm toluene pressures. The logarithms of these values were then plotted against $1/T^{\circ}\text{K}$. This showed an almost linear relationship for the data at 0.4 mm, one discordant experiment being quite discernible. The data at 0.8 mm showed much greater scatter but in view of the relationship applying to the 0.4 mm data the best straight line was drawn in this case also (see figure 45).

From these lines one can take data to plot the variations of α_0 and β with temperature. These are drawn (data in Table VIII) in figures 46 and 47 where the true rate constants have been used in Arrhenius type plots. The slopes lead to an activation energy of 66.7 k.cals/mole and a frequency factor of $10^{11.86} \text{ sec}^{-1}$ from the variation of k_0 and a value of 63.2 k.cals/mole for the activation energy of the toluene dependence.

TABLE VIII(a) Data from Figure 45 to obtain β and k_t .

$(1/T^{\circ}\text{K}) \times 10^4$	<u>% dec./sec.</u>		β (<u>% dec./sec. mm</u>)
	<u>0.8 mm</u>	<u>0.4 mm</u>	
9.2	6.40	4.78	4.05
9.5	2.45	1.81	1.61
9.8	0.946	0.691	0.638
10.0	0.501	0.363	0.345
10.1	0.364	0.263	0.253

$(1/T^{\circ}\text{K}) \times 10^4$	k_t ($\text{sec}^{-1}\text{mm}^{-1}$)	k_t (sec^{-1} moles $^{-1}$ litres)	$\log_{10} k_t$
9.2	0.0413	2.79×10^3	3.446
9.5	0.0163	1.06×10^3	3.027
9.8	0.00640	0.408×10^3	2.610
10.0	0.00345	0.214×10^3	2.331
10.1	0.00253	0.156×10^3	2.194

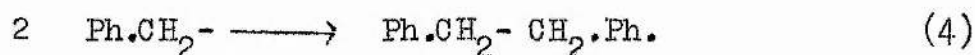
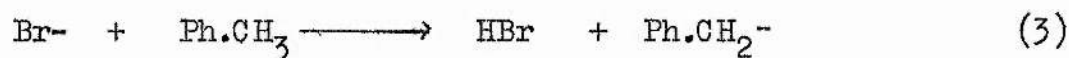
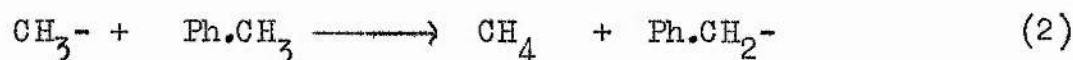
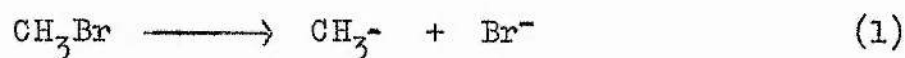
(b) Evaluation of α_0 and k_0 .

$(1/T^{\circ}\text{K}) \times 10^4$	α (<u>% dec./sec.</u>)	α_1 [Argon]*	α_0 (<u>% dec./sec.</u>)	$\log_{10} k_0$
9.2	3.16	0.514	2.646	$\bar{2}.429$
9.5	1.17	0.204	0.966	$\bar{3}.985$
9.8	0.436	0.081	0.355	$\bar{3}.550$
10.0	0.225	0.044	0.181	$\bar{3}.255$
10.1	0.162	0.032	0.130	$\bar{3}.114$

* An average value of 0.85 mm for [Argon] was used in the calculations.

B. Possible reaction sequences and mechanistic considerations

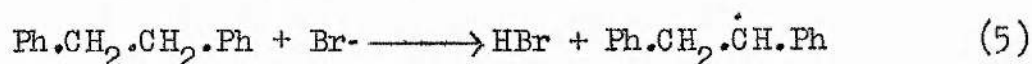
The pyrolysis of methyl bromide in the presence of toluene is assumed by Szwarc (39) to follow fairly closely the reaction scheme:



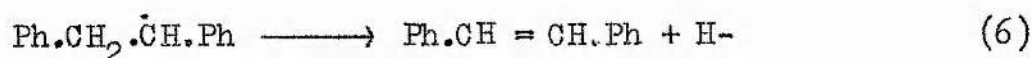
Reaction (1) was assumed to be the slow rate determining step in the sequence and reactions (2) and (3) were assumed to be rapid. Finally dibenzyl was formed by dimerization of two $\text{Ph}\cdot\text{CH}_2^-$ radicals. Reaction (2) has been widely studied (see page 17) and proceeds with an activation energy of about 10 k.cals/mole. Reaction (3) similarly proceeds with a low activation energy (see page 19) of about 7 k.cals/mole. With toluene in excess the above reactions should represent the fate of the methyl radicals and bromine atoms.

The reaction, however, is not as straightforward as one might hope or anticipate on the above scheme. For example, in the experiments of Schon and Szwarc, the amounts of dibenzyl and methane produced were smaller than expected on the basis of the above sequences. Their analysis was obtained by subtracting the dibenzyl, methane and hydrogen produced by the decomposition of the toluene alone from the decomposition products of the reacting mixture. They

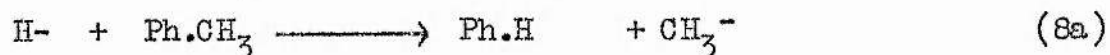
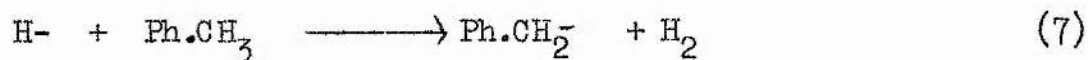
explain the reduced dibenzyl and methane by the possible association of methyl and benzyl radicals. They also observed increased amounts of hydrogen compared with the yield from toluene alone. The dibenzyl formed contained impurities which led to one suggestion of a partial dibenzyl decomposition into stilbene and hydrogen. Their alternative explanation was that bromine atoms attacked dibenzyl to form a dibenzyl radical and HBr:



The dibenzyl radical could then decompose as follows:



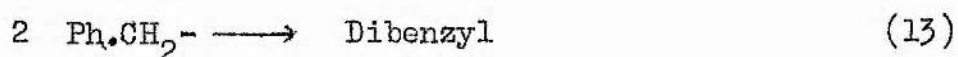
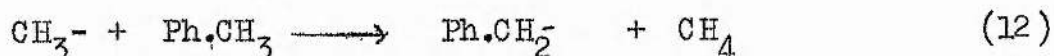
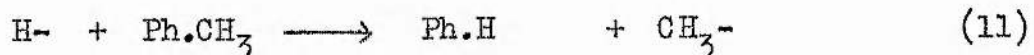
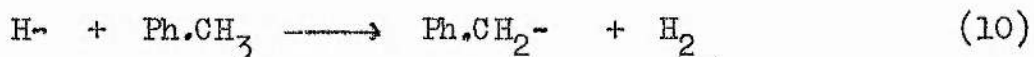
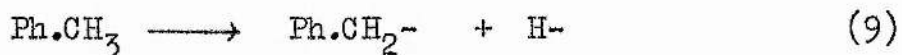
followed by:



Reactions (7) and (8) produced the hydrogen and methane in the ratio 6:4. The workers assumed that HBr produced by (5) was small and that HBr production was approximately equivalent to the rate of the dissociation process (1).

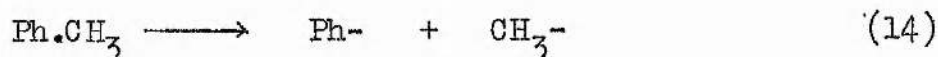
We can perhaps make alternative suggestions if we first of all examine the toluene decomposition. A thorough examination has been made by Smith (8), and by others (43, 44, 45, 46).

In the temperature range 1000 to 1150°K the toluene decomposition has been stated to follow the reaction scheme set out below:

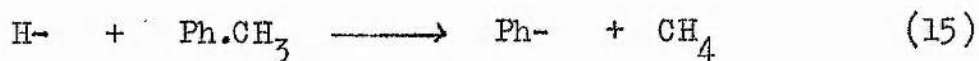


That the decomposition is, in fact, much more complex than the above scheme, has been shown by Smith (8) who found the composition of the solids produced to be not 100% dibenzyl but 50 to 60 mole per cent dibenzyl and the remaining solids a mixture of dimethyl diphenyls and monomethyl diphenyls in the ratio 4:1.

Further she estimated the heat of dissociation of reaction (14) at 92 k.cals./mole compared with the 84 k.cals./mole of reaction (9).



Deducing entropy changes for reactions (9) and (14) by using Trotman-Dickenson's method for estimating entropies of large radicals, namely by the addition of 1.4 e.u. for the electronic degeneracy of the radical to the parent molecule, and relating this entropy change to the A factors suggested that at 1100°K reaction (14) could approach the rate of (9). Reaction (15) is also postulated as a possible additional source of methane.



For the above reasons Smith was cautious about identifying her activation energy with the side-chain C-H bond dissociation energy. More recent work however as discussed in the introduction to this thesis has shown that a value of $D(\text{Ph}\cdot\text{CH}_2-\text{H}) = 84 \text{ k.cal./mole}$ is now generally acceptable.

The decomposition of methyl bromide requires a fairly high temperature (about 1000°K); as a result there must be some degree of decomposition of toluene. Being in excess its primary decomposition products may be present in such concentrations as to initiate decomposition of methyl bromide and so to interfere with a simple kinetic scheme whereby the radical products from the halide arise only by its dissociation and are quickly and efficiently removed by the toluene present.

We may estimate the relative extents of the toluene and methyl bromide decompositions. Taking toluene to have a rate constant given by

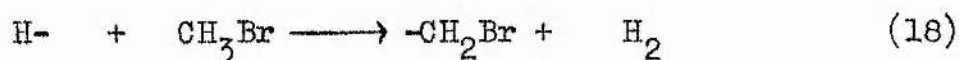
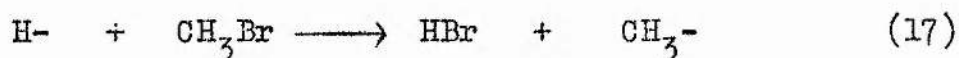
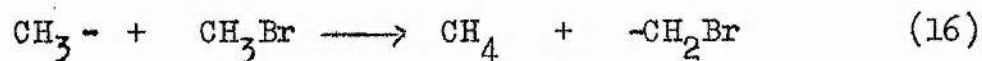
$$k_{\text{Tol}} = 10^{15.1} \exp. (-84700/RT) \text{ sec.}^{-1}$$

as obtained by Smith (8) and assuming the methyl bromide rate of unimolecular decomposition to be given by $k_{\text{MeBr}} = 10^{11.86} \times \exp(-66700/RT) \text{ sec.}^{-1}$ obtained in this work, one can see that, if the toluene/methyl bromide ratio is about 20/1, the relative extents of decomposition at 1000°K , under our conditions, are:

$$\begin{aligned} \frac{\text{Toluene decomposition}}{\text{Methyl bromide decomposition}} &= \frac{20 \times 10^{15.1} \times 10^{-84700/4570}}{1 \times 10^{11.86} \times 10^{-66700/4570}} \\ &= \underline{4.} \end{aligned}$$

Such a calculation illustrates the extent of the toluene decomposition at the temperatures used. Experimental evidence of this was available from the early data when the reaction was being followed by methane and hydrogen production rates as described on Page 54. Figure 20 shows that the methane from a blank experiment was about two thirds of the methane obtained in a run with both reactants present.

In view of the above it would not be unreasonable to propose that the 'impurities' of Szwarc may have been decomposition products of toluene alone, or the results of such products attacking the methyl bromide. Possible reactions which one might consider are:



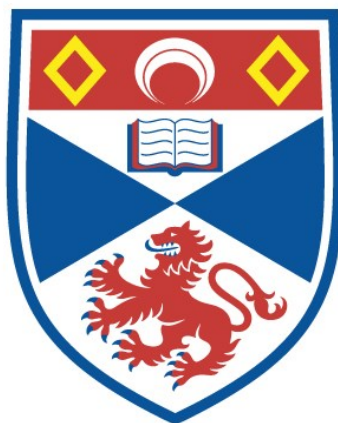
The fate of the $\cdot\text{CH}_2\text{Br}$ radical could be represented by reaction with toluene to reform a methyl bromide molecule by hydrogen abstraction. Alternatively, a unimolecular decomposition could lead to a bromine atom and a methylene radical ($\cdot\text{CH}_2$). The former would be lost by the desirable reaction (3) while methylene radicals have been said to produce carbon and methane (147, 148).

Reaction (16) is approximately thermoneutral and proceeds with an activation energy of about 10 k.cals/mole. Steacie (150) quotes 10.1 k.cals/mole relative to the methyl radical combination reaction

THE DEVELOPMENT OF AN IMPROVED KINETIC
FLOW TECHNIQUE AND ITS APPLICATION TO THE
PYROLYSIS OF METHYL BROMIDE

Gordon Robert Woolley

A Thesis Submitted for the Degree of PhD
at the
University of St Andrews



1965

Full metadata for this item is available in
St Andrews Research Repository
at:

<http://research-repository.st-andrews.ac.uk/>

Please use this identifier to cite or link to this item:

<http://hdl.handle.net/10023/14802>

This item is protected by original copyright

and Gordon and Taylor obtained a value of 6.6 k.cals/mole (149). Reaction (17) is exothermic to the extent of about 20 k.cals/mole. Chadwell and Titani (145) quote an activation energy of 6 → 7 k.cals/mole for reaction (17) assuming a steric factor of unity. Polanyi et al. (146) quote a value not greater than 3.2 k.cals/mole. It is thus a possible cause of loss of methyl bromide as is the approximately thermoneutral reaction (18). If increasing the toluene concentration led to increased hydrogen atom concentrations in the reacting system, then reactions (17) and (18) could explain the increased rate. In order to assess the possible extent of reactions (17) and (18) one must compare them with the rate of loss of hydrogen atoms by the alternative reaction (10).

The activation energy for (17) may be taken as about 5 k.cals/mole. There appears to be no reliable value for the activation energy for the attack of H- on toluene. The relative extents of the hydrogen atom abstraction reactions with methyl bromide and with toluene, assuming a 20:1 excess of the latter will be given by:

$$\frac{\text{Rate from toluene}}{\text{Rate from CH}_3\text{Br}} = \frac{20}{1} \cdot e^{\Delta E/RT}$$

where ΔE is the difference in activation energies between attack on toluene and on methyl bromide. Even for equal activation energies the rate from toluene will be 20 times greater simply because it is in excess. One might anticipate an activation energy for attack on toluene to be the same or slightly larger than for the methyl

bromide case which would tend to increase the above ratio.

Reactions of bromine atoms with methyl bromide have been omitted. These are unfavourable on energetic grounds and the bromine atom concentration is likely to be very low since it is derived only from the decomposition of methyl bromide.

C. Analysis of the rate equation

It is the purpose of this section to attempt an explanation of the experimentally observed rate equation:

$$-d[\text{MeBr}]/dt = k_o[\text{MeBr}] + k_T[\text{MeBr}] [\text{Tol.}] + k_A[\text{MeBr}] [\text{Argon}].$$

The analysis and verification of this equation presented so far in the discussion has used experimental data from the unlined furnace. The data corresponds to rates determined for a fixed surface/volume ratio. Until it was realized that the reaction was strongly dependent upon surface area, the possibility of the second term in the above equation being due to a homogeneous bimolecular reaction in the gas phase had not been rejected. Klemm and Bernstein (140), showed that the gas phase decomposition of methyl iodide in toluene at 326 to 374°C was represented in part by a bimolecular reaction:

$$-d[\text{MeI}]/dt = k_1[\text{MeI}] [\text{Tol.}] + k_2[\text{MeI}]^{1/2} [\text{Tol.}]^{1/2}$$

No surface effect was observed by Bernstein, but this may have been due to the higher pressures used (18→78 cm Hg.)

An explanation of our rate equation must therefore involve the surface. The seasoning effect of our reaction and the results obtained have been presented on page 69 et seq. A brief survey of

EFFECT OF VARIATION OF TOLUENE PRESSURE IN LINED FURNACE.

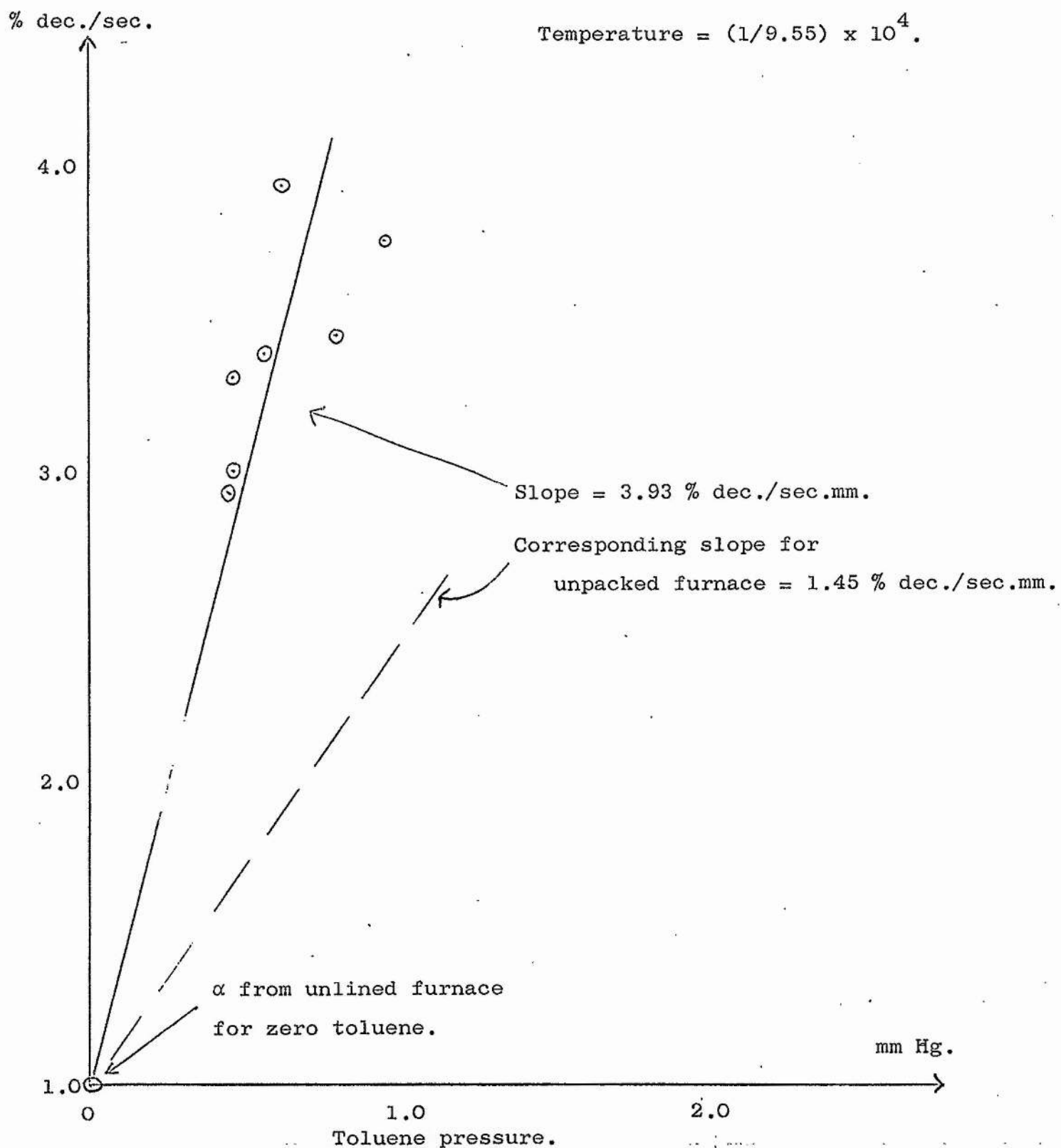


FIG. 48.

current aspects of wall coatings is given in Appendix X. Subsequent experiments to examine the effect of an increased surface area and its variation with temperature have been given on page 81. The temperature coefficient of the overall rate constant for the lined furnace appears to have a lower activation energy than the unlined furnace (see figure 39). Such behaviour would be expected if homogeneous and heterogeneous reactions were operative in about the same temperature range.

From the analysis outlined above whereby we are able to derive rate constants for the toluene dependence and for the plain first order decomposition of methyl bromide, the temperature coefficient of the former, although of the same order of magnitude as the temperature coefficient of the latter, is about 3 k.cals/mole smaller. When these two items are combined into an overall rate constant, and if the toluene term in the empirical analysis is a surface dependent term, then we can see why the surface effect has appeared to be less at the higher temperatures. We have, in this argument, ignored the argon dependence but this is small and in no way affects the conclusions.

If one plots a graph of the type of figure 40 but this time for the lined furnace, then a steeper line is obtained if the "toluene term" of the empirical equation is surface dependent. Such a graph is shown in figure 48 where % decomposition per second is plotted against toluene pressure. The argon pressures used in the

two furnaces were about the same. The value of α for the unpacked furnace is shown and the points on the graph are seen to lie about a steeper line with a fair approximation to the same α for both furnaces. The ratio of $\beta_{\text{packed}}/\beta_{\text{unpacked}} = 2.7$. The surface/volume ratio increase was 2.85. This strongly suggests that the toluene term is the surface dependent term and should strictly be written as $k_{\text{T}}[\text{Toluene}] [\text{MeBr}] [\text{Surface}]$.

Precisely what role the surface plays in this term is a matter for conjecture. The rate of such a reaction will depend upon the product of the concentrations of the two reactants and it may be that the surface adsorbs toluene in a dissociated form which reacts with methyl bromide during collisions of the latter at the wall or vice versa. Alternatively both reactants may be chemisorbed on to the wall and react in this state. This latter suggestion would be expected to lead to cross products of the reactants namely ethylbenzene and benzyl bromide. Examination of the furnace effluent gas by the mass spectrometer showed the presence of a small peak increase over the bypass gas at $m/e = 106^+$ suggesting the presence of only a trace of ethylbenzene in the gas mixture.

It was pointed out earlier that the possibility exists of H-atom attack on the methyl bromide. An increase, from any cause, of the stationary state concentration of H- atoms would therefore be reflected in the rate of decomposition of the halide.

The rate of formation of H- atoms is $k_9[\text{Tol}]$. The rate of loss of hydrogen atoms allowing for loss at the surface as well as in the gas phase is given by:

$$(k_{10}+k_{11}) [\text{H-}] [\text{Tol.}] + (k_{17} + k_{18}) [\text{H-}] [\text{MeBr}] + k_s [\text{H-}] [\text{Surface}]$$

whence

$$[\text{H-}] = k_9[\text{Tol}] / \left\{ (k_{10} + k_{11})[\text{Tol}] + (k_{17} + k_{18})[\text{MeBr}] + k_s[\text{Surface}] \right\}$$

To try to explain the toluene dependence term of the empirical rate equation on the lines of a chemical reaction between F- atoms and methyl bromide would lead to a term:

$$k_9[\text{Tol.}][\text{MeBr}] / \left\{ (k_{10} + k_{11})[\text{Tol}] + (k_{17} + k_{18})[\text{MeBr}] + k_s[\text{Surface}] \right\}$$

In order to understand the effect of the denominator, it is convenient to consider extreme cases i.e. for one term dominating the others. Thus if the $(k_{10} + k_{11})[\text{Tol}]$ term is dominant, the equation reduces to $k_9[\text{MeBr}]$ and one loses the toluene rate dependence. If the second term predominates, then the first order in methyl bromide is lost. Should the last term dominate, we observe first order behaviour in methyl bromide and toluene but the reaction would be surface inhibited.

All of these cases are against the experimental observations, and one must conclude that the suggestion of a H- atom reaction accounting for the toluene dependence is unjustified. This, along with the evidence proposed earlier, emphasises the acceptability of this term being a surface dependent term.

COMPARISON OF TEMPERATURE VARIATION OF OVERALL FIRST ORDER RATE CONSTANTS.

$3 + \log_{10} k_1$

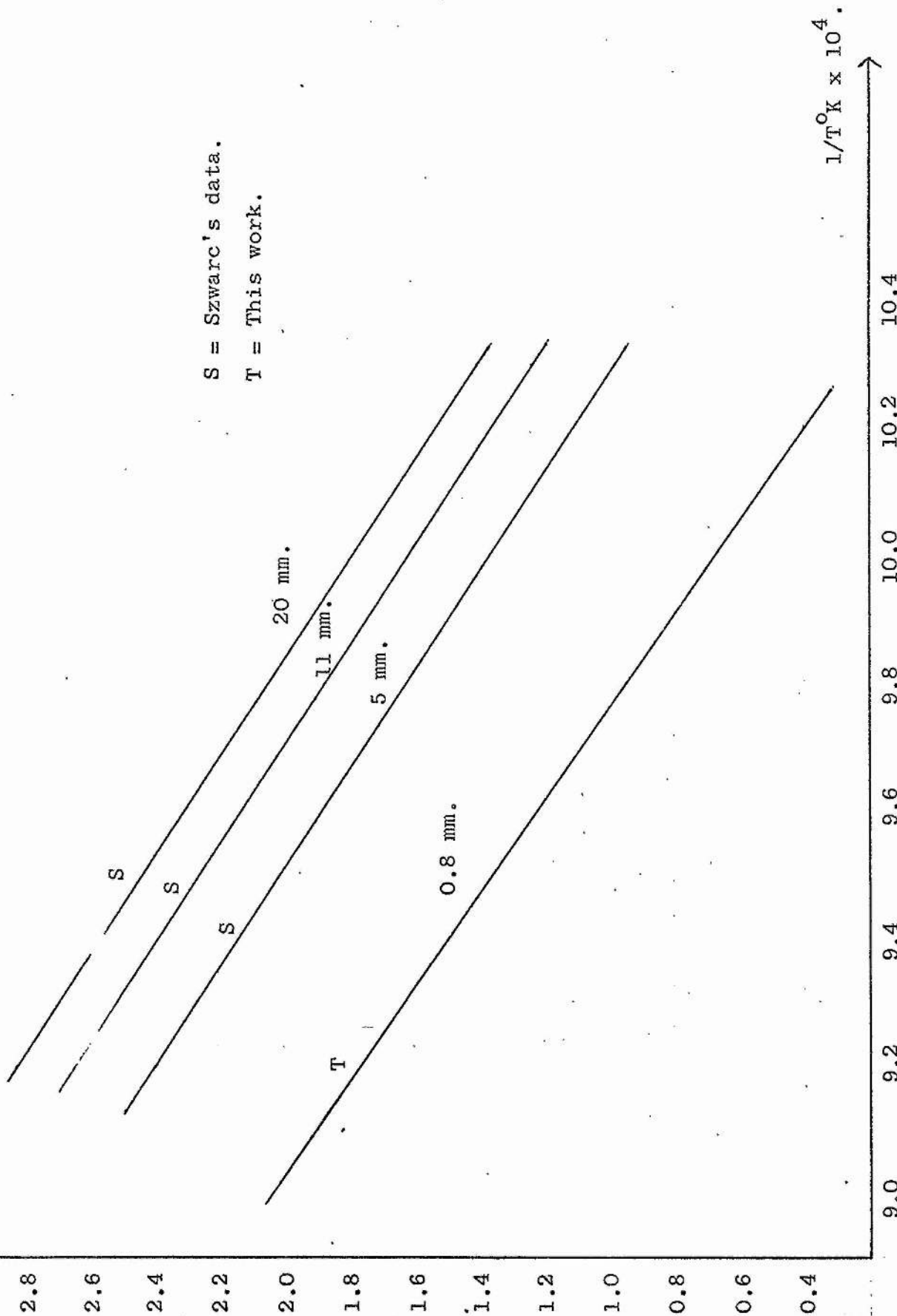


FIG. 49.

It is of interest that, using the kinetic parameters derived in this work and Szwarc's reactant concentrations, we are able to calculate the extent of his reaction. Szwarc (39) had used higher toluene pressures in a similar type of system. The comparison of the two sets of results is shown in figure 49 using overall first order rate constants. Using run 9 at 1019°K of Szwarc's published data as being the one nearest to our own extensive data at 1018°K, the toluene pressure was 11.45 mm Hg and the methyl bromide pressure was 0.55 mm. In the absence of a carrier gas we can use our values of β and α_0 to synthesise an extent of decomposition as follows:

$$\alpha_0 = 0.38 \text{ \% dec./sec.}$$

$$\beta = 0.5 \text{ \% dec./sec. mm.}$$

$$\begin{aligned} \text{Then \% dec./sec} &= 0.38 + 0.5 \times 11.45 \\ &= \underline{6.11} \end{aligned}$$

Szwarc's experimental value is $3.24/0.41 = 7.9\%$ dec./sec. Considering that Szwarc's temperature is slightly higher and that we have inherently assumed a similar surface/volume ratio between the two sets of work, the agreement is very reasonable. It must be emphasised that on the basis of our analysis only 6% of Szwarc's decomposition of methyl bromide occurred unimolecularly and without the aid of toluene as a co-reactant.

Turning now to the term $k_A [\text{Argon}][\text{MeBr}]$ in the empirical rate equation we have to explain an observed increase in rate with increasing argon pressure. The possibility of an energising process

has been discussed and discarded and one can only suggest that the argon, a completely inert species, will act in preventing the loss of some active entity at the wall. Thus an increase in argon pressure might increase the H- atom concentration in the bulk of the gas by preventing diffusion to the walls. This will increase the rate of loss of methyl bromide by reactions (17) or (18). The argon term then may be analysed on the lines of a homogeneous reaction between H- and methyl bromide. The $k_A [\text{Argon}][\text{MeBr}]$ of the empirical equation would become:

$$k'_A [\text{H-}] [\text{MeBr}] = k'_A [\text{MeBr}] k_9 [\text{Tol}] / \left\{ (k_{10} + k_{11}) [\text{Tol}] + (k_{17} + k_{18}) [\text{MeBr}] + k_s [\text{Surface}] \right\}$$

It is necessary to examine the relative importance of the terms in the denominator. In view of the evidence on page 99 the hydrogen atoms will react preferentially with the toluene. Since k_{10} and k_{11} represent the rates for reaction with toluene we may consider this term larger than the $(k_{17} + k_{18})$ term and may, as an approximation, ignore the latter.

The effect is therefore to give a toluene and surface dependence in the denominator. Such a reaction scheme would give a first order dependence in methyl bromide, approximately zero dependence in toluene and the effect of the argon would be to alter slightly the value of k_s , which represents the destructive efficiency of the surface to the hydrogen atoms. As the concentration of argon increases, the value of k_s will fall and so the observed decomposition

rate of methyl bromide will rise. One cannot present more than a qualitative explanation of this effect without further experiments.

There remains the first order decomposition term $k_0[\text{CH}_3\text{Br}]$ for discussion. Clearly such a term will be the unimolecular first order decomposition of the methyl bromide. Its rate will depend upon the rate of fission of the $\text{CH}_3\text{—Br}$ bond and the temperature dependence of the rate constant will, if the recombination reaction has zero activation energy, give the value of $D(\text{CH}_3\text{—Br})$, the bond dissociation energy. The value for the activation energy from figure 47 is 66.7 k.cals/mole and the A factor is $10^{11.86}\text{sec.}^{-1}$.

From a thermochemical standpoint the bond dissociation energy in methyl bromide is readily calculated from the heats of formation of the parent and the radicals formed.

$$\text{Thus } D(\text{CH}_3\text{—Br}) = \Delta H_f^\circ (\text{CH}_3\text{—}) + \Delta H_f^\circ (\text{Br}\cdot) - \Delta H_f^\circ (\text{CH}_3\text{Br})$$

Szwarc (39) calculated the thermochemical value of $D(\text{CH}_3\text{—Br})$ at 67.5 ± 0.5 k.cals/mole. His value for $\Delta H_f^\circ (\text{CH}_3\text{—})$ was based on the heats of formation of H \cdot and of methane and on the C—H bond dissociation energy in methane. He used a value of -8.6 for $\Delta H_f^\circ (\text{CH}_3\text{Br})$.

With regard to the above equation, $\Delta H_f^\circ (\text{Br}\cdot)$ is well established at 26.71 k.cals/mole (151) at 25°C. The value for $\Delta H_f^\circ (\text{CH}_3\text{Br})$ at 25°C is quoted at -8.5 k.cals/mole (151), and -8.6 k.cals/mole (126). A value of -10.0 k.cals/mole is quoted by Maslov and Maslov (152). The value -8.5 appears to be preferred. The value of $\Delta H_f^\circ (\text{CH}_3\text{—})$ at

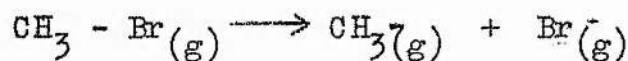
25°C appears a little less certain. Skinner et al (127, 128) quote 32.5 k.cals/mole and a value 32.0 k.cals/mole is also quoted (151). Eckstein (72) used a value 34.0 k.cals/mole and Benson recently tabulated 34.0 ± 1 k.cals/mole (80). Trotman-Dickenson (153) quoted 33.9 k.cals/mole. A value of 32.0 k.cals/mole may be deduced from $\Delta H_f^\circ (\text{CH}_4) = -17.89$ k.cals/mole, $\Delta H_f^\circ (\text{H}^-) = 52.09$ k.cals/mole $D(\text{CH}_3 - \text{H}) = 102$ k.cals/mole.

Using a value of 32.0 k.cals for $\Delta H_f^\circ (\text{CH}_3^-)$ and -8.5 k.cals/mole for $\Delta H_f^\circ (\text{CH}_3\text{Br})$, one obtains $D(\text{CH}_3\text{-Br}) = 32.0 + 26.71 + 8.5$
 $= \underline{67.21 \text{ k.cals/mole}}$

An upper limit would use $\Delta H_f^\circ (\text{CH}_3^-) = 34$ k.cals/mole and give 69.21 k.cals at 25°C.

In order to compare this with our experimental activation energy which was obtained at higher temperature we must calculate the correction involved.

Our temperature range was centered on about 1030°K. In order to find the ΔH° for the reaction



we must have heat content data for $\text{CH}_3\text{-Br}$, CH_3 and Br^- over the temperature range 298° \rightarrow 1030°K.

We may treat the Br^- atoms as a perfect monatomic gases with $C_p = C_v + R$. Then for Br^- atoms:

$$\begin{aligned} H_{1030}^\circ - H_{298}^\circ &= 5/2 R [1030 - 298] \\ &= \underline{3.62 \text{ k.cals/mole}} \end{aligned}$$

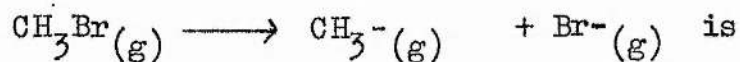
For methyl bromide, heat content and specific heat data are listed by Gelles and Pitzer (154) for the temperature range 100 \rightarrow 1500°K. Interpolation of their data yields a value for

$$\begin{aligned} H_{1030}^{\circ} - H_{298}^{\circ} &= 13.87 - 2.54 \\ &= \underline{11.33 \text{ k.cals/mole}} \end{aligned}$$

The methyl radical heat content data is not so readily available. However a value of 8.9 k.cals/mole is obtained by interpolation of data by Ribaud (155) for the value $(H_{1030}^{\circ} - H_{298}^{\circ})$ for CH_3^{\cdot} .

This value may carry a small error.

Thus ΔH_{1030}° for the dissociation:



given by:

$$\begin{aligned} \Delta H_{298}^{\circ} + (H_{1030}^{\circ} - H_{298}^{\circ})_{\text{CH}_3^{\cdot}} + (H_{1030}^{\circ} - H_{298}^{\circ})_{\text{Br}^{\cdot}} \\ - (H_{1030}^{\circ} - H_{298}^{\circ})_{\text{CH}_3\text{Br}} \\ = \Delta H_{298}^{\circ} + 8.9 + 3.62 - 11.33 = \Delta H_{298}^{\circ} + 1.19 \text{ k.cals/mole} \end{aligned}$$

The experimental value of 66.7 k.cals/mole obtained in this work when corrected to 298°K by subtracting 1.19 k.cals/mole yields a value 65.51 k.cals/mole. In view of the complexity of the empirical rate equation and the difficulties inherent in deducing the first order constant in such a system, the agreement with other workers on $\text{D}(\text{CH}_3 - \text{Br})$ must be considered as fair. With our increased understanding of the apparent mechanism operating at the

pressures used, the data should now be capable of being extended to produce a more reliable estimate.

The A factor of $10^{11.86} \text{sec.}^{-1}$ is low for a unimolecular decomposition. It is however not 'abnormal'. Gowenlock (156) considers A factors outside the limits of $10^{11.5}$ and $10^{14.5}$ to be abnormal. We may note here that the experimental data has produced a value of the activation energy somewhat smaller than one might anticipate on thermochemical grounds. Should an extension of this work produce a value more in keeping with the thermochemical value, an associated A factor would be nearer to the expected 10^{13}sec.^{-1} for the unimolecular split.

D. General assessment of the method.

This survey of the decomposition of methyl bromide in excess toluene was undertaken to test for applicability of the techniques developed in the early part of the thesis. The complexities disclosed cannot be regarded as a failure of the technique, but rather as an indication of its utility. In most studies of small fractional decompositions the assumption of a particular stoichiometry is a necessary step in deriving velocity constants since analyses are usually made for products. The present technique offers the opportunity of dealing with a wide range of substances without the

necessity to study the stoichiometry at all temperatures of interest. So far as can be assessed from this one test reaction the procedures adopted seem valuable. It would be helpful if the technique could be applied to higher gas pressures. This is largely a matter of the porosity of the mass spectrometer leaks employed, although difficulties are likely to be encountered when pressures of, say 100 mm or higher, are used.

The technique has been applied here to a flow system. The validity of data from similar systems has been criticised recently and a relevant survey is given in Appendix XI. It is not impossible to extend the method to a static system in which one would have to include an inert gas as a reference concentration (in the flow system, the reference is the bypass gas). We consider that the technique developed in this work is a distinctly useful tool.

In the case of the test reaction used there are clearly many further lines of development. Studies ought to be made with more widely varying surface areas, particularly with regard to its effect on the k_o , k_A and k_T values. Work at higher gas pressures might help to reduce the effect of surface and should be undertaken for clarification of the position. The ultimate aim of any such work ought clearly to be the establishment of conditions, if this is possible, where the k_o term is dominant and the other terms negligible. The conditions used in this work and in Szwarc's previous study are

clearly not free from complexity. It is, of course, possible that the self decomposition of toluene will always induce a decomposition of RX when $D(R - X)$ is as high as in methyl bromide. A more exhaustive study would be of value to our understanding of the processes involved.

SUMMARY

1. The first object of this work was to produce a technique of analysing continuously the exit gases of flow reactors under conditions where the extent of decomposition is small, and to do this with particular reference to the small changes in reactant concentration. This was preferred to analysis for products since the translation of the data for the latter into kinetic rate equations requires a knowledge or assumptions of the stoichiometry.

The second aim of the work was to apply the technique to typical systems as used for bond dissociation energy determinations and test the method on a reaction of importance.

2. Details have been given of the development of the system where the analyses can be performed mass spectrometrically and continuously on both the inlet and exit gases, with about 30 seconds between each sampling. The technique minimises the chance that variations in flow conditions or changes in reactor efficiency will pass undetected. It permits also variations in kinetic parameters to be studied without opening up the reactor but merely by altering the variables and waiting for new steady state conditions.

In order to deal with the small variations in the large signals given by the reactant decomposition, an electrical backing off device was used after sufficient stability had been obtained. The details of this have been given.

3. In order to check the flexibility of the technique, the thermal decomposition of methyl bromide in excess toluene, previously investigated by Szwarc, was carried out in the flow system.

4. It was shown experimentally that the rate of decomposition of the methyl bromide was given by:

$$-d [\text{MeBr}]/dt = \left\{ k_0 + k_T [\text{Toluene}] + k_A [\text{Argon}] \right\} [\text{MeBr}]$$

when using up to 0.1 mm CH_3Br in about 1 mm of toluene and 1 mm of argon carrier gas. The reaction was shown to be surface dependent and was studied in two furnaces of different S/V ratio.

5. Methods of analysis of the data have yielded k_0 , k_T and k_A . The temperature coefficient of k_0 has been shown to be

$$k_0 = 10^{11.86} \exp(-66,700/RT) \text{ sec}^{-1} \text{ in the range } 960^\circ \rightarrow 1090^\circ \text{K.}$$

The activation energy from the k_T temperature variation is 63.2 k.cals/mole.

6. The kinetic data have been discussed and k_0 is ascribed to the first order decomposition process while the second term has been considered to be a surface reaction. The small increase of the rate with rise in argon pressure is thought to be caused by increases in the steady state concentration of hydrogen atoms, due to argon impeding the partial wall removal of this entity.

7. The activation energy of 66.7 k.cals/mole for the unimolecular decomposition has been compared with other data on $\text{D}(\text{CH}_3 - \text{Br})$.

8. Finally, suggestions have been made for further work in the study of this reaction to aid a more complete understanding of the apparently complex mechanism involved.

APPENDICESAPPENDIX I. Calculation of contact times.

It may be readily calculated that the residence time in seconds of a gas passing through a furnace is given by the formula:

$$t_c = \frac{V \times P \times 273}{n \times 22400 \times 760 \times T}$$

where V = furnace volume in ml.

= 280 ml. for unpacked furnace,

P = furnace pressure in mm. Hg.,

T = furnace temperature in degrees Kelvin,

and n = total moles per second passing through the furnace.

The furnace pressure, P, is calculated from a knowledge of the pressures at the flow McLeod gauges and the flow capillary or capillaries in use for the run. Reference to the table on page 46 shows the percentage increase to be applied to the McLeod gauge reading to give the actual furnace pressure.

If the total moles per second passing through the furnace and the bypass is

$$N = n_{\text{MeBr}} + n_{\text{tol.}} + n_{\text{argon}}$$

then n, the number of moles passing through the furnace = α N where α is the fraction passing down the furnace line.

n_{MeBr} and $n_{\text{tol.}}$ are obtained from calibration graphs (figures 6 and 7), n_{argon} is obtained from calibration graph figure 9 from a knowledge of the capillary in use and P_1 and P_2 , the flow McLeod gauge readings. The sum of these quantities yields the total moles per second and reference to figures 25 and 26 (or 29 and 30 in the case of the packed furnace) allows the fraction, α , of the gases passing down the furnace line to be calculated.

The extent of decomposition is given by:

$$\% \text{ decomposed} = \frac{\Delta (\text{mV.})}{\text{Bypass} (\text{mV.})} \times 100$$

where $\Delta (\text{mV.}) = (\text{bypass reading} - \text{furnace reading})$ in millivolts of peak height of 96^+ .

$\text{Bypass (mV.)} = \text{total bypass reading in millivolts} = (\text{recorder scale reading}) + (\text{backing off reading}) - (96^+ \text{ zero reading}).$

The average of four or six readings of percentage decomposition was taken as the value for a particular run.

The partial pressure of substance x in the furnace is given by:

$$p'_x = \left(\frac{n_x}{n} \right) P/n,$$
 the letters having the above described significance.

First order rate constants may then be calculated from the rate equation:

$$k_1 (\text{sec.}^{-1}) = \frac{2.303}{t_0} \log_{10} [100/(100-x)]$$

where $x = \text{percentage decomposition.}$

APPENDIX II. Gas distribution data.

Data on the distribution of gas between furnace and bypass lines were as follows.

(a) Unpacked furnace. Effect of temperature variation at a constant pressure of 1.0 mm. Flow capillary No.4. See figure 25.

<u>Furnace Temp. ($^{\circ}$K)</u>	<u>% through furnace. (i)</u>
943	45.9
951	45.3
971	45.2
983	45.2
997	44.8
1018	45.0
1037	44.3
1039	44.5
1070	43.8

(b) Unpacked furnace. Effect of pressure variation at a constant temperature of 1037° K. See figure 26.

<u>Pressure (mm Hg.)</u>	<u>% through furnace</u> (i)	<u>Capillary</u>
0.77	43.4	4
1.05	44.4	4
1.48	46.2	4
1.90	47.0	4
0.65	46.5	1
0.91	46.8	1
1.46	48.0	1
1.94	48.1	1
1.03	48.0	2
1.84	48.0	2
0.83	48.0	1 + 2 + 4

(i) The error is estimated to be not greater than $\pm 0.6\%$ on the percentage quoted. See Appendix VIII.

(c) Packed furnace. Temperature variation at a constant pressure of 1 mm Hg. Flow capillary No. 4.

<u>Temperature ($^{\circ}$K)</u>	<u>% through furnace.</u> (ii)
974	33.5
995	33.8
995	32.2
996	32.8
1017	31.7
1019	32.2
1033	31.8
1034	31.6

(d) Packed furnace. Effect of pressure variation at 1018°K. See figure 30.

<u>Pressure (mm Hg.)</u>	<u>% through furnace.</u> ⁽ⁱⁱ⁾	<u>Capillary</u>
0.43	29.1	4
0.43	29.3	4
1.09	32.2	4
1.05	32.9	4
1.60	34.9	4
2.07	35.4	4
2.57	36.3	4
2.60	36.4	4
1.20	37.1	1
0.58	34.6	1

(ii) The error is estimated to be not greater than $\pm 2.3\%$ on the percentage quoted. See Appendix VIII.

APPENDIX III. Seasoning rate data.

Variation of the extent of decomposition with seasoning time for packed ($s/v = 5.2$) and unpacked ($s/v = 1.82$) furnaces. The values have been related to one second of residence time. Flow capillary No. 4

(a) Unpacked furnace at 1000°K.

<u>Run no.</u>	<u>% dec./sec.</u> (iii)	<u>Seasoning time (mins.)</u>
56	0.66	15
57	0.57	56
58	0.49	87
59	0.44	111
60	0.46	143
61	0.45	169
62	0.46	199
63	0.46	225
64	0.44	283

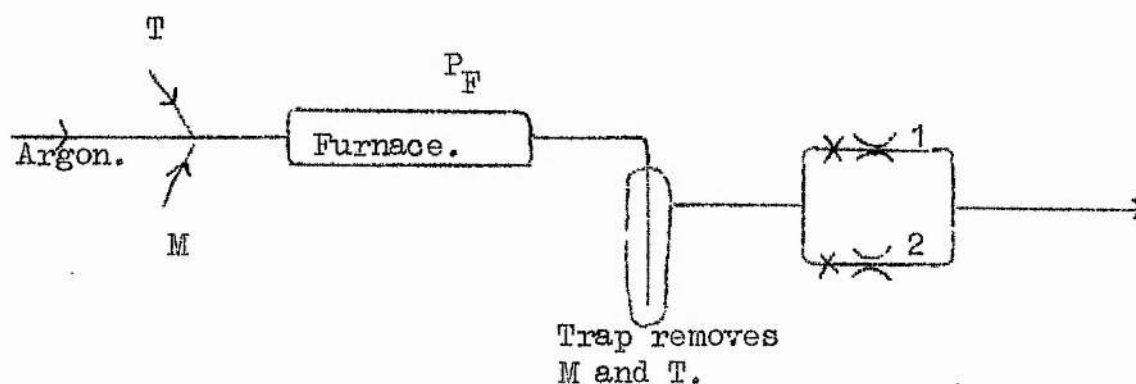
(b) Packed furnace at 1005°K.

<u>Run no.</u>	<u>% dec./sec.</u> (iii)	<u>Seasoning time (mins.)</u>
115	2.55	14
116	1.92	34
117	1.61	57
118	1.43	80
119	1.29	117
120	1.22	154
121	1.19	177

(iii) An average error of $\pm 2.0\%$ in the figure quoted is estimated. See Appendix VIII.

APPENDIX IV. Variation of partial pressure with contact time.

Let n_A and n_B moles/sec. of argon carrier gas flow through capillaries 1 and 2 respectively and let n_T and n_M be the moles/sec. of injected reactants which remains constant. The situation is represented diagrammatically below:



The partial pressure of M in the furnace when using capillary 1 is:

$$p'_{M_1} = \frac{n_M}{n_M + n_T + n_A} \cdot P_F$$

For capillary 2:

$$p'_{M_2} = \frac{n_M}{n_M + n_T + n_B} \cdot P'_F$$

where P_F and P'_F are the furnace pressures in the two cases.

The contact time is given by

$$t_c = \frac{K \cdot P_F}{\sum_i n_i} \quad \text{where } K \text{ is a temperature dependent apparatus constant.}$$

Thus

$$\begin{aligned} p'_{M_1} &= \frac{n_M}{n_M + n_T + n_A} \cdot \frac{t_1 \sum_i n_i}{K} \\ &= \frac{n_M t_1}{K} \end{aligned}$$

$$\text{and } p'_{M_2} = \frac{n_M t_2}{K}$$

Thus the ratio of the partial pressures of a reactant under the above conditions at a given temperature is the same as the ratio of the contact times. The partial pressures of the carrier gas in the two cases are

$$p'_{A_1} = \frac{n_A}{n_M + n_T + n_A} \cdot \frac{t_1 \sum_i n_i}{K}$$

$$\text{and } p'_{B_2} = \frac{n_B}{n_M + n_T + n_B} \cdot \frac{t_2 \sum_i n_i}{K}$$

$$\text{or } \frac{p'_{A_1}}{p'_{B_2}} = \frac{n_A t_1}{n_B t_2}$$

thus involving both the mole ratio and the contact time ratio.

APPENDIX V. Temperature coefficient of first order rate constant in
unpacked furnace. (a)

TABLE V

<u>Run</u>	<u>% dec.</u>	<u>t_c (secs)</u>	<u>p' to l. (mm Hg.)</u>	<u>3+log₁₀ k₁</u>	<u>1/T (°K) x 10⁴</u>	<u>Flow Capillary</u>
1	3.93	2.86	0.346	1.16	9.606	1
2	3.71	2.81	0.438	1.12	"	1
3	3.29	2.84	0.334	1.07	"	1
4	4.02	2.85	0.327	1.16	9.643	4
5	9.44	5.79	0.650	1.23	9.625	2
6	2.02	1.69	0.196	1.08	9.634	4
7	0.82	6.00	0.671	0.56	10.320	4
8	2.49	5.70	0.675	0.64	9.970	4
9	22.55	5.46	0.694	1.67	9.276	4
10	9.82	2.65	0.347	1.59	9.268	1
11	4.39	5.87	0.651	0.88	9.824	4
21	1.43	5.20	0.811	0.44	10.107	4
22	0.68	2.69	0.432	0.40	"	1
23	0.80	2.76	0.442	0.46	10.091	1
24	1.65	5.02	0.777	0.52	"	4
25	3.33	5.04	0.804	0.81	9.911	4
26	1.46	2.65	0.434	0.74	"	1
27	1.07	1.74	0.288	0.79	"	2
28	1.77	1.71	0.288	1.02	9.681	2
29	2.72	2.59	0.432	1.03	"	1
30	6.71	4.97	0.804	1.14	"	4
31	12.24	4.94	0.808	1.42	9.488	4
32	5.00	2.56	0.432	1.30	"	1
33	2.81	1.68	0.280	1.23	"	2

TABLE V continued.

Run	% dec.	t_o (secs.)	$p'_{to1.}$ (mm Hg.)	$3+\log_{10} k_1$	$1/T(^{\circ}K) \times 10^4$	Flow Capillary
34	4.31	1.73	0.295	1.41	9.352	2
35	7.52	2.58	0.437	1.49	"	1
36	16.94	4.78	0.792	1.58	"	4
37	7.05	1.69	0.291	1.64	9.195	2
38	11.79	2.53	0.432	1.69	"	1
39	25.96	4.84	0.803	1.79	"	4
45	3.42	5.06	0.824	0.81	9.930	4
46	1.43	2.59	0.437	0.75	9.901	1
47	3.49	5.03	0.824	0.85	"	4
48	1.05	5.19	0.812	0.31	10.290	4
50	8.82	1.20	0.216	1.88	9.046	1 + 2 + 4
51	10.57	1.61	0.286	1.84	"	2
52	17.73	2.42	0.439	1.91	"	1
53	12.50	1.51	0.249	1.96	8.979	1 + 2 + 4
54	14.18	1.61	0.288	1.98	8.971	2
55	0.82	4.98	0.780	0.22	10.370	4
64	2.29	5.16	0.855	0.65	10.000	4
69	0.87	4.59	0.889	0.28	10.331	4
70	0.96	4.61	0.885	0.32	"	4
71	0.75	4.62	0.887	0.21	10.395	4
72	0.63	5.29	0.753	0.07	"	4
73	1.10	5.10	0.826	0.37	10.309	4
74	1.21	5.62	0.710	0.34	"	4
75	3.76	5.12	0.807	0.88	9.911	4
76	1.39	2.71	0.437	0.71	"	1
77	6.28	4.85	0.780	1.13	9.737	4
78	2.29	2.61	0.439	0.95	"	1
79	1.37	5.03	0.792	0.44	10.173	4

TABLE V continued.

Run	% dec.	t_c (secs.)	$p'_{tol.}$ (mm Hg.)	$3+\log_{10} k_1$	$1/T(^{\circ}K) \times 10^4$	Flow Capillary
80	1.56	5.04	0.798	0.49	10.173	4
81	1.69	5.05	0.812	0.53	"	4
87	2.38	2.59	0.479	0.97	9.823	1
88	2.21	2.54	0.486	0.94	"	1
96	1.60	2.45	0.463	0.82	"	1
103	1.44	2.14	0.436	0.83	"	1

(d) For an estimate of errors see Appendix VIII.

APPENDIX VI. Temperature coefficient of first order rate constant for packed furnace.^(c)

TABLE VI

Run	% dec.	t_c (secs.)	$p'_{tol.}$ (mm Hg.)	$3+\log_{10} k_1$	$1/T(^{\circ}K) \times 10^4$
121	6.14	5.15	0.744	1.09	9.95
122	1.22	5.12	0.748	0.38	10.38
123	2.09	5.13	0.751	0.62	"
124	9.39	2.84	0.461	1.54	9.55
125	8.57	2.85	0.461	1.50	"
126	17.64	5.13	0.796	1.58	"
127	16.45	3.14	0.461	1.76	9.33
128	15.18	3.08	0.478	1.73	"
129	9.98	2.05	0.320	1.71	"
130	3.89	3.80	0.953	1.00	10.15
131	2.17	2.16	0.619	1.01	"
132	3.14	3.83	0.963	0.92	"
133	8.41	2.14	0.622	1.61	9.55

TABLE VI. continued.

Run	% dec.	t_c (secs.)	$p'_{tol.}$ (mm Hg.)	$3 + \log_{10} k_1$	$1/T(^{\circ}K) \times 10^4$.
134	14.47	3.86	0.954	1.61	9.55
135	7.88	2.33	0.566	1.55	"
136	8.23	2.81	0.454	1.49	"
137	6.29	5.22	0.760	1.09	10.09
138	3.77	2.83	0.446	1.13	"
139	5.65	5.13	0.739	1.06	"
140	3.23	2.86	0.449	1.06	"
141	2.58	1.93	0.672	1.13	"

(e) For an estimate of errors see Appendix VIII.

APPENDIX VII. Rate of molecular diffusion to the furnace wall.

Consider a molecule placed centrally between the outer wall and the thermocouple well wall. In the present apparatus this is 0.5 cm. from the wall.

The average number of collisions (n) suffered by a particle when diffusing through a distance, y , is given by (17):

$$n = \frac{3 \pi y^2}{4 \lambda^2} \quad \text{where } \lambda \text{ is the mean free path.}$$

The mean free path may be calculated (18) by:

$\lambda = 1/\sqrt{2} \pi \sigma^2 n^*$ where n^* is the number of molecules per cm.³.

$$\text{Thus } n = \frac{3}{2} \pi^3 y^2 \sigma^{-4} n^{*2}$$

A value of n^* may be obtained from the relation (16):

$$n^* = \frac{9.652 \times 10^{18} \times P}{T} \quad \text{molecules/cm}^3.$$

where P is the pressure in mm Hg. and T is the temperature of the gas.

Inserting typical values of 2 mm pressure at 1000°K we have

$$n^* = 19.3 \times 10^{16} \text{ molecules cm.}^{-3}$$

Continuing to estimate the diffusion time by basing our calculations on argon we have $\sigma = 3.7 \times 10^{-8}$ cm., and a molecular weight of 40.

Then the number of collisions a centrally placed molecule will make in diffusing the 0.5 cm. to the wall is:

$$\begin{aligned} n &= \frac{3}{2} \pi^3 (0.5)^2 [3.7 \times 10^{-8}]^4 [19.3 \times 10^{16}]^2 \\ &= \underline{8.11 \times 10^5 \text{ collisions.}} \end{aligned}$$

The number of collisions one molecule makes per second is given by (18):

$$Z_1 = \sqrt{2} \pi \sigma^2 \bar{c} n^*$$

where \bar{c} is the average molecular velocity and is given by:

$$\bar{c} = \sqrt{\frac{8RT}{\pi M}}$$

where the symbols have their usual significance.

Then

$$\begin{aligned} Z_1 &= \sqrt{2} \pi (3.7 \times 10^{-8})^2 \sqrt{\frac{8 \times 8.3 \times 10^{10}}{\pi \times 40}} \times (19.3 \times 10^{16}) \\ &= \underline{8.5 \times 10^7 \text{ collisions sec.}^{-1}} \end{aligned}$$

Thus the time taken for the centrally placed molecule to reach the wall is given by the value of n/\bar{z}_1 .

$$\begin{aligned} n/\bar{z}_1 &= 8.11 \times 10^5 / 8.5 \times 10^7 \\ &= \underline{9.5 \times 10^{-3} \text{ secs.}} \end{aligned}$$

The result, had the calculation been based on toluene taking $\sigma \approx 11\text{\AA}$, and $M = 92$, would have given an n/\bar{z} value of 1.3×10^{-1} secs.

Such values would, with a typical accommodation coefficient of about 0.2, suggest that in times of the order of 0.5 sec. even molecules which are initially placed centrally will have reached wall temperature by direct contact with the wall. This time, then, represents an upper limit.

The value of n varies with the square of the distance, y , and the majority of molecules in the furnace will therefore have a much lower value of n than the above calculation suggests. Many of the collisions made on the way to the wall will be with molecules which have already visited the wall and possess higher energies. This will have the effect of heating the molecules before they even get to the wall or of increasing the value of the accommodation coefficient towards unity. Such quantities are difficult to assess but it is felt that in view of the above calculations a warm-up time of 0.5 secs. is not conceivable.

APPENDIX VIII. An assessment of errors and error limits.

The error limits quoted at the foot of the tables in Appendix II

were estimated from the extent of the spread of the readings. The error involved in weighing the toluene to obtain the percentage through furnace figure was of the order of 0.1%. In addition collection errors caused by possible differences in trap efficiencies gave rise to the error limits quoted. A greater spread was observed in the packed furnace. The majority of values fall within a much smaller range than the error quoted.

Errors in the percentage decomposition figure were estimated by calculating the standard deviation of the several experimental readings obtained. The arithmetic mean of the readings was the figure used in calculations. The standard deviations calculated varied from better than $\pm 1.0\%$ to about 5.5%. Instrumental instabilities were a contributing factor to these deviations.

The partial pressures of the reactants quoted are considered to be within $\pm 2.0\%$. They were estimated from the possible errors involved in reading the manometer in the case of the methyl bromide injection and in the steadiness of the water bath temperature in the case of the toluene injection. The carrier gas partial pressure error was of about the same order since the McLeod gauges were considered accurate to about $\pm 1.0\%$.

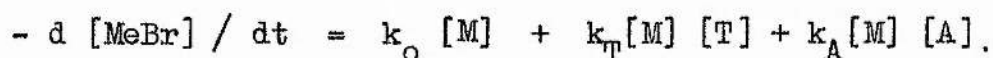
An error in the knowledge of the furnace temperature of one degree at 750°C will produce an uncertainty of $0.01 \times 10^{-4} \text{ K}^{-1}$ in the reciprocal temperatures quoted. The furnace temperature control was to within $\pm 0.5^{\circ}\text{C}$. The smoothing of the furnace on

the other hand was known to be $\pm 1 \text{ C}^{\circ}$ producing an uncertainty of $\pm 0.01 \times 10^{-4} \text{ K}^{-1}$.

The probable error in the contact time may be deduced by the normal method (84). Insertion of the above quoted errors into the formula in Appendix I leads to a probable error in t_0 of about $\pm 4.0\%$. This produces a maximum probable error in the value of the rate constant of about $\pm 5.0\%$.

APPENDIX IX. Effect of contact time variation and removal of Toluene dependence.

The data for decomposition rate against contact time drawn in Figure 34, if treated as a linear graph showed intercepts of the order of 0.5 seconds on the time axis. As pointed out earlier these data were obtained before it was established that the rate of decomposition increased with increase in the pressure of toluene, and the data of Figure 34 involved higher toluene pressures as contact times increased — because of the method of experimentation. In this section a correction is applied to the data of Figure 34 in order to remove the disturbing influence of the variation in toluene pressure. The correction will be based on the established rate equation:



where $[M]$ = methyl bromide concentration, $[T]$ = toluene concentration and $[A]$ = argon concentration.

Rewriting this we have

$$\% \text{ dec.}/t_c = \alpha_0 + \beta [T] + \alpha_A [A]$$

where t_c is the contact time and the equation applies to small extents of decomposition. α_0 is the intercept (in % decomposition/sec) corresponding to zero contribution from toluene and from argon and β and α_A are the slopes (in % decomposition/sec per mm pressure) for the toluene and argon variations respectively. An accurate treatment would require the equation

$$\log[1/(1 - \text{fraction decomposed})] = \{ \alpha_0 + \beta [T] + \alpha_A [A] \} t_c$$

rather than merely $(\% \text{ decomposition})/t_c$. An expansion of the logarithmic term allows one to calculate the error involved in the approximate treatment. Thus for a fractional decomposition of 0.1 (i.e. 10%), the error involved is about 5% in the decomposition figure and for 20% decomposition the error rises to about 10%.

For most of the runs, $[A]$ was about constant at 0.7 to 0.8 mm Hg and also the effect of variation of argon pressure is small compared with the toluene effect. We may therefore write as a good approximation

$$(\% \text{ decomposition}) = \{ \alpha + \beta [T] \} t_c$$

where α represents $(\alpha_0 + \alpha_A [A])$.

It can be shown that for the experimental technique used the toluene partial pressure is proportional to the contact time (see

Appendix IV) i.e. as we increase t_c , so $[T]$ increases if the injection rate is unchanged.

A plot of % decomposition against time of contact will therefore be expected to show an upward curvature with increasing time of contact. The points shown in Figure 34 could reasonably be held to lie on an upward curve through the origin rather than on the straight line drawn in that graph. The more accurate treatment outlined above would have the effect of increasing slightly the upward curvature of the plots. Since the $\beta[T]$ contribution amounts to some 50% of the total $(\alpha + \beta[T])$ and since no quantitative use is to be made of data obtained from this correction, the less accurate treatment is considered to be adequate.

We can now correct the points for the effects caused by toluene pressure variations by the following procedure. Since we have three points, obtained from each of the three flow capillaries at several temperatures, we may write three simultaneous equations. For example, consider runs 31, 32, 33 at 1054°K . We can set up three equations from the experimental data, using concentrations of toluene in mm Hg, as follows:

$$12.24 = (\alpha + 0.808 \beta) 4.94 \quad (1)$$

$$5.0 = (\alpha + 0.432 \beta) 2.56 \quad (2)$$

$$2.81 = (\alpha + 0.280 \beta) 1.68 \quad (3)$$

TABLE IX

<u>Run</u>	<u>Temp (°K)</u>	<u>% dec.</u>	<u>t_c (secs)</u>	<u>p'_{tol} (mm)</u>	<u>α</u>	<u>β</u>	<u>Av. α</u>	<u>Av. β</u>	<u>Corrected % dec.</u>
4	1038	4.02	2.85	0.327	1.19	0.68			2.96
5	"	9.44	5.79	0.650	1.00	0.97	1.02	1.11	5.52
6	"	2.02	1.70	0.196	0.86	1.68			1.66
31	1054	12.24	4.94	0.808	1.34	1.41			6.04
32	"	5.00	2.56	0.432	1.16	1.84	1.25	1.59	3.22
33	"	2.81	1.68	0.280	1.24	1.53			2.07
37	1087	7.05	1.69	0.291	2.34	6.25			5.28
38	"	11.79	2.54	0.432	4.65	0.89	3.49	3.17	8.49
39	"	25.96	4.84	0.803	3.47	2.37			15.00
50	1106	8.82	1.21	0.216	-	-			7.32
51	"	10.57	1.61	0.286	-	-	5.18	4.90	8.40
52	"	17.73	2.42	0.439	5.18	4.9			12.55

REMOVAL OF TOLUENE DEPENDENCE FROM CONTACT TIME VARIATION.

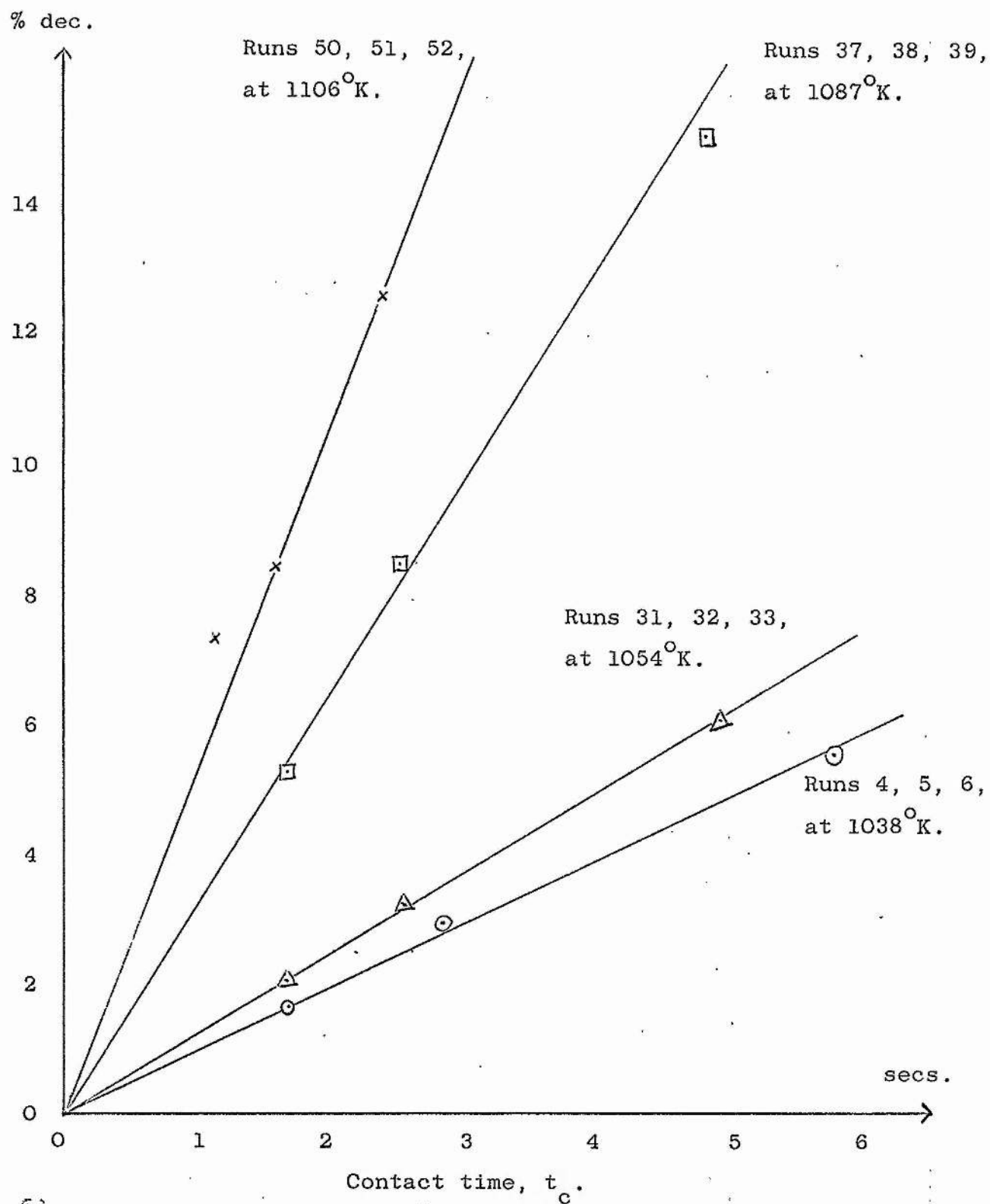


FIG. 5.

Since the values in the equations are actual experimental values it is unlikely that they will fit the curve exactly. The values of α and β were therefore determined by solving equations (1) and (2), (2) and (3), and (3) and (1) and averaging the values of α and β so obtained. The values for the above set were:

$$\alpha = 1.34, 1.16, 1.24 ; \text{ average value } 1.25$$

$$\beta = 1.41, 1.84, 1.53 ; \text{ average value } 1.59$$

The percentage decomposition corrected for zero toluene contribution then becomes

$$\text{Observed \% decomposition} \times \frac{\alpha}{(\alpha + \beta[T])}$$

Such corrected data for several sets of runs are given in Table IX and plots of corrected percentage decomposition are shown in Figure 50 as good straight lines through the origin with slope α . The upper point of the 1087°K data may be in error because of too high a decomposition figure.

COMPARISON OF THEORETICAL AND EXPERIMENTAL DECOMPOSITION RATES.

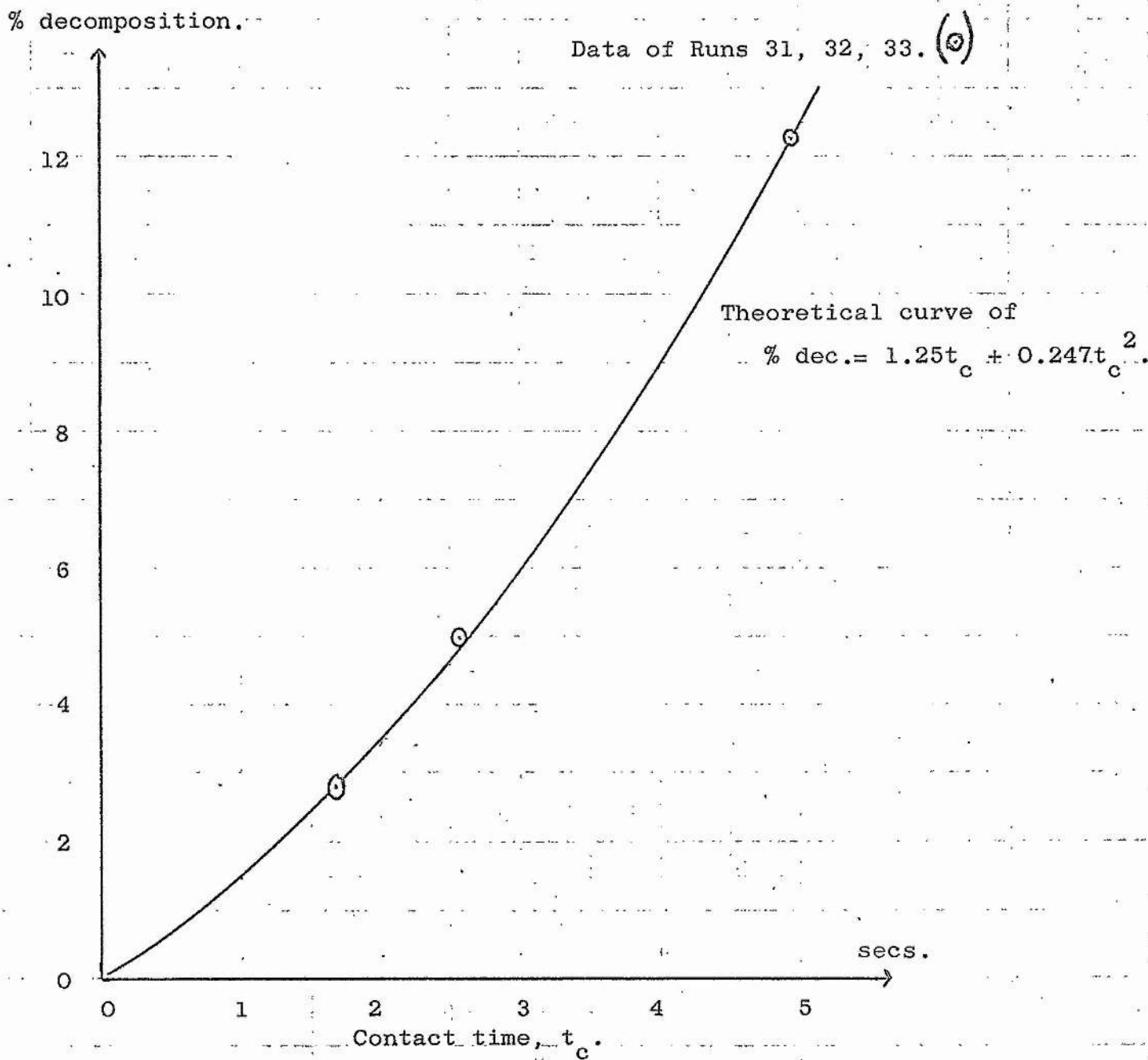


FIG. 51.

It will be noted that a large spread exists in the individual values of α and β . This is a common feature when one is curve fitting to experimental points by exact mathematical treatments. Small errors in the values become large percentage errors when subtracted. However, averaging the α and β values should give a reasonably reliable result, and since the α/β ratio is about unity at several temperatures the corrected decomposition is relatively insensitive to values of α/β and more sensitive to $[T]$. One should correctly apply a statistical treatment involving the minimizing of the sum of the standard deviations from a calculated straight line.

That the above described treatment would appear valid is shown by taking the average values of α and β and calculating values of % decomposition for the experimental $[T]$ and t_c values. The calculated curve, a parabola of the form $y = ax+bx^2$, may be drawn. The constant of proportionality between $[T]$ and t_c is found by a plot of these quantities. Thus the equation for runs 31, 32, 33 becomes:-

$$\% \text{ decomposition} = 1.25 t_c + 0.247 t_c^2,$$

since $[T] = 0.166 t_c$ in this case.

The curve is shown in Figure 51. The experimental points are seen to be in good agreement with the theoretical curve.

APPENDIX X Furnace seasoning.

The production of furnace wall coatings by the reactants to produce relatively inert surfaces has been widely noted. The general tendency is for a surface to be more active when clean and so, as a reaction proceeds and the walls become coated, the rate slows down. Brearley et. al.(143) in work on t-amyl chloride showed that prolonged treatment in a packed vessel with a surface/volume ratio of 10 times the unpacked furnace ratio was necessary to bring the rate down to the value for the unpacked vessel. As has been shown by experiments in this research the coating appears to be essentially of carbon from the decomposition of methyl bromide in the presence of toluene. A similar effect for the pyrolysis of toluene was observed by Smith (8). Szwarc (39), too, in the particular case of methyl bromide pyrolysis in toluene as a carrier reported a carbonaceous deposit on the walls. It is of interest to note that he did not observe this for the pyrolyses of other halomethanes. In pyrolytic work on methyl iodide alone (in pyrex vessels), Klemm and Bernstein (140) reported an extensive carbon deposition but when toluene was present the reaction was clean with no surface film at all.

Cullis et al. (141) with the aid of electron diffraction photographs, have studied the structures of pyrolytic carbon crystallite deposits produced in a silica furnace at 850 to 950°C.

They suggested that halogen can remain in the solid and so affect the properties of the coating. Holbrook (142) emphasized the care needed in assuming that carbon deposits are inert and showed that surfaces from ethyl chloride pyrolysis behaved differently from those produced by pyrolysis of allyl bromide. He produced e.s.r. evidence for free radicals in the carbon deposits from the allyl halide and warned of the use of such a compound in the production of inactive surfaces.

In general a heterogeneous decomposition will have a lower activation energy than a corresponding homogeneous decomposition, thus, if both are present, the extent of the former will be greater at the lower temperatures. Rice and Herzfeld (144) have discussed the effect of surface on supposedly homogeneous gas reactions and also the effects of different surfaces on the reaction rates.

The process of seasoning is probably not sufficiently well understood to formulate theories. However, the importance that surfaces can play in gas phase decomposition studies has to be noted and one must ensure that the surface in use is yielding reproducible data.

APPENDIX XI: Flow conditions and design characteristics.

The conventional method of studying a reaction with reasonably short reaction times in a flow system involves flowing the material through a reaction vessel, either with or without a carrier gas.

Calculation of the contact time is made by assuming the flow to be laminar or plug flow along the length of the reaction vessel. Several workers have recently pointed out the possible sources of error in such an assumption. Gilbert (120) in a re-examination of the decomposition of hydrazine showed it to favour a second order process, which was in line with calculations from flame theory, rather than the first order reaction as deduced by Szwarc. Gilbert suggested that Szwarc's (123) experiments were not under isothermal reaction conditions and that a strong effect was present due to heat transfer in the reactor entrance region. Reinterpretation of Szwarc's data by assuming the tubular reactor to be isothermal only downstream of the entrance led to a consistency with flame theory.

Batten (132) has investigated the validity of the assumed plug flow. By photographing the mixing of bromine vapour with carbon tetrachloride vapour at various flow rates he concluded that over a wide range of conditions the bulk of the gas flowed through without diffusing laterally to the walls. However, the flow would appear to be laminar for values of Reynolds number (R_e) of less than about three. It should be pointed out that his photographs were taken shortly after the bromine vapour was allowed to enter the reaction zone and that therefore steady state conditions may not apply.

A calculation on typical flow conditions with the reactor used in this research indicates R_e values of considerably less than unity. For example, a flow rate of about 3.0×10^{-6} moles/sec at 1.7 mm Hg pressure through a furnace at 1023°K becomes a volumetric flow rate of 110 mls/sec.

Reynolds number is defined by $R_e = \rho u d / \eta$, a dimensionless quantity where ρ is the density of the fluid, d the tube diameter, u the linear velocity and η the viscosity. The value R_e indicates the limiting region between laminar and turbulent flow. Thus for values of $\rho u d / \eta$ greater than this limiting value (e.g. with high flow velocities), turbulent flow will be present and for laminar flow the value R_e must not be exceeded.

Basing our calculation on argon, the carrier gas, using typical values $\eta = 550 \mu\text{P}$ at 750°C and $d = 3.0 \text{ cm}$, the Reynolds number is calculated at 0.09. This is two orders of magnitude less than the value required by Batten for laminar flow. Furthermore the reactor was equipped with a re-entrant thermocouple well which would tend to prevent channelling and probably also introduce a swirling action if the well was not mounted exactly centrally. This would help the lateral diffusion to the walls.

Mulcahy and Pethard (133) have also estimated possible errors in flow systems. They base their calculations on toluene vapour, because of its popularity as a carrier in flow work, at 1000°K

in a 2 cm diameter furnace and deduce that for a rate constant to be accurate to within 10% then the value of t_c/p must lie between the limits $Z > t_c/p > 0.5$ where Z is 3 for 50% conversion, 10 at 25% conversion and infinity at 0% conversion. t_c (secs) is the contact time and p (cms Hg) is the reactor pressure.

Typical values of t_c/p from the present work are 13 at 8.8% conversion and 18 at 1.2% conversion. These values along with Reynolds number calculations suggest no serious errors in the methods of calculating residence times and in assuming laminar flow.

Such work, however, emphasises the need for care in the design of gas flow reactors. Melville and Gowenlock (16) have discussed the problem briefly. A steady state or capacity flow reactor for the study of homogeneous gas phase reactions has been described by De Graaf and Kwart (134) in which they claimed elimination of the normal flow reactor difficulties. Mulcahy and Williams (135) also described a stirred flow reactor to remove the uncertainties of temperature and flow conditions in conventional flow methods. Kinetic data deduced in these reactors, in the former case on ethyl acetate pyrolysis and in the latter ditertiary butyl peroxide pyrolysis, agree well with other authors. The methods involve essentially vigorous mixing and stirred flow.

Other authors using stirred flow gas phase reactors are Herndon et al. (136, 137, 138) who claimed a much more simplified arrangement than De Graaf and Kwart and they obtained good

consistency with other workers on pyrolysis of chlorocyclohexane.

A discussion of the errors resulting from temperature gradients in spherical reaction vessels for the case of slower reactions has been given by Benson (139). The treatment applied to both liquid and gaseous systems and attempts to calculate the quantitative effect of convection were made. The method involved the estimation of Reynolds number by assuming that the flow within the reaction vessel consisted of a central column of low density fluid moving upwards and an equal flow of high density fluid moving downwards.

REFERENCES

1. Barraclough, Ph.D. Thesis, St. Andrews, (1958).
2. Szwarc, J. Chem. Physics, 1948, 16, 128.
3. Handbook of Chemistry and Physics, (Chemical Rubber Publishing Company, Cleveland, Ohio), 34th. ed., 1952.
4. Moore, Ph.D. Thesis, Manchester.
5. Nier, Rev. Sci, Instr., 1947, 18, 398.
6. Davidson, Ph.D. Thesis, St. Andrews, (1958).
7. Peirson, Electronic Engineering, 1950, 22, 48.
8. Smith, Ph.D. Thesis, St. Andrews, (1959).
9. Szwarc, Proc. Roy. Soc., 1951, 209A, 118.
10. American Petroleum Institute Research Project 44, Mass Spectral data.
11. Field and Franklin, Electron Impact Phenomena, (Academic Press, New York, 1957).
12. Sanderson, Vacuum Manipulation of Volatile Compounds, (Chapman and Hall Ltd., London, 1948).
13. Halstead and Nier, Rev. Sci. Instr. 1950, 1019.
14. Lapage, Ph.D. Thesis, St. Andrews, (1950).
15. Wood, Proc. Roy. Soc., 1923, 102A, 1.
16. Melville and Gowenlock, Experimental Methods in Gas Reactions, (MacMillan, London, 1964).
17. Semenov, Chemical Kinetics and Chain Reactions, (Clarendon Press, Oxford, 1935).
18. Barrow, Physical Chemistry, (McGraw Hill, New York, 1961).
19. Mearns, Ph.D. Thesis, St. Andrews, (1959).
20. Knox and Palmer, Chem. Rev., 1961, 247.
21. Reed and Sneddon, Trans. Faraday Soc., 1959, 55, 876.
22. Pitzer, J. Amer. Chem. Soc., 1948, 70, 2140.
23. Cottrell, The Strengths of Chemical Bonds, (Butterworths, London, 1958).
24. Cox, Tetrahedron, 1962, 18, 1337.

25. Bernstein, *Trans. Faraday Soc.*, 1962, 58, 2285.
26. Skinner, *J. Chem. Soc.*, 1962, 4396.
27. Errede, *J. Phys. Chem.*, 1960, 64, 1031.
28. Errede, *J. Org. Chem.*, 1962, 27, 3425.
29. Sehon and Szwarc, *Ann. Rev. Phys. Chem.*, 1957, 8, 439.
30. Szwarc, *Chem. Rev.*, 1950, 47, 75.
31. Reed, *Ion Production by Electron Impact*, (Academic Press, London, 1962).
32. Mortimer, *Reaction Heats and Bond Strengths*, (Pergamon, New York, 1961).
33. Steacie, *Atomic and Free Radical Reactions*, (Reinhold, New York, 1954).
34. Vedenev, Gurvich, Kondratev and Frankevich, *Bond Dissociation Energies, Ionisation Potentials and Electron Affinities*, (Acad. of Sciences, U.S.S.R., Moscow, 1962).
35. Trotman-Dickenson, *Gas Kinetics*, (Butterworths, London, 1955).
36. Herzberg, *Spectra of Diatomic Molecules*, (van Nostrand, New York, 1950).
37. Gaydon, *Dissociation Energies and Spectra of Diatomic Molecules*, (Chapman and Hall, London, 1953).
38. Baughan, Evans and Polanyi, *Trans. Faraday Soc.*, 1941, 37, 377.
39. Sehon and Szwarc, *Proc. Roy. Soc.*, 1951, 209A, 110.
40. Roberts and Skinner, *Trans. Faraday Soc.*, 1949, 45, 339.
41. Szabo, *Advances in Kinetics of Homogeneous Gas Reactions*, (Methuen, London, 1964).
42. Szwarc and Ghosh, *J. Chem. Physics*, 1949, 17, 744.
43. Szwarc, *J. Chem. Physics*, 1948, 16, 128.
44. Blades, Blades and Steacie, *Canad. J. Chem.*, 1954, 32, 298, 1142.
45. Takahasi, *Bull. Chem. Soc. Japan*, 1960, 33, 808, 801.
46. Price, *Canad. J. Chem.*, 1962, 40, 1310.
47. Anderson, Scheraga and Van Artsdalen, *J. Chem. Physics*, 1953, 21, 1258.
48. Benson and Buss, *J. Phys. Chem.*, 1957, 61, 104.

49. Schissler and Stevenson, *J. Chem. Physics*, 1954, 22, 151.
50. Esteban, Kerr and Trotman-Dickenson, *J. Chem. Soc.*, 1963, 3873.
51. Meyerson, *J. Amer. Chem. Soc.*, 1963, 85, 3340.
52. Rylander, Meyerson and Grubb, *J. Amer. Chem. Soc.*, 1957, 79, 842.
53. Busfield and Ivin, *Trans. Faraday Soc.*, 1961, 57, 1044.
54. Farmer, Henderson, McDowell and Lossing, *J. Chem. Physics*, 1954, 22, 1948.
55. Takahasi, *Bull. Chem. Soc. Japan*, 1956, 29, 625.
56. Rhind, Ph.D. Thesis, St. Andrews, (1963).
57. Cher, *J. Phys. Chem.*, 1964, 68, 1316.
58. Johnston and Parr, *J. Amer. Chem. Soc.*, 1963, 85, 2544.
59. Burkley and Rebbert, *J. Phys. Chem.*, 1963, 67, 168.
60. Berezin, Kazanskaya and Martinek, *Zhur. Obshchei. Khim.*, 1960, 30, 4092.
61. Meyer and Burr, *J. Amer. Chem. Soc.*, 1963, 85, 478.
62. Gomer and Kistiakowsky, *J. Chem. Physics*, 1951, 19, 85.
63. Frost and Pearson, *Kinetics and Mechanism*, (Wiley, New York, 1961, 2nd. ed.).
64. Szwarc and Roberts, *Trans. Faraday Soc.*, 1950, 46, 625.
65. Price and Trotman-Dickenson, *J. Chem. Soc.*, 1958, 4205.
66. Trotman-Dickenson and Steacie, *J. Chem. Physics*, 1951, 19, 329.
67. Taylor and Smith, *J. Chem. Physics*, 1940, 8, 543.
68. Rebbert and Steacie, *J. Chem. Physics*, 1953, 21, 1723.
69. Wilen and Eliel, *J. Amer. Chem. Soc.*, 1958, 80, 3309.
70. Brook and Glazebrook, *Trans. Faraday Soc.*, 1960, 56, 1014.
71. Fettis, Knox and Trotman-Dickenson, *J. Chem. Soc.*, 1960, 4177.
72. Eckstein, Scheraga and Van Artsdalen, *J. Chem. Physics*, 1954, 22, 28.
73. Givens and Willard, *J. Amer. Chem. Soc.*, 1959, 81, 4773.
74. Tsuda, Melton and Hanill, *J. Chem. Physics*, 1964, 41, 689.
75. Kistiakowsky and Van Artsdalen, *J. Chem. Physics*, 1944, 12, 469.

76. Benson and Buss, *J. Chem. Physics*, 1958, 28, 301.
77. Hirschfelder, *J. Chem. Physics*, 1941, 9, 645.
78. Trotman-Dickenson, *Chem. and Ind.*, 1965, 379.
79. *Chem. Soc. Special Publication No. 16*, 1962.
80. Benson, *J. Chem. Ed.*, 1965, 42, 502.
81. Brickstock and Pople, *Trans. Faraday Soc.*, 1954, 50, 901.
82. Franklin and Lumpkin, *J. Chem. Physics*, 1951, 19, 1073.
83. Miller and Steacie, *J. Chem. Physics*, 1951, 19, 73.
84. Bond, *Probability and Random Errors*, (Ed. Arnold and Co., London, 1935).
85. *Proceedings of Kekule Symposium on Theoretical Organic Chemistry*, 1958, (Butterworths, London, 1959).
86. Goldberg and Daniels, *J. Amer. Chem. Soc.*, 1957, 79, 1314.
87. Blades, *Canad. J. Chem.*, 1958, 36, 1129.
88. Blades, *Canad. J. Chem.*, 1958, 36, 1043.
89. Thomas, *J. Chem. Soc.*, 1959, 1192.
90. Agius and Maccoll, *J. Chem. Soc.*, 1955, 973.
91. Semenov, Sergeev and Kapralova, *Doklady Akad. Nauk S.S.S.R.*, 1955, 105, 301.
92. Blades and Murphy, *J. Amer. Chem. Soc.*, 1952, 74, 6219.
93. Maccoll and Thomas, *J. Chem. Physics*, 1951, 19, 977.
94. Maccoll and Thomas, *J. Chem. Soc.*, 1955, 979.
95. Maccoll and Thomas, *J. Chem. Soc.*, 1957, 5033.
96. Maccoll and Thomas, *J. Chem. Soc.*, 1955, 2445.
97. Sergeev, *Doklady Akad. Nauk S.S.S.R.*, 1956, 106, 299.
98. Kale, Maccoll and Thomas, *J. Chem. Soc.*, 1958, 3016.
99. Harden and Maccoll, *J. Chem. Soc.*, 1955, 2454.
100. Wing Tsang, *J. Chem. Physics*, 1964, 40, 1498.
101. Harden and Maccoll, *J. Chem. Soc.*, 1959, 1197.
102. Harden, *J. Chem. Soc.*, 1957, 5024.
103. Wing Tsang, *J. Chem. Physics*, 1964, 41, 2487.
104. Barker and Maccoll, *J. Chem. Soc.*, 1963, 2839.
105. Blades, Gilderson and Wallbridge, *Canad. J. Chem.*, 1962, 40, 1533.

106. Kale and Maccoll, J. Chem. Soc., 1964, 1513.
107. Maccoll and Thomas, Nature, 1955, 176, 392.
108. Ingold, Proc. Chem. Soc., 1957, 279.
109. Barton and Head, Trans. Faraday Soc., 1950, 46, 114.
110. Harrison, Kebarle and Lossing, J. Amer. Chem. Soc., 1961, 83, 777.
111. Herndon, Sullivan, Henley and Manion, J. Amer. Chem. Soc., 1964, 86, 5691.
112. Teranishi and Benson, J. Chem. Physics, 1964, 40, 2946.
113. Flowers and Benson, J. Chem. Physics, 1963, 38, 882.
114. Benson and Bose, J. Chem. Physics, 1962, 37, 2935.
115. Benson, J. Chem. Physics, 1963, 38, 1945.
116. Holmes and Maccoll, J. Chem. Soc., 1963, 5919.
117. Teramoto, Kitabatake and Onouchi, J. Chem. Soc. Japan, Ind. Chem. Sect., 1964, 67, 460.
118. Lane, Linnett and Oswin, Proc. Roy. Soc., 1953, 216A, 361.
119. Pritchard and Thommarson, J. Phys. Chem., 1964, 68, 568.
120. Gilbert, Combustion and Flame, 1958, 2, 149.
121. Branson and Smith, J. Amer. Chem. Soc., 1953, 75, 4133.
122. Stevenson, Disc. Faraday Soc., 1951, 10, 35.
123. Szwarc, Proc. Roy. Soc., 1949, 198A, 267.
124. Lossing, Ingold and Henderson, J. Chem. Physics, 1954, 22, 1489.
125. McDowell and Cox, J. Chem. Physics, 1952, 20, 1496.
126. Carson, Carson and Wilmshurst, Nature, 1952, 170, 320.
127. Hartley, Pritchard and Skinner, Trans. Faraday Soc., 1950, 46, 1019.
128. Hartley, Pritchard and Skinner, Trans. Faraday Soc., 1951, 47, 254.
129. Evans and Polanyi, Trans. Faraday Soc., 1938, 34, 11.
130. Goy and Pritchard, J. Phys. Chem., 1965, 69, 3040.
131. Boyd, Ph.D. Thesis, St. Andrews, (1962).
132. Batten, Austral. J. Appl. Sci., 1961, 12, 11.
133. Milcahy and Pethard, Austral. J. Chem., 1963, 16, 527.

134. De Graaf and Kwart, J. Phys. Chem., 1963, 67, 1458.
135. Mulcahy and Williams, Austral. J. Chem., 1961, 14, 534.
136. Herndon, Henly and Sullivan, J. Phys. Chem. 1963, 67, 2842.
137. Lewis and Herndon, J. Amer. Chem. Soc., 1961, 83, 1955.
138. Herndon and Lowry, J. Amer. Chem. Soc., 1964, 86, 1922.
139. Benson, J. Chem. Physics, 1954, 22, 46.
140. Klemm and Bernstein, J. Amer. Chem. Soc., 1960, 82, 5987.
141. Cullis, Manton, Thomas and Wilman, Acta. Cryst. 1959, 12, 382.
142. Holbrook, Proc. Chem. Soc., 1964, 418.
143. Brearley, Kistiakowsky and Stauffer, J. Amer. Chem. Soc., 1936, 58, 43.
144. Rice and Herzfeld, J. Phys. Chem., 1951, 55, 975.
145. Chadwell and Titani, J. Amer. Chem. Soc., 1933, 55, 1363.
146. Cremer, Curry and Polanyi, Z. physik. Chem. 1933, 23, 445.
147. Meissner and Schumacher, Z. physik. Chem., 1940, 185, 435.
148. Whittingham, Disc. Faraday Soc., 1947, 2, 175.
149. Gordon and Taylor, J. Amer. Chem. Soc., 1941, 63, 3435.
150. Raal and Steacie, J. Chem. Physics, 1952, 20, 578.
151. National Bureau of Standards Circular 500, 1952.
152. Maslov and Maslov, Khim. i Tekhnol. Topliv i Masel 3, 1958, 10, 50.
153. Fettis and Trotman-Dickenson, J. Chem. Soc., 1961, 3037.
154. Gelles and Pitzer, J. Amer. Chem. Soc., 1953, 75, 5259.
155. Ribaud, Publ. Sci. et Tech. du ministere de l'air, 1952, 266, 141
156. Gowenlock, Quart. Rev. 1960, 14, 133.